

Osteoblast physiology and morphology on
cell adhesive plasma-polymerized
allylamine and ethylenediamine layers

Kumulative Dissertation
zur
Erlangung des akademischen Grades
doctor rerum naturalium (Dr. rer. nat.)
der Mathematisch-Naturwissenschaftlichen Fakultät
der Universität Rostock

vorgelegt von

Henrike Rebl geb. Jesswein

geb. am 05.04.1983 in Rostock

Rostock, Mai 2014



Universität
Rostock



Traditio et Innovatio

Datum der Einreichung: 11.07.2014

Datum der Verteidigung: 24.04.2015

Gutachter:

Prof. Dr. J. Barbara Nebe,

Universitätsmedizin Rostock, Zentrum für Medizinische Forschung, AB Zellbiologie

Prof. Dr. Uwe Pieleis,

Hochschule für Life Sciences (MuttENZ, Schweiz), Institut für Chemie und Bioanalytik

PD Dr. Sergei Kuznetsov,

Universität Rostock, MNF, Institut für Biowissenschaften

Content

Abbreviations.....	I
1. Introduction.....	1
1.1 Motivation.....	1
1.2 Physico-chemical surface modifications.....	2
1.3 Molecular mechanisms of the initial cell adhesion.....	4
1.4 Cell types.....	7
1.5 Working hypotheses and objectives.....	8
2. Publications.....	9
2.1 <i>Study I:</i> H. Rebl, B. Finke, K. Schroeder, J.B. Nebe; Time-dependent metabolic activity and adhesion of human osteoblast-like cells on sensor chips with a plasma polymer nanolayer.....	9
2.2 <i>Study II:</i> H. Rebl, B. Finke, J. Rychly, K. Schröder, J.B. Nebe; Positively charged material surfaces generated by plasma polymerized allylamine enhance vinculin mobility in vital human osteoblasts.....	21
2.3 <i>Study III:</i> H. Rebl, B. Finke, R. Lange, K.D. Weltmann, J.B. Nebe; Impact of plasma chemistry versus titanium surface topography on osteoblast orientation.....	31
2.4 <i>Study IV:</i> H. Testrich, H. Rebl, B. Finke, F. Hempel, B. Nebe, J. Meichsner; Aging effects of plasma polymerized ethylenediamine (PPEDA) thin films on cell- adhesive implant coatings.....	44
3. Discussion.....	51
3.1 Introduction of a new method for monitoring cells on nano-surface coatings.....	52
3.2 Initial cell adhesion is significantly improved on plasma-modified surfaces.....	53
3.3 Initial cell spreading is promoted on PPAAm.....	55
3.4 Mobility and length of vinculin contacts is enhanced on positively charged surfaces.....	55

3.5	Morphology of osteoblastic cells is flattened on PPAAm.....	56
3.6	Contact guidance along grooves is abrogated on plasma-modified surfaces.....	57
3.7	Differentiation of osteoblastic cells is promoted on structured PPAAm surfaces.....	57
3.8	Comparative analyses with PPEDA and stored surfaces show that the amino group density is not deciding for the elevated cell adhesion.....	58
3.9	<i>In vivo</i> results.....	59
4.	Conclusions and future prospects.....	61
5.	Summary.....	63
6.	Zusammenfassung.....	64
7.	References.....	65
8.	Appendix.....	72

Abbreviations

AP	alkaline phosphatase
BSP	bone sialoprotein
Col I	collagen I
ECM	extracellular matrix
FA	focal adhesion
FACS	fluorescence-activated cell sorting
FRAP	fluorescence recovery after photobleaching
FTIR	fourier transform infrared spectroscopy
GDA	glutardialdehyde
HA	hyaluronic acid
PEG-DA	polyethylene glycol-diacid
PPAAm	plasma-polymerized allylamine
PPEDA	plasma-polymerized ethylenediamine
rf	radio frequency
RGD	arginine-glycine-aspartic acid peptide sequence
SAM	self-assembled monolayer
TFBA	trifluoromethylbenzoicanhydride
Ti	titanium
WCA	water contact angle measurement
XPS	X-ray photoelectron spectroscopy

1. Introduction

1.1 Motivation

Defects and inflammation of bone and joints annually affect several million people worldwide. As one of the most prevalent operations, 390,000 hip and knee prostheses are implanted annually in Germany. Additionally, 37,000 replacement operations are necessary each year [<http://www.eprd.de> Endoprothesenregister Deutschland; 22.1.2013]. The number of hip fractures in the European Union is predicted to rise from 414,000 in the year 2000 up to 972,000 in 2050. This represents an increase by 135%. The number of vertebral fractures is estimated to increase from 23.7 million to 37.3 million [COMPSTON *et al.* 1998]. It was anticipated that 25% of all health expenditures in developing nations go towards providing trauma-related care by the year 2010 [DELMAS *et al.* 2000]. Short convalescence times are of growing importance as, at least in industrial countries, there is a growing need for an employable population to keep the economy stable and to ensure the supply of the older generations. Due to improved healthcare systems, people reach an advanced age. At the same time there is a growing will to stay physically and mentally healthy and have high fitness and self-dependence in seniority. Moreover, expectancies after an operation have changed in the last decades. Patients who overcame a total hip replacement do not only want to be reconstituted but expect to walk stairs and do sports without pain.



Figure 1: Radiograph of the hip with prosthesis (AML; DePuy, Warsaw, Indiana) after total hip arthroplasty. The arrows show regions of osteolysis and wear of the polyethylene. Published in PULLIAM *et al.*, 1997.

Bone fractures, dorsal pain, osteoporosis, scoliosis, bone cancer and other diseases of the musculoskeletal system can in part only be cured by operations and the use of permanent, temporal or degradable implants. Orthopedic biomaterials therefore have to be designed in a way that they can replace different tissue or stimulate the bone to restore/recover/heal. High demands are made on the

materials properties because the human body exerts a highly corrosive milieu. The materials need to have (I) high mechanical stability, (II) abrasion resistance, (III) load capacity, (IV) biocompatibility and potentially (V) bioactivity and osteoinductive potential [NAVARRO *et al.* 2008]. On account of this, intensive research on improved materials or coatings is of great importance since the last decades.

1.2 *Physico-chemical surface modifications*

The use of metals is widespread in dentistry or surgery. Especially titanium and titanium alloys are commonly used due to their fracture toughness and load bearing capacity. However, their ingrowth in living bone is rather poor [YAN *et al.* 1997]. While temporary implants, which have to be removed from the patient after a certain time, should be rather inert and require no bone bonding, long-term implants have to possess a bioactive surface to enable good integration into the patient's bone. The fabrication of a rough surface by mechanical methods such as grinding, machining and blasting [BARBOUR *et al.* 2007, LANGE *et al.* 2002, LUETHEN *et al.* 2005], or chemical methods such as etching and anodization [PARK *et al.* 2007, SZMUKLER-MONCLER *et al.* 2004] increases the bone-bonding-ability. Cell culture experiments have shown that rough surfaces promote cell adhesion, spreading [LUETHEN *et al.* 2005, RANUCCI *et al.* 2001], gene expression of differentiation markers and synthesis of proteins of the extracellular matrix [BOYAN *et al.* 1996, HATANO *et al.* 1999]. Moreover, polished titanium, due to its low roughness and low wettability, is likely to be colonized by fibroblasts, which are unwanted in the bone-implant-interface [PESAKOVA *et al.* 2007]. On the one hand, the high surface roughness of corundum blasted surfaces adversely affects cell spreading and proliferation. On the other hand, the rough topography is essential for the successful long-term functionality of "close-to-bone implants". Clinical trials have shown that a high surface roughness leads to a better distribution of the forces acting on the bone, resulting in decreased occurrence of micro-fractures [WISKOTT *et al.* 1999].

Additionally, there are different approaches optimizing cell adhesion to metallic surfaces. Coatings are deposited to improve the biocompatibility and bioactivity of a surface compared to a solely inert surface. Coatings are also applied to inhibit bacterial adhesion and colonization. Gristina has postulated in 1987 that human body cells and bacteria compete in a "race for the surface". Those cells, who reach the surface first and build up a firm layer, will determine the fate of the implant. Thus it would be a great benefit, if the adhesion of human body cells, especially bone cells, could be improved [GRISTINA 1987].

A widespread approach to create biologically active implant surfaces comprises the deposition of an additional layer on top of the metal by physicochemical or biochemical means [MORRA *et al.* 2003, NARAYANAN *et al.* 2008]. A well-accepted method to increase the bioactivity of metals is the deposition of an hydroxyapatite layer using electrophoretic techniques [DUCHEYNE *et al.* 1990] or *via* plasma-

spraying [THULL *et al.* 2001]. With respect to chemical modifications, one focus is placed on the grafting of lipid-layers or proteins, i.e. adhesion proteins, growth factors or peptides that function as ligands for adhesion receptors. Considering peptides, especially the amino acid motif RGD (arginine-glutamine-asparagine), present in the extracellular matrix (ECM) proteins fibronectin or vitronectin, is under intensive research [SCHULER *et al.* 2006, WILLUMEIT *et al.* 2007, WOJTOWICZ *et al.* 2010].

The use of poly-D-lysine (PDL) coated surfaces in research and development is widespread. However, due to the lack of mechanical stability, this coating was not established at the implant market. Thus, as described above, there are several preconditions that have to be fulfilled by orthopedic implant coatings. They have to be mechanically stable, have a high load capacity and need to be highly biocompatible [NAVARRO *et al.* 2008]. This accounts for the bulk material as well as for the potential coating.

Another main research area is concerned with the coupling of functional groups on implant surfaces. Different techniques can be used to deposit layers with various terminating groups (CH₃, NH₂, COOH, OH) on a surface. Different approaches showed that the highest adhesion of osteoblasts could be reached on NH₂ groups compared to polyethylenglycol and methyl groups [FAUCHEUX *et al.* 2004, SCHWEIKL *et al.* 2007]. A very common technique is to use self-assembled monolayers (SAMs), where organic molecules adsorb to a surface and organize due to the different chemistry of the head and tail-domains [FAUCHEUX *et al.* 2004].

Besides these techniques, plasma technology offers advantages to modify metal surfaces with reactive groups. Cold plasma processes are energy-efficient, dry techniques that can be performed in a large range of pressure. These plasma processes are characterized by a low degree of ionization when operated at low pressure, thereby altering only the upper layer of the material leaving the characteristics of the bulk material unchanged. This is highly desired in the orthopedic field because it allows for modification of existent, commercially available materials thereby improving their performance in the biomedical field without changing the mechanical features [DENES *et al.* 2004]. Such processes include (I) the deposition of chemical groups, (II) the deposition of micro- or nanolayers generating varying roughness or (III) the creation of cell adhesive coatings with defined chemical composition, which can be functionalized subsequently with immobilized molecules [INTRANUOVO *et al.* 2011, SCHRÖDER *et al.* 2010a]. Direct applications for this technique are drug eluting stents or vascular prosthesis, releasing substances that prevent from thrombosis, blood coagulation or restenosis [REN *et al.* 2008, WALSCHUS *et al.* 2011]. In principal, reactive surfaces like polymers can easily be equipped with nitrogen-containing groups by plasma treatment with a simple process gas like ammonia. Depending on treatment condition, this can lead to high nitrogen content and amino group density on the surface. However, these surfaces undergo a fast restructuring process, which results in a rapid change of the hydrophilicity during storage on air. For this reason ammonia-treated surfaces are not applicable in orthopedics or dental surgery [GRIESSER *et al.* 1994].

However, inert surfaces like titanium can well be equipped with amino groups by depositing polymer layers. Different amines, for example allylamine ($C_3H_5NH_2$), are used as precursors for functionalizing materials using different coating techniques. The surfaces are equipped with a net positive surface charge. The amine layer allows further covalent coupling of proteins or peptides *via* suitable linkers [FINKE *et al.* 2007, HAMERLI *et al.* 2003, J.H. ZHAO *et al.* 2011]. By functionalizing the surface of the implant material titanium with positively charged amino groups, their cell adhesive characteristics can be significantly altered. Polished titanium surfaces usually possess a water contact angle of 70° . In contrast to this, human cells adhere best, when the surface has a water contact angle of $40-60^\circ$ - the so-called “biocompatibility window” [LIM *et al.* 2004]. The functionalization of titanium surfaces with plasma technology offers the possibility to render the surface more hydrophilic (50°) and additionally to generate positively charged amino groups [FINKE *et al.* 2007, NEBE *et al.* 2010]. Among different amines, allylamine ($C_3H_5NH_2$) is used as a precursor in plasma processes to generate surfaces with a biocompatible water contact angle and a positive surface charge ($\sim 9.1mV$) [HAMERLI *et al.* 2003, HARSCH *et al.* 2000, NEBE *et al.* 2007, REN *et al.* 2008]. But also ethylenediamine ($C_2H_8N_2$) or heptylamine ($CH_3(CH_2)_6NH_2$) can be used to generate positively charged plasma layers [KIM *et al.* 2007, ZHAO *et al.* 2011].

1.3 Molecular mechanisms of the initial cell adhesion

The majority of tissue cells, apart from blood cells, need to adhere to the extracellular matrix or other cells in order to survive. The quality of this first adhesion is decisive for the further growth and differentiation of the cells. Cell adhesion is playing a central role in the development of all metazoans [HYNES 1999]. Studies on cell-matrix and cell-cell contacts indicate that these complexes consist of multiple components, including transmembrane adhesion receptors (integrin family), components of the actin cytoskeleton and interconnecting anchoring proteins (focal adhesion kinase, paxillin), which link the cytoskeleton with the membrane [ZAMIR *et al.* 2001]. These protein complexes influence the integration of single cells into the tissue. Moreover, they play a major role in the transduction of transmembrane signals, which regulate important cellular processes. These processes are often overlapping and are connected to each other, such as proliferation, migration, differentiation or apoptosis of cells [GEIGER *et al.* 2001, GIANCOTTI *et al.* 1999].

Due to the complexity of the processes being involved during cell adhesion, it is necessary to divide the processes in temporary defined events. Primarily the cell exhibits many unspecific weak bondings, which taken together are sufficient to hold the cell near the surface. This creates the temporal and spatial frame for the production and organization of adhesion proteins [HANEIN *et al.* 1995].

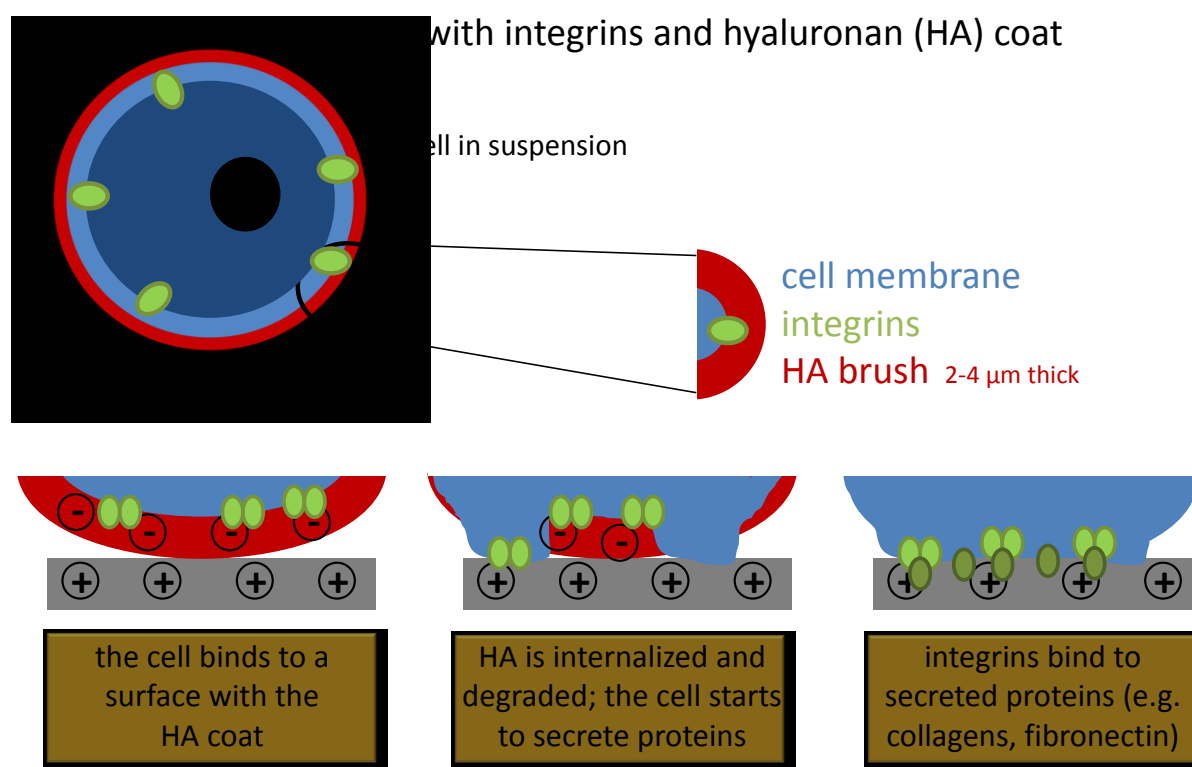


Figure 2: Scheme of the initial cell adhesion to a positively charged surface. The negatively charged hyaluronan (HA) coat facilitates a weak bonding to the surface until the cell has established strong adhesion bonds *via* integrins. Adapted from [COHEN *et al.* 2004]

The formation of integrin contacts requires a time frame of several minutes and a maximum distance to the surface of a few dozen nm [ZIMMERMAN *et al.* 2002]. Subsequently, these contacts mature into focal contacts representing a stable connection to the surface. Recently, it was discovered that the pericellular matrix-component hyaluronan (HA) plays a decisive role during the first cell-surface contact [M. COHEN *et al.* 2006, ZIMMERMAN *et al.* 2002]. HA is a large linear glucosaminoglycane (10^6 - 10^7 kD) composed of several disaccharides of glucuronic acid and n-acetylglucosamin [COHEN *et al.* 2004, TOOL 2001]. Due to the carboxy-group of the glucuronic acid, HA is strongly negatively charged at physiological pH [COHEN *et al.* 2003, TOOLE 2004]. The thickness of the hyaluronan coat may vary from 2-4 μm depending on the cell type [COHEN *et al.* 2003]. HA mediates the fast adhesion of cells to a surface. If the hyaluronan coat of the cell is removed by hyaluronidase, the binding of cells is diminished [FINKE *et al.* 2007]. Likewise, cell adhesion can be inhibited if both partners - cell and surface - exhibit HA [ZIMMERMAN *et al.* 2002]. This initial phase, where only weak forces are developed between cell and surface may last 2-10 minutes. During this time, no focal adhesions are formed. In order to make way for receptor-integrin contacts, HA has to be modified or removed. HA is then dislocated to the cell periphery or hydrolyzed by hyaluronidase [COHEN *et al.* 2004]. During cell spreading, the HA is remaining in pockets, few μm^2 in size, underneath the cell [M. COHEN *et al.* 2006]. Subsequently, as the cell reaches a closer distance to the surface, it starts building up focal contacts resulting in a strong

bonding to the surface. Subsequently, different adapter proteins like vinculin, paxillin, or focal adhesion kinase can bind to this agglomeration of adhesion proteins that is referred to as ‘focal adhesions’ or the ‘adhesome’ [GEIGER *et al.* 2011]. Due to the complexity of the focal adhesions, it is not possible to analyze all proteins involved. In lieu thereof only one or two representative proteins out of this agglomeration are analyzed. We and others have decided to use vinculin as a model protein to investigate the flexibility and motility of the adhesion process [M. COHEN *et al.* 2006, CRITCHLEY 2004, DIENER *et al.* 2005, MOHL *et al.* 2009].

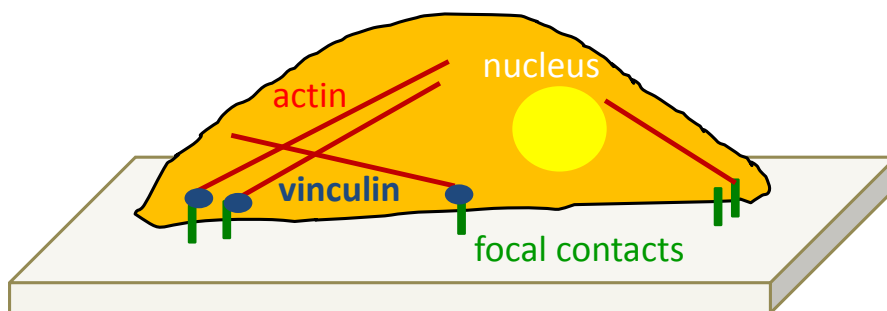


Figure 3: Scheme of an adherent cell on a material surface. The main attachment is facilitated by the focal adhesions which include integrin proteins. These bind to extracellular surface ligands. Intracellularly they are connected to adapter proteins such as vinculin that bind to the actin cytoskeleton [Adapted from REBL *et al.* 2010].

Vinculin is an actin-binding protein which serves as a marker for both cell–cell and cell–extracellular matrix (focal adhesion) junctions. Vinculin is expressed ubiquitously, thus it can be assumed that vinculin is involved in multiple other signalling pathways [ZIEGLER *et al.* 2006]. Recent findings have shown for example the role of vinculin in apoptotic pathways [SUBAUSTE *et al.* 2004]. Vinculin is a 116 kDa protein and it is composed of a globular head followed by a short proline-rich sequence and a tail domain. In the cytoplasm vinculin is thought to exist in an inactivated state, where an interaction between the head and tail masks the various ligand binding sites in the protein. Vinculin in focal adhesions was found to be in an activated state where ligand binding is feasible [CHEN *et al.* 2005]. Among these binding partners of vinculin are talin, F-actin or paxillin. In focal adhesions vinculin is thought to play a stabilizing role, thereby down-regulating the cell motility [ZIEGLER *et al.* 2006].

The formation, maturation and protein composition of the focal adhesions strongly depend on the protein composition of the extracellular matrix (ECM) that is secreted on the implant surface. [GEIGER *et al.* 2001] In human bone, 90% of the ECM is made up of collagenic proteins. From these, collagen I makes up the major part with 97%. The minor part is composed of osteonectin, bone sialoproteins or fibronectin [ANSELME 2000]. For this reason, we and others preferred to use whole collagen I proteins to study the

defined cell interaction with the surface coating [ZHU *et al.* 2006]. Another approach to improve the cell adhesion towards a surface is to use proteins or small peptides instead of proteins. In the biomaterials field, the ECM proteins fibronectin (with its motif Arg-Gly-Asp: RGD) or collagen I (with the collagen-mimetic peptide GFOGER) are under intensive research. During the cell adhesion process, the integrins, large transmembrane proteins can bind to these ECM-proteins or small peptides. These large transmembrane proteins establish a firm adhesion of the cell to a surface [TAKADA *et al.* 2007]. The reason for sometimes using rather peptides than proteins for surface coatings can be found in the detailed look at the implantation site. During the implantation operation, a wound is created and a lot of blood is present surrounding the freshly inserted implant. The protein or peptide layer might be degraded by hydrolyses or enzymatic activity. The matrix metalloproteinases contained in the blood could destroy the ECM proteins [MANNELLO 2008]. Peptides are less susceptible to destruction so they might maintain their efficiency. However, the biological effect is not as high compared to whole proteins due to their reduced length that results in a generally poor specificity and a reduced conformational flexibility [COLLIER *et al.* 2011, GEIGER *et al.* 2011].

1.4 Cell types

Biomaterial tests are usually performed using primary cells or cell lines of human origin. Primary human cells from healthy tissue are ideal to test materials before their clinical application. Unfortunately, there are some restrictions in their practical use. On the one hand, these cells are only available to a limited degree and on the other hand, there is a high variability of cells coming from identical tissue but from different donors [CZEKANSKA *et al.* 2012]. This variability gives rise to the necessity to perform many independent experiments to conduct significant statistical analyses. These restrictions have led to the prevalent use of tumor-derived cell lines. The advantage of human cell lines is the high proliferation rate leading to a nearly unrestricted availability. Even though osteoblastic cell lines like SaOs-2 or MG-63 are derived from a sarcoma, they have conserved the main properties of primary osteoblasts i.e. the expression of osteogenic differentiation markers like osteocalcin and bone sialoprotein (BSP) or the activity of the alkaline phosphatase (AP) [GRAUSOVA *et al.* 2009, G. ZHAO *et al.* 2007]. Moreover, a systematic study [CLOVER *et al.* 1992] revealed that MG-63 cells and primary human osteoblasts express a similar integrin subunit pattern. This makes them very attractive for studies on the initial attachment to material surfaces.

1.5 Working hypotheses and objectives

The present thesis arose from the joint research project “Campus PlasmaMed” subproject “PlasmaImp” (www.campus-plasmamed.de, 10/2012, grant No. 13N9775, 13N11183). Concomitantly to this dissertation at hand different plasma depositions were established and physico-chemically evaluated at the Leibniz Institute for Plasma Science and Technology (Dr. B. Finke and Dr. K. Schröder, INP) in Greifswald and the University of Greifswald/Department of Physics (Prof. J. Meichsner). In the context of this dissertation, the cellular behavior on these positively charged allylamine plasma layers was characterized.

Most of the techniques used for the characterization of surface coatings are performed on plane substrates. This is due to the fact that a lot of methods for surface characterization, e.g. ellipsometry for the measurement of layer thickness or water contact angle measurements to determine surface hydrophilicity, can hardly be performed on rough substrates. However, orthopedic implants often require a rough surface topography to ensure fast and good primary stability and to minimize the appearance of micro fractures. We therefore decided to perform a comparative study on how the cell behavior changes on a certain chemical layer, when combined with defined surface topography.

Our hypothesis was that (I) this positively charged surface would facilitate a faster cell adhesion and thus induce the faster creation of focal adhesions. These focal adhesions would mature and the cell would spread on the surface, grow, proliferate and finally differentiate faster than on an uncoated surface.

Moreover we hypothesized that (II) the density of the amino groups would play a major role in controlling the adhesion and growth of the cells. This is why we decided to compare layers generated from different precursors (allylamine and ethylenediamine).

Finally, we assumed that (III) the combination of the plasma layer with surface roughness would influence the cell adhesion and potentially further processes.

2. Publications

2.1 Study I

Henrike Rebl, Birgit Finke, Karsten Schroeder, J Barbara Nebe.

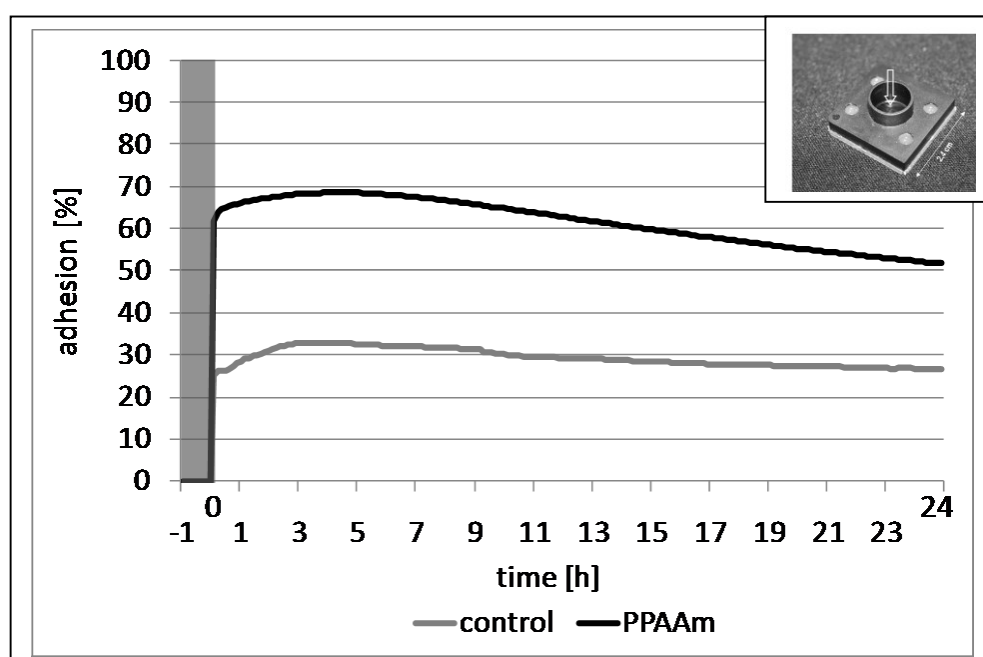
Time-dependent metabolic activity and adhesion of human osteoblast-like cells on sensor chips with a plasma polymer nanolayer.

Int J Artif Organs 2010; 33: 738 – 748 .

Abstract

This journal article introduces the use of a sensor chip based assay (BIONAS®) for the characterization of cell behavior on a chemical surface layer. So far these (“Lab-on-chip”) systems had only been used for observing the influence of soluble substances on cell behavior. Here, cell adhesion and metabolic activity of osteoblast-like cells grown on a plasma layer of PPAAm were monitored over a time period of 24 h. The surface coating did not interfere with the sensor performance. We determined that adhesion of vital cells on PPAAm is enhanced shortly (1 h) after cell seeding and remained continuously higher for 24 h. The nanometer-thin PPAAm layer did not change the overall metabolic activity of MG-63 cells during 24 h. This indicates that the plasma polymer layer enhances cell adhesion without affecting cell metabolism. Moreover, scanning electron images revealed that the cells spread out very flat on the sensor surface leading to a strong interaction between the cell and the underlying surface.

Graphical abstract:



ORIGINAL ARTICLE

Time-dependent metabolic activity and adhesion of human osteoblast-like cells on sensor chips with a plasma polymer nanolayer

Henrike Rebl¹, Birgit Finke², Karsten Schroeder², J. Barbara Nebe¹

¹University of Rostock, Biomedical Research Center, Dept. of Cell Biology, Rostock - Germany

²Leibniz-Institute for Plasma Science and Technology e.V. (INP), Greifswald - Germany

ABSTRACT

Purpose: To improve orthopedic implant ingrowth, knowledge of the effect of chemical surface modifications on vital cell function *in vitro* is of importance. Early in our investigations we recognized that amino groups, positively charged via plasma polymerized allylamine, increased cell growth and the actin-filament formation in the initial cell-material contact phase. To gain insight into continuous vital cell behavior on this plasma polymer layer, here we present the metabolic activity of osteoblasts and their time-dependent adhesion using the sensor chip technology.

Methods: We demonstrate a new method for continuous 24 hour-measurements with vital human osteoblast-like cells (MG-63, ATCC) on sensor chips (Bionas[®] SC 1000) modified with plasma polymerized allylamine (PPAAm). The PPAAm film deposited on the chip is a cross-linked, strongly fixed plasma polymer with relatively high amino functionality and well defined chemical surface composition. We assessed continuous cell adhesion and the metabolic activity, i.e., oxygen consumption and acidification.

Results: We determined that adhesion of vital cells on PPAAm is not only enhanced shortly (1 h) after cell seeding but remained continuously higher for 24 h, which is significant. This nanometer-thin PPAAm layer did not change the overall metabolic activity of MG-63 cells during 24 h.

Conclusion: This tool – using adhesion and metabolic sensor chips – appears to be a suitable method for the recognition of vital cell physiology in biocompatibility measurements of plasma chemical treated surfaces.

KEY WORDS: Biocompatible materials, Polymer, Biosensing techniques, Osteoblasts, Cell adhesion, Metabolic activation

Accepted: August 17, 2010

INTRODUCTION

Control of tissue physiology by biomaterial surfaces is fundamental in bone tissue engineering. In the last decade many strategies have been introduced to improve the cell-material-interaction via chemical surface modifications of an implant material (1-4). In this context, adhesion, cell spreading and migration are vitally important for the im-

mediate occupation of an implant surface by osteoblasts as well as for the induction of tissue regeneration (5, 6). After the initial cell contact phase at the material interface further adhesion events were mediated via the adhesion receptors, named integrins. Therefore, for a decade immobilized proteins and peptides (e.g., type I collagen, RGD peptides) that function as ligands for adhesion receptors have commonly been used to improve the biomaterial. A

common approach to the creation of a biologically active implant surface involves the application of an additional coating onto the material surface by means of physico-chemical and biochemical deposition techniques (7, 8). One focus in the chemical surface modification involves coating with proteins, peptides and/or growth factors as well as lipid bilayers (5, 9, 10). Another strategy, owing to the net negative charge of eukaryotic cells, is to provide the surface with positive charge carriers, for example, NH_2 groups (11-14). Allylamine is widely used as a precursor for functionalizing materials with a net positive surface charge and for allowing further covalent coupling of proteins or peptides via suitable linkers (7, 15, 16). By functionalizing the surface of the implant material titanium with positively charged amino groups, their cell growth characteristics can be significantly improved, as our previous studies involving plasma polymerized allylamine (PPAAm) showed (13, 14, 17-19). However, in the experiments, the influence of the PPAAm-modified surface chemistry on cells was only tested with endpoint measurements. This does not allow a conclusion to be drawn on the course of the effect at any given time point. Biochips offer an ideal noninvasive online measurement platform to obtain precise and reproducible data on basic functional parameters such as the metabolic activities of living, adherent cells over longer time periods. In order to determine reasonable time points for more precise testing methods, chip-based assays are of great benefit. Global cellular metabolic activity, the rate of mitochondrial oxygen consumption and morphological changes are typically investigated (20, 21). Generally these assays are extremely useful for monitoring drug effects and dosage influence. The evaluation of functional layers has not been the center of interest so far.

To our knowledge this is the first study reporting the permanent effect of an allylamine plasma polymer with a continuous adhesion measurement method, monitoring metabolic activity in the same time frame. Using continuous measurements of cell metabolic parameters allows for better characterization and understanding of the influence of different substrata on cell accretion. The Bionas[®] 2500 analyzing system (Bionas GmbH, Rostock, Germany) enables the measurement of relevant parameters like adhesion (impedance), respiration and acidification in parallel (22). These parameters are recorded continuously to obtain an overview of the relevant cell behavior characteristics at any given time point. This will help to gain a better understanding of cell adhesion processes at the material interface.

The aim of the study was to find a stable and reproducible method to evaluate adhesion and especially metabolism (oxygen consumption, acidification) of living cells on surfaces chemically modified with a plasma polymer nanolayer. In detail we wanted to find out sensor efficacy of Bionas[®] chips after the plasma chemical treatment.

MATERIALS AND METHODS

Sensor chips

The Bionas[®] 2500 analyzing system with the metabolic chips SC 1000 (Bionas GmbH, Rostock, Germany) was used (Fig. 1A). This chip type is equipped with three sensor types: IDES (interdigitated electrode structure) sensors for cell adhesion, Clark type sensors for respiration and ISFET (ion-sensitive field effect transistor) sensors for acidification measurements (Fig. 1B). The chip surface was functionalized with plasma polymerized allylamine (PPAAm) as described below. The Bionas[®] 2500 analyzing system technology is based on a flow system, where fresh medium (in our experiments Dulbecco's modified Eagle medium + 0.1% fetal calf serum) is steadily supplied to the cells. The Bionas[®] auto sampler was designed to support the medium supply during the measurement. To prevent contamination, the medium racks were sealed with a sterile membrane (BREATHseal, Greiner Bio-One GmbH, Frickenhausen, Germany) which could be penetrated easily by the aspiration needle. During the entire course of the experiment a pump phase of 4 minutes was followed by a steady phase (no flow) of 4 minutes. The flow rate in the system was adjusted to the lowest value of 56 $\mu\text{l}/\text{min}$ to avoid shear stress. The temperature in the

TABLE I - MEASUREMENTS OF CAPACITANCE OF THE CELL-FREE SENSOR CHIPS BEFORE AND AFTER PLASMA TREATMENT

	Capacitance prior to plasma-modification [nF]	Capacitance after to plasma-modification [nF]
Chip 1	48	48
Chip 2	49	49
Chip 3	47	47
Chip 4	47	47

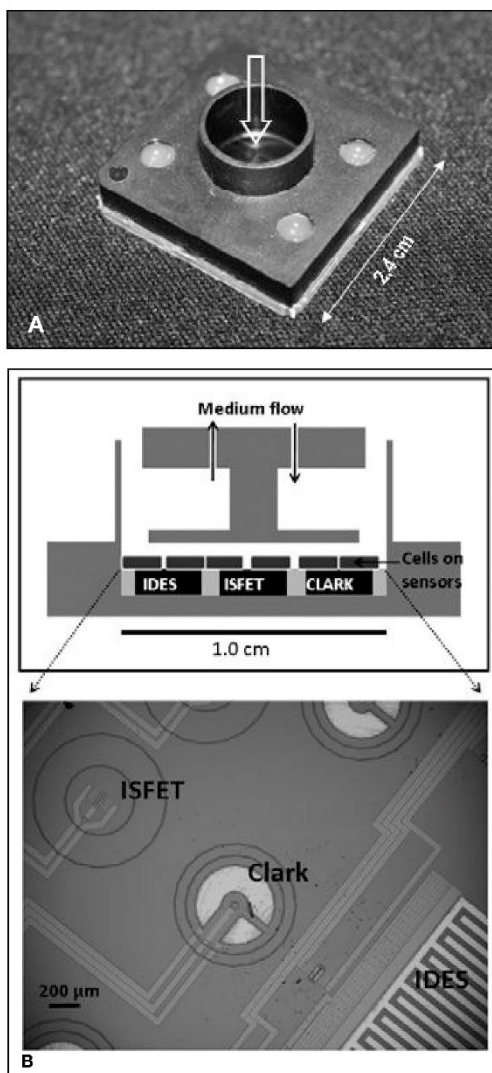


Fig. 1 - (A) Image of the metabolic chip SC 1000 (Bionas GmbH, Rostock, Germany; Canon 350D). The cell culture surface (arrow) of the chip is 70.88 mm². A scheme of the chip and a magnification of the surface are shown in **(B)**. This chip type is equipped with three sensor types to measure cell adhesion (interdigitated electrode structure sensors, IDEs), respiration (Clark type sensors), and acidification (ion-sensitive field effect transistor sensor, ISFET).

operating chamber was 37°C. Prior to the experiments, the metabolic chips SC 1000 used as controls were decontaminated with 70% ethanol and washed with phosphate buffer solution (PBS; PAA Laboratories GmbH, Pasching, Austria). In the Bionas[®] 2500 analyzing system, six measurement places work in parallel; therefore we can directly compare different surface treatments in the same experiment.

Plasma treatment

Amino functionalization was performed in a low-pressure plasma process reactor V55G (plasma finish, Schwedt, Germany, volume=60 l) in a two-step procedure: first, the chip surface was decontaminated and activated by pulsed oxygen plasma (500 W, 50 Pa, 100 sccm O₂/25 sccm Ar, 10 ms on/90 ms off, 30 s effective) and immediately coated by the plasma polymerization of the precursor allylamine (PPAAm) using a pulsed, low-pressure microwave plasma (2.45 GHz, 500 W, 50 Pa) for an effective treatment duration of 18 seconds (brutto 120 s, 300 ms on/1700 ms off, PPAAm nanolayer thickness d≤50 nm) (13, 14, 18, 19, 23). Allylamine was fed from a liquid handling system (50 sccm allylamine), which was carefully purified from air by evacuating and purging with N₂ prior to use. Argon was applied as carrier gas (50 sccm Ar). The substrate was located 9 cm below the coupling window in a downstream plasma position.

Surface characterization

Film thickness and stability in water

A silicon wafer was partially coated with cellulose acetate before plasma deposition. After coating with plasma polymer, the cellulose acetate film was removed, taking along the plasma polymer situated thereon. This was measured with a surface profiler Dektak3ST (Veeco, Santa Barbara, CA, USA). The stylus had a tip radius of 2.5 μm. The layer thickness was measured as the difference between the average of 25 points before and after this step. The stability of the PPAAm coatings in water (14) was proved by sonication in the ultrasonic bath Transsonic T570H (Elma, Singen, Germany) with a radio frequency of 35 kHz for 10 minutes. XPS spectra were applied before and after sonication to investigate chemical alterations.

X-ray Photoelectron Spectroscopy (XPS)

The elemental chemical surface composition and chemical binding properties of the surfaces were determined by high resolution scanning X-ray photoelectron spectroscopy (XPS). The XPS (Kratos Axis Ultra, Manchester, UK) ran with the monochromatic Al K_α line at 1486 eV (150 W). Charge neutralization was implemented. C1s, O1s, N1s, and Si2p spectra were recorded at pass energy of 80 eV for the quantification of the chemical surface composition, or 10 eV for highly resolved peaks. The C-C/C-H component of the C1s peak was adjusted to 285 eV (24). A chemical derivatization technique for the determination of amino groups was applied to label the amino groups for detection since these groups do not lead to significant shifts in the binding energy of the N1s electrons. Amino groups were reacted with 4-trifluoromethylbenzaldehyde (TFBA; Sigma-Aldrich, Taufkirchen, Germany) at 40°C for 2 hours in a saturated gas phase. Three fluorine atoms mark one primary amino group.

Fourier Transform Infrared Spectroscopy (FT-IR)

The chemical composition of the PPAAm films was further analyzed by means of infrared absorption spectra taken with the help of the diamond attenuated total reflectance unit (ATR) of an FT-IR spectrometer (Spectrum One; Perkin-Elmer, Rodgau-Jügesheim, Germany). In this case, Au-sputtered polystyrene samples were used to improve sensitivity (14).

Zeta-potential

Surface charges were estimated on the basis of the zeta-potential by determining the streaming potential dependent on the pressure with an Electrokinetic Analyzer (A. Paar, Ostfildern, Germany). Subsequently the zeta-potential was calculated according to the method of Fairbrother and Mastin (25). The measurements were performed in 0.001 M KCl solution at pH 6.0.

Water contact angle, surface energy

Contact angle and surface energy of native and treated sensor chip surfaces were ascertained by the sessile drop method using the contact angle measuring system OCA 30 (Data Physics Instruments GmbH, Filderstadt, Germany).

The determination of the angle between the solid surface and the tangent of the drop was performed by computer control. The polar and disperse parts of the surface free energy were calculated from measurements of contact angles with different liquids such as water, ethylene glycol, and methylene iodide. The calculation of the surface free energy (software SCA20) was made using the methods of Owens and Wendt (26).

Cell culture

The human osteoblast cell line MG-63 (ATCC, CRL-1427; LGC Promochem, Wesel, Germany) was used for all experiments. Before seeding onto the sensor chips cells were cultured in Dulbecco's modified Eagle medium (DMEM) with 10% fetal calf serum (FCS Gold; PAA Laboratories GmbH, Pasching, Austria), and 1% gentamicin (Ratiopharm GmbH, Ulm, Germany) at 37°C in a humidified atmosphere with 5% CO₂. Cells were seeded onto each sensor chip with a density of 6x10⁴ cells/chip and allowed to adhere for 1 hour at 37°C and 5% CO₂ in DMEM with 0.1% FCS before starting the experiments. The cell culture surface of the chip is 70.88 mm². Measurements of adhesion and cell metabolism were performed in DMEM + 0.1% FCS but without NaHCO₃, because this non-buffered medium was required for acidification measurements. Therefore DMEM powder (Invitrogen, Carlsbad, CA, USA) was solubilized in Water for Injection purposes (Aqua ad iniectionem; Baxter, Unterschleißheim, Germany) and supplemented with 0.1% FCS and 1.0% gentamicin (Ratiopharm GmbH, Ulm, Germany). The pH value was set at 7.2 and the osmolality was 270-340 mOsmol/kg. Finally the medium was sterile filtered.

Continuous measurements of adhesion and metabolism

For cell adhesion measurements, the metabolic chips SC 1000 (total area of the cell culture surface=70.88 mm²) were equipped with IDES sensors (Fig. 1B). For this purpose, impedance measurements were used to detect insulating cell membranes near the measuring electrodes. The cell culture surface of the IDES-sensor is 29 mm², with a finger width and interfinger space of 50 μm each (22, 27, 28). Cell adhesion was calculated using the raw values of capacitance (nF) obtained with the IDES sensors. The empty, cell-free chip (ca. 47 nF) was referred to as 0% ad-

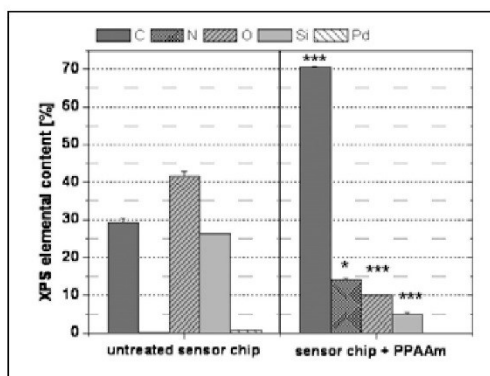


Fig. 2 - Elemental composition of an untreated and PPAAm coated sensor chip determined by XPS ($n=3$, Student's t -test, $***p<0.001$, $^*p<0.05$). The thin PPAAm film covered the sensor chip surface; only about 5% of Si can be detected after plasma polymerization with allylamine. The film thickness of PPAAm is smaller than 10 nm, the detection depth of the XPS.

hesion; 0 nF corresponds to 100% adhesion.

The metabolic activity was assessed by respiration (Clark type sensor) and acidification (ISFET) measurements. The details were described earlier (22, 28). Briefly, the accumulation of metabolic products, e.g., lactate leads to a decrease in the pH-value of the medium. When fresh medium is supplied, the pH-value rises again. This creates characteristic peaks and the slope of the curve represents the acidification rate. The respiration rate was calculated analogously. For further processing of the values, Microsoft Excel software (Microsoft® Office 2007) was used. To evaluate the ISFET sensor sensibility after the coating process with PPAAm, we tested the system with empty, cell-free chips using the cell culture medium with differing pH values: DMEM with 0.1% FCS but without NaHCO_3 was adjusted to pH 7.0 and pH 8.0, using 6 M NaCl or 10 M NaOH (Zentralapotheke University Rostock, Rostock, Germany). Then, the medium was changed every 10 minutes from pH 8.0 to pH 7.0, and finally to pH 8.0.

Scanning electron microscopy (SEM)

Cells were cultivated on the chip surfaces for 4 hours, washed with PBS and fixed with 2.5% glutaraldehyde. Afterwards, cells were dehydrated through a graded series of acetone (30% 5 min, 50% 5 min, 75% 10 min, 90%

10 min, and 100% 2x 10 min) and dried in a critical point dryer (K850; EMITECH, Taunusstein, Germany). Gold sputtering was performed with the coater (SCD 004; BAL-TEC, Leica Microsystems, Welzlar, Germany). Images were obtained with the scanning electron microscope SEM DSM 960A (Carl Zeiss, Oberkochen, Germany).

The cell areas (in μm^2) of osteoblasts were calculated using the ImageTool software (Windows Vers. 3.0, The University of Texas Health Science Center, San Diego).

Statistics

Statistical analyses were performed with the software SPSS Vers. 15.0 for Windows (SPSS Inc., Chicago, IL, USA) using the Student's t -test and Mann-Whitney-U-Test. Data were presented as a mean (\pm standard deviation); a probability value of $p<0.05$ was considered significant.

RESULTS

Surface characterization

Due to plasma treatment a very thin, adherent, cross-linked PPAAm film, which is resistant to hydrolysis and delamination and equipped with a sufficient density of positively charged amino groups (13, 14, 18, 19) could be deposited. Therefore, it is of value to characterize the film properties in more detail. In the present case, coatings were selected not only for high stability in aqueous environments but also with an adequate, very thin layer for the investigation of the metabolic activity of MG-63 cells on sensor chips. The film thickness was approximately determined to be about <10 nm. This is slightly weaker than the analysis depth of XPS. XPS revealed the C, O, and N content of the coating as well as Si from the substrate (Fig. 2). The element ratio N/C of about 20% ($N=14\%$) does not reach the theoretical N/C ratio of the monomer allylamine $\text{H}_2\text{C}=\text{CH}-\text{CH}_2-\text{NH}_2$ ($N/C=33.3\%$; $N=25\%$). Oxygen is not a constituent of the monomer. Its existence is most probably a consequence of free radicals in the coating, which can react with oxygen after air contact. O/C is relatively high at 14% ($O=10\%$), some oxygen from the SiO_2 chip surface, and Si/C at 7% ($\text{Si}=5\%$). These values can be explained by the short duration of treatment and consequential small film thickness <10 nm. The $-\text{NH}_2/\text{C}$ ratio is about

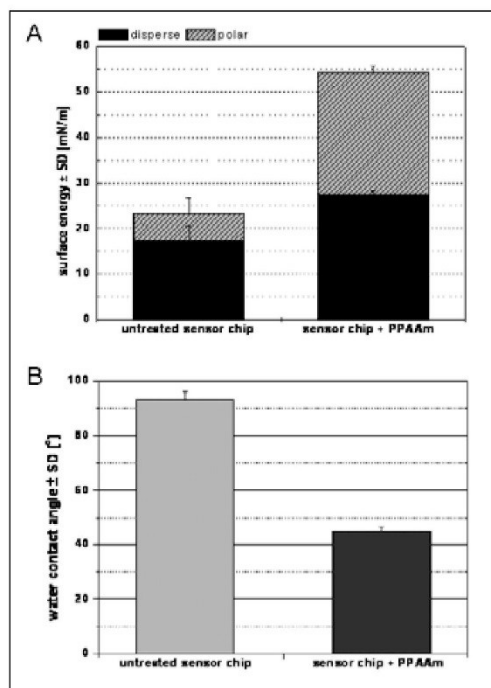


Fig. 3 - Surface energy (A) and water contact angle (B) of the untreated and PPAAm coated sensor chip surface ($n=2$). Note the tendency to an enhanced surface energy (dispersed and polar part) and a reduced water contact angle (i.e., higher hydrophilicity) on PPAAm.

2%, which is relatively low compared to the maximum value of 18% reported for a special radio frequency-plasma (29). This is a consequence of the cross-linking of the precursors and formation of different amines, amides, and nitriles, as demonstrated in (14) by FT-IR analyses. Therefore, some oxygen is found in the coating. The amount of oxygen increases only marginally after sonication in water (15); no hydrolysis or delamination occurred, verifying a stable plasma polymer film in aqueous media (30).

The PPAAm film showed a positive zeta-potential (14 mV), whereas pure glass surfaces were negatively charged (-44 mV) (17). Contact angle measurements (Fig. 3) demonstrated a medium hydrophilic surface advantageous for cell adhesion (31). PPAAm surfaces on sensor

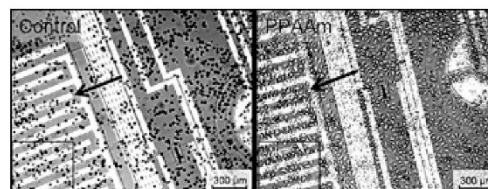


Fig. 4 - MG-63 osteoblasts were cultivated on the chip surface for 1 h before the start of the experiment and monitored with the light microscope (Olympus). The arrows point to the IDES sensors on the chips. The growth density was adjusted to nearly 80% on the PPAAm surface at the start of the experiment. Calculation of areas covered by cells revealed a density of 34.9% on untreated and 72.4% on PPAAm sensor chips (gates).

chips have a water contact angle value of about $45^\circ \pm 1.4$. Correspondingly, the surface energy of PPAAm on sensor chips is strongly enhanced, both the dispersed and polar part, in comparison with the untreated sensor surface (Fig. 3).

PPAAm did not interfere with the sensor output

All sensors of the chip: 1x IDES, 2x Clark and 5x ISFET performed well and transmitted a signal after PPAAm functionalization. Moreover, the values of the sensors in the empty, cell-free state were not changed by plasma modification. The capacitance values were measured prior to and after plasma-modification with allylamine. The measurements revealed that the IDES values remained unchanged (Tab. I). Measurements with cell culture medium with differing pH values showed that the ISFET sensors after PPAAm modification still reacted to the change of pH; the resulting differences of the slope were nearly the same with steps of the gate-source-voltage of 0.1 V.

PPAAm enhances continuous cell adhesion

Human osteoblast-like MG-63 cells were cultivated on the Bionas[®] SC 1000 chip for 1 hour before the measurement was started. We were able to observe on the light-microscopic images that already after the short time span of one hour, the coverage by cells was notably higher on the PPAAm functionalized sensor surface (Fig. 4). However, it was not possible to start the experiment directly after seeding the cells due to the fact that the medium flow

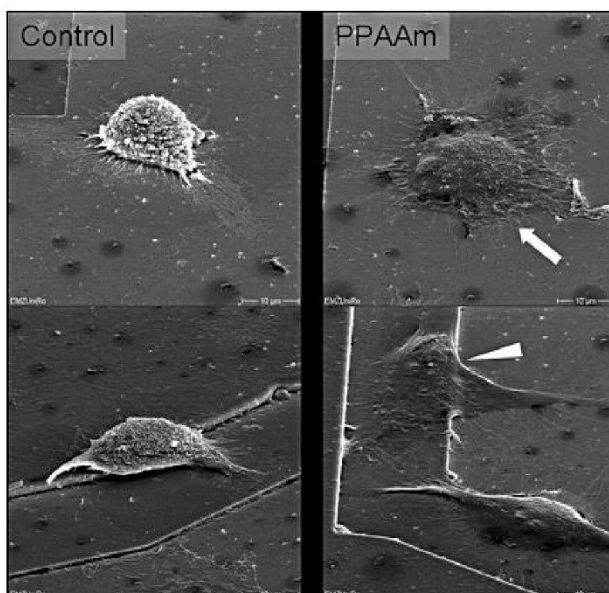


Fig. 5 - SEM images of human MG-63 osteoblasts on untreated (left) and on PPAAm biofunctionalized (right) sensor chips at $t=4$ h. Notice that plasma coating (PPAAm) results not only in an accelerated spreading behavior (arrow) but also allows the cells to literally melt with the relief of the chip surface (arrowhead). DSM 960A, Carl Zeiss, $\times 2,000$, 10 kV, 45° .

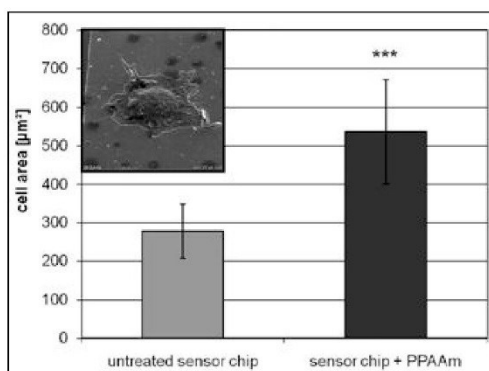


Fig. 6 - The cell area at $t=4$ h is significantly elevated (nearly 1.9-fold) on a PPAAm coated sensor chip (control: $n=7$ cells; PPAAm: $n=8$ cells; Mann-Whitney-U-Test, $p \leq 0.05$). Data (in μm^2) were obtained from SEM images (DSM 960A, Carl Zeiss) see Fig. 5 and analyzed with the ImageTool software (insert).

in the chamber would wash away all cells in the solution. Under one hour in duration, not enough cells were attached to the control surface, so continuous measurement could only begin 1 hour after cell seeding. The growth den-

sity was adjusted to nearly 80% on the plasma modified surfaces at the start of the experiment. Therefore further spreading and cell division over the longer measurement period (24 h) was possible. SEM images of MG-63 cells on the SC 1000 chip surface 4 hours after cell seeding demonstrate the increased spreading behavior on PPAAm (Fig. 5). One can see that the osteoblasts demonstrate an extremely flattened phenotype on sensor chips with PPAAm compared to the untreated sensor chip surface already after this short contact time. Cell area at this time point of 4 hours is significantly elevated (nearly 1.9-fold) on PPAAm coated sensor chips (Fig. 6).

Adhesion was calculated using measurements of capacitance (nF). The cell-free chip was referred to as 0% adhesion; 0 nF corresponds to 100% adhesion. Continuous adhesion measurements (Fig. 7) reveal that osteoblast attachment is highly, and significantly, increased in the first adhesion phase on the chip surface with PPAAm although the same number of cells (6×10^4) was seeded onto all surfaces (2 h: 2.31 times, 4 h: 2.08 times, 6 h: 2.11 times, 8 h: 2.10 times that of the untreated control). After 24 hours the cell adhesion (capacitance measurement) was still 1.95 times higher on PPAAm modified surfaces (significance

Rebl et al

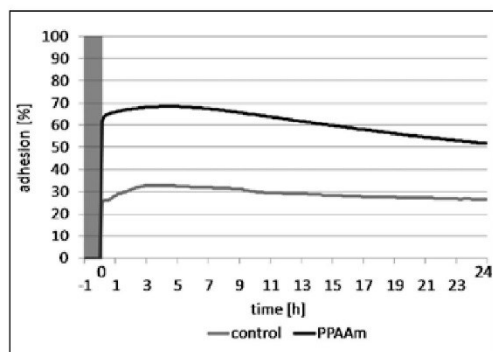


Fig. 7 - Continuous adhesion measurement of vital human MG-63 cells on IDES sensors of chip SC 1000. Before the start, cells were allowed to adhere for 1 h on the chips (gray area). Start of the capacitance measurements (nF) was defined as 0 h. The empty chip was referred to as 0% adhesion; 0 nF corresponds to 100% adhesion. Note that the adhesion, i.e., the grade of surface coverage, is significantly higher on PPAAm at every time point compared to controls ($n=4$, Student's *t*-test, $p \leq 0.05$).

$p \leq 0.05$). We can assume that for periods longer than 24 hours as well, cells on PPAAm are at a growth advantage compared to cells on untreated surfaces. In two experiments with an analyzing time of 40 hours, using a thicker PPAAm layer ($d \sim 50$ nm), we could observe that cell adhesion was increased by nearly 40% and remained higher throughout the entire measurement time (data not shown).

PPAAm did not influence cell metabolic activity

The time-dependent measurement of the metabolic activity of the osteoblasts reveals that the acidification (Fig. 8A) and oxygen consumption (Fig. 8B) are not significantly different on PPAAm compared to the control chip surface at every time point, and they reach a steady state. The first decrease in oxygen consumption between start (0 h) and 2 hours occurs due to the adjustment of the cell-medium-system to the conditions in the operating chamber.

Generally, cell metabolism is stable although the adhesion of the vital human osteoblasts is significantly enhanced on plasma functionalized allylamine surfaces and the cells seem to be more active in spreading.

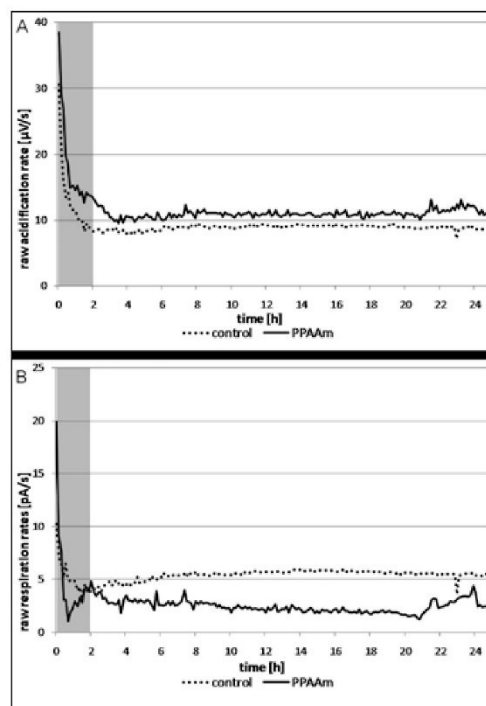


Fig. 8 - Measurements of cell metabolic activity for 24 h on PPAAm modified sensor chip surfaces compared to the controls: acidification (A) and oxygen consumption (B). No significant differences can be observed over the whole time period ($n=4$, Student's *t*-test). Note that the first decrease (grey area) occurs due to the adjustment of the cell-medium-system to the conditions in the operating chamber.

DISCUSSION

The use of biochips is common for the testing of potential drugs or the determination of the correct dosage. The preminent advantage is that cellular effects can be monitored noninvasively for different parameters and on-line over a long period of time. Cell-based assays are more expensive, often require a larger number of cells, are time consuming and seldom provide information about the dynamics of the cells. Nonetheless, they do yield more detailed information. Chip-based assays are therefore a good

means to gain general information about the behavior of a living cellular system and enable the determination of reasonable time points for more precise testing methods (20, 32). The *in vitro* method introduced here is not intended to replace specific analyzing methods for gaining insights into the synthetic activities of differentiated osteoblastic cells producing collagen I, bone sialoprotein and calcium phosphate ions, for example, or, likewise proteins accompanying cell cycle phases. Instead, it is designed especially for vital cell analysis to get additional long-term information for these specific parameters regarding adhesion and metabolism. Although not introduced here, it is possible to observe cell reaction immediately after the addition of substances to the medium flow (22). Thus, one can observe the vital cell behavior on a functionalized chip surface in combination with growth stimulating factors, for example.

Surface functionalization with positively charged NH_2 groups is known to enhance cell adhesion. Faucheux et al describe that NH_2 end groups outperform CH_3 or OH end groups on self-assembled monolayers in terms of cell attachment and spreading (3). However, these conclusions were drawn from results collected at distinct time points. In this paper we present for the first time a method by which cell adhesion can be recorded continuously on a plasmachemically-modified surface. This offers new possibilities for the characterization of innovative surface modifications. We were able to show that plasma modification does not destroy the sensors or alter the capacitance values recorded with untreated, cell-free chips.

Continuous adhesion measurements reveal that osteoblast attachment is highly increased in the first adhesion phase on the chip surface with PPAAm (nearly 2-fold compared to the control). This correlates with our previous results, where we showed that cell spreading is significantly enhanced on PPAAm at distinct time points (13, 14). This plasma treatment is an ideal tool for functionalizing biomaterial surfaces with desired properties.

The spreading data in our experiments on the PPAAm coated chips can be correlated with the impedance values: on the untreated control, the spreading data reveal 35% cell coverage and an impedance measurement of 25%. On the PPAAm coated surface, the spreading values indicate a cell area of 72% and the impedance measurement has a value of 62%.

Gaining full insight into the progression of cell adhesion is, nevertheless, very time consuming. Our new approach is a simple and fast means of tracking cell adhesion on

plasma-modified surfaces over a longer time span.

A precondition for the use of the BIONAS® sensor chips in biocompatibility investigations is the intact sensor function after the surface modification, regardless of what is used for the coating (e.g., plasma activation, protein layer of matrix molecules, chemical groups, spacer for additional binding such as PEG DA). We therefore tested the sensitivity of the sensor function in empty, cell-free chips. All sensors – IDES, ISFET and Clark – were still active after plasma functionalization (for IDES, see Tab. I). This test should be done prior to each study concerning the influence of each study concerning the influence of surface coatings on cell metabolic and adhesion function.

Sarravia and Toca-Herrera (33) used the combination of quartz crystal microbalance with dissipation (QCM-D) and atomic force microscopy (AFM) to study online the adhesion process of hepatoma cells. However, these methods require expensive equipment, a long period of training and, finally, interpretation of the data might turn out to be very complicated. The authors admit that for some measured values there is not yet a theoretical model to correlate the changes measured by QCM-D with cell response, although it is stated that they are proportional to cell-surface contact area. This makes the interpretation of the data quite difficult. However, parameters like elastic modulus or cell height give a clearer understanding of cell behavior on the modified substrates. After 24 hours, the difference in increase of the capacitance between the control and the plasma functionalized PPAAm surface is minor but still significant. This might be due to the fact that cells have to detach in order to migrate over the surface. Common cellular properties like proliferation and cell migration require a “loose” bonding of the cell to the substrate (34). We could show that our human MG-63 osteoblasts have a higher migration potential on PPAAm than on untreated surfaces. Cells are highly motile after 48 hours on PPAAm compared to untreated titanium surfaces (17). This indicates that the improvement of the early adhesion phases, as shown by higher adhesion and spreading values due to amino functionalization of the surfaces, strongly influences subsequent cell responses.

Measuring the *metabolic activity*, the acidification rate of MG-63 is slightly, but not significantly, increased on PPAAm. This may indicate a slightly higher activity level of the cells, resulting in an increase in metabolic products, such as lactate or CO in the surrounding medium (22). However, the respiration rate of the cells is slightly decreased on

PPAAm-surfaces. These minor changes in metabolic activity are not significant over the whole 24-hour time span, indicating that the osteoblasts are not stressed on the PPAAm-surface and the nano-scaled layer of PPAAm is stable and not cytotoxic. On the other hand, we can also speculate that our MG-63 cells will be supported in their adhesion and spreading activities by the surface charges due to PPAAm but without disturbing, affecting or stimulating the metabolic activity.

Strikingly, we found that the morphology of osteoblasts demonstrates an extremely flattened phenotype on allylamine-modified surfaces and the cells seem to merge with the sensor relief of the surface. Other groups also found that surfaces equipped with NH_2 groups enhance cell attachment, spreading and growth. Morphological analyses of cells on the surfaces displayed extensive cell spreading, indicating good cell-contacting properties (3, 15, 16). This close surface contact of cells due to positively charged amino groups could indicate a strong cell-material-interaction.

CONCLUSIONS

Plasma treatment of sensor chip surfaces with resulting positively charged amino groups continuously enhances time-dependent adhesion of vital human osteoblasts. Nevertheless, the metabolic activity, i.e., the acidification and the oxygen consumption, on PPAAm is equal to control surfaces. This indicates a significant improvement in cell adhesion without affecting cell metabolism. Furthermore, the flattened cell morphology and the close surface contact of the MG-63 osteoblasts after only a short time of cultivation implies an increase in the bone-bonding ability of plasma-biofunctionalized material surfaces. The method introduced here, using metabolic and adhesion sensor chips, appears suitable for the evaluation of the behavior of vital, adherent cells after plasma-chemical surface treatment.

NOMENCLATURE

Ar	argon
ATR	attenuated total reflection
IDES	interdigitated electrode structure
ISFET	ion-sensitive field effect transistor
PPAAm	plasma polymerized allylamine

RF	radio frequency
SEM	scanning electron microscopy
sccm	standard cubic centimeter
XPS	X-ray photoelectron spectroscopy
1s	1s atomic orbital
2p	2p atomic orbital

ACKNOWLEDGEMENTS

We kindly thank Prof. Dr. J. Gimsa (University of Rostock) for providing the Bionas® 2500 analyzing system. We are thankful to Drs. S. Drechsler and A. Kob (Bionas) for technical support and discussion. The authors thank their technicians U. Kellner, M. Brüser, U. Lindemann and G. Friedrichs (all INP Greifswald) for excellent assistance. We acknowledge the technical support of the electron microscopy center (EMZ, Medical Faculty, Dr. M. Laue) of the University of Rostock.

Financial support: The authors are grateful to the German Ministry of Education and Research (BMBF, grant no. 13N9779) for financial support as part of the Campus PlasmaMed, Plasmalmp project.

Conflict of interest statement: The authors do not have proprietary interests and disclose any financial arrangement with a company.

Meeting presentation: Some of the data have been presented (poster) at the third international congress "Interface Biology of Implants" (IBI) in Rostock-Warnemuende, Germany in May 2009.

Address for correspondence:

PD Dr. J. Barbara Nebe
University of Rostock, Medical Faculty, BMFZ, Dept. of Cell Biology
Schillingallee 69
D-18057 Rostock, Germany
e-mail: barbara.nebe@med.uni-rostock.de

REFERENCES

- Hildebrand HF, Nebe JB, San Roman J, Amedee J. Editorial, Surface functionalization and activation of biomaterials. *Biomol Eng* 2007; 24: 423-42.
- Faucheaux N, Schweiss R, Lutzow K, Werner C, Groth T. Self-assembled monolayers with different terminating group as model substrates for cell adhesion studies. *Biomaterials* 2004; 25: 2721-30.

Metabolic activity and plasma polymer

3. Petrie TA, Raynor JE, Reyes CD, Burns KL, Collard DM, Garcia AJ. The effect of integrin-specific bioactive coatings on tissue healing and implant osseointegration. *Biomaterials* 2008; 29: 2849-57.
4. Nebe JB, Mueller L, Luethen F, et al. Osteoblastic adhesion and function response to biomimetically altered titanium surfaces. *Acta Biomater* 2008; 4: 1985-95.
5. Schuler M, Owen GR, Hamilton DW, et al. Biomimetic modification of titanium dental implant model surfaces using the RGDSP-peptide sequence: a cell morphology study. *Biomaterials* 2006; 27: 4003-15.
6. Petrie TA, Capadona JR, Reyes CD, Garcia AJ. Integrin specificity and enhanced cellular activities associated with surfaces presenting a recombinant fibronectin fragment compared to RGD supports. *Biomaterials* 2006; 27: 5459-70.
7. Morra M, Cassinelli C, Cascardo G, et al. Surface engineering of titanium by collagen immobilization. Surface characterization and in vitro and in vivo studies. *Biomaterials* 2003; 24: 4639-54.
8. Narayanan R, Seshadri SK, Kwon TY, Kim KH. Calcium phosphate-based coatings on titanium and its alloys. *J Biomed Mater Res B Appl Biomater* 2008; 85: 279-99.
9. Wojtowicz AM, Shekaran A, Oest ME, et al. Coating of biomaterial scaffolds with the collagen-mimetic peptide GFOGER for bone defect repair. *Biomaterials* 2010; 31: 2574-82.
10. Willumeit R, Schuster A, Iliev P, et al. Phospholipids as implant coatings. *J Mater Sci Mater Med* 2007; 18: 367-80.
11. Faucheux N, Tzoneva R, Nagel MD, Groth T. The dependence of fibrillar adhesions in human fibroblasts on substratum chemistry. *Biomaterials* 2006; 27: 234-45.
12. Schweikl H, Müller R, Englert C, et al. Proliferation of osteoblasts and fibroblasts on model surfaces of varying roughness and surface chemistry. *J Mater Sci Mater Med* 2007; 18: 1895-1905.
13. Nebe JB, Finke B, Lüthen F, et al. Improved initial osteoblast's functions on amino-functionalized titanium surfaces. *Biomol Eng* 2007; 24: 447-54.
14. Finke B, Lüthen F, Schröder K, et al. The effect of positively charged plasma polymerization on initial osteoblastic focal adhesion on titanium surfaces. *Biomaterials* 2007; 28: 4521-34.
15. Hamerli P, Weigel T, Groth T, Paul D. Surface properties of and cell adhesion onto allylamine-plasma-coated polyethylene terephthalat membranes. *Biomaterials* 2003; 24: 3989-99.
16. Ren TB, Weigel T, Groth T, Lendlein A. Microwave plasma surface modification of silicone elastomer with Allylamine for improvement of biocompatibility. *J Biomed Mater Res* 2008; 86A: 209-19.
17. Rebl H, Finke B, Ihrke R, et al. Positively charged material surfaces generated by plasma polymerized allylamine enhance vinculin mobility in vital human osteoblasts. *Adv Mater* DOI: 10.1002/adbi.200900070.
18. Schroeder K, Finke B, Polak M, et al. Gas discharge plasma-assisted functionalizations of titanium implant surfaces. *Mater Sci Forum* 2010; 638-42: 700-5.
19. Finke B, Schröder K, Jesswein H, et al. Thin aminofunctional coatings improve early stage of cellular response to titanium in vitro and in vivo. *Biomaterialien* 2009; 10 (S1): 64.
20. Becker B, Eitzbach S, Schmidhuber M, et al. Real-time screening system using living cells for chemosensitivity testing. *Eurocon 2009: International IEEE conference devoted to the 150 anniversary of Alexander S. Popov, 2009; 1-4 proceedings: 87-93.*
21. Wiest J, Brischwein M, Ressler J, Otto AM, Grothe H, Wolf B. Cellular assays with multiparametric bioelectronic sensor chips. *Chimia (Aarau)* 2005; 59: 243-6.
22. Thedinga E, Kob A, Holst H, et al. Online monitoring of cell metabolism for studying pharmacodynamic effects. *Toxicol Appl Pharmacol* 2007; 220: 33-44.
23. Ohl A, Schröder K. Plasma assisted surface modification of biointerfaces. In: Hippler R, Kersten H, Schmidt M, Schoenbach KH (eds). *Low temperature plasma physics*. Berlin: VCH Wiley; 2008. p 803-19.
24. Beamson G, Briggs D. *The scientia ESCA 300 database*. New York, NY: Wiley J & Sons; 1992.
25. Fairbrother H, Mastin J. *Studies in electro-endosmosis*. *J Chem Soc* 1924; 75: 2318.
26. Owens DK, Wendt RC. Estimation of the surface free energy of polymers. *J Appl Polym Sci* 1969; 13: 1741-7.
27. Thedinga E, Ullrich A, Drechsler S, et al. In vitro system for the prediction of hepatotoxic effects in primary hepatocytes. *ALTEX* 2007; 24: 22-34.
28. Ehret R, Baumann W, Brischwein M, Schwinde A, Wolf B. On-line control of cellular adhesion with impedance measurements using interdigitated electrode structures. *Med Biol Eng Comput* 1998; 36: 365-70.
29. Friedrich J, Kühn G, Mix R, et al. Polymer surface modification with monofunctional groups of variable types and densities. *J Adhes Sci Technol* 2003; 17: 1591-1617.
30. Schröder K, Finke B, Ohl A, et al. Capability of Differently Charged Plasma Polymer Coatings for Control of Tissue Interactions with Titanium Surfaces. *J Adhes Sci Technol* 2010; 24: 1191-1205.
31. van Wachem PB, Beugeling T, Feijen J, et al. Interaction of cultured human endothelial cells with polymeric surfaces of different wettabilities. *Biomaterials* 1985; 6: 403-8.
32. Ceriotti L, Kob A, Drechsler S, et al. Online monitoring of BALB/3T3 metabolism and adhesion with multiparametric chip-based system. *Anal Biochem* 2007; 371: 92-104.
33. Saravia V, Toca-Herrera JL. Substrate influence on cell shape and cell mechanics: HepG2 cells spread on positively charged surfaces. *Microsc Res Tech* 2009; 72: 957-64.
34. Cox E, Huttenlocher A. Regulation of integrin-mediated adhesion during cell migration. *Microsc Res Tech* 1998; 43: 412-9.

2.2 Study II

Henrike Rebl, Birgit Finke, Joachim Rychly, Karsten Schröder, J. Barbara Nebe

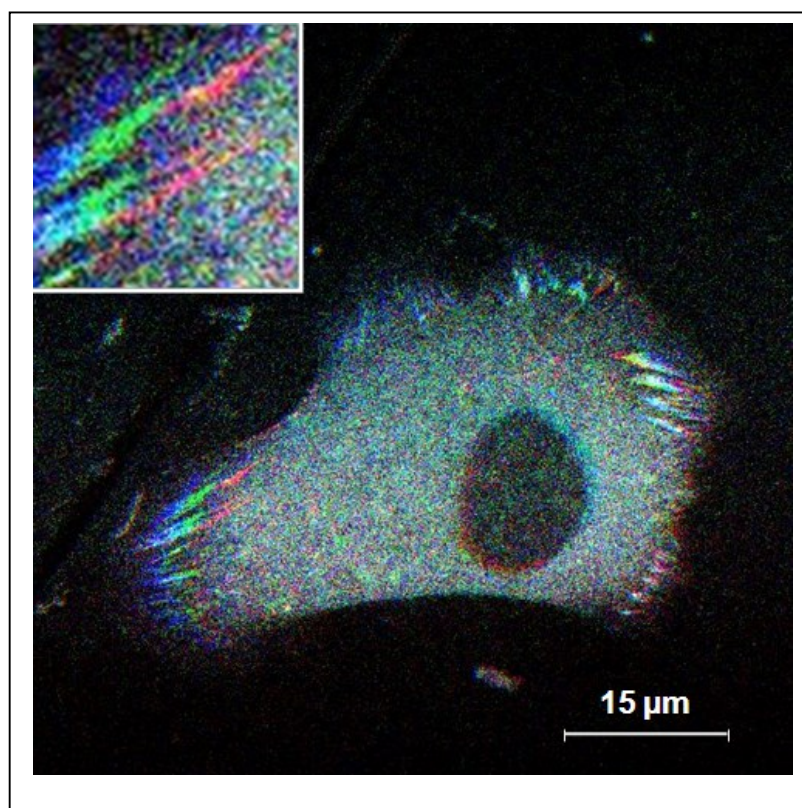
Positively charged material surfaces generated by plasma polymerized allylamine enhance vinculin mobility in vital human osteoblasts.

Advanced Biomat. 12 (2010) 356-364.

Abstract

The second article summarizes results of vinculin mobility analyses on the plasma polymer layer of allylamine. In living, GFP-vinculin transfected osteoblastic cells we determined a significant increase in vinculin mobility and vinculin contact length on PPAAm compared to collagen I coated surfaces during the initial adhesion phase. Cell migration was increased as observed by fibronectin-staining after 48h. The fibronectin “footprints”, and thus the distance the cells had moved, was much longer on surfaces coated with plasma-polymerized allylamine. Surface analyses of the PPAAm layer confirmed that the surface potential is positive, as it was hypothesized.

Graphical abstract:



DOI: 10.1002/adem.200980070

Positively Charged Material Surfaces Generated by Plasma Polymerized Allylamine Enhance Vinculin Mobility in Vital Human Osteoblasts**

By Henrike Rebl, Birgit Finke, Roland Ihrke, Holger Rothe, Joachim Rychly, Karsten Schroeder and Barbara J. Nebe*

Several studies suggest that the modification of an implant surface by chemical means plays an important role in bone tissue engineering. Previously we have shown that osteoblast cell adhesion and spreading can strongly be increased by a positively charged surface. Cell adhesion and migration are two vital processes that are completely dependent on coordinated formation of focal adhesions. Changes in the organization of the actin cytoskeleton and the focal adhesions are essential for numerous cellular processes including cell motility and tissue morphogenesis. We examined the mobility of the cytoskeletally associated protein vinculin on functionalized surfaces using plasma polymerized allylamine (PPAAm), a homogenous plasma polymer layer with randomly distributed amino groups. In living, GFP–vinculin transfected osteoblastic cells we determined a significant increase in vinculin mobility and vinculin contact length on PPAAm compared to collagen I coated surfaces during the initial adhesion phase. We suggest that positive charges control the cell physiology which seems to be dominant over the integrin receptor binding to collagen I. The results emphasize the role of the surface charge for the design of artificial scaffolds in bone repair.

[*] Dr. J. Barbara Nebe, H. Rebl, J. Rychly
Department of Cell Biology, Medical Faculty, University of Rostock, Biomedical Research Center Schillingallee 69, D-18057 Rostock, Germany
E-mail: barbara.nebe@med.uni-rostock.de, henrike.rebl@med.uni-rostock.de, joachim.rychly@med.uni-rostock.de
B. Finke, R. Ihrke, K. Schroeder
Leibniz-Institute for Plasma Science and Technology e.V. (INP) Felix-Hausdorff-Str. 2, D-17489 Greifswald, Germany
E-mail: finke@inp-greifswald.de, ihrke@inp-greifswald.de, schroeder@inp-greifswald.de
H. Rothe
Department of Biomaterials, Institute for Bioprocessing and Analytical Measurement Techniques (iba) e.V., Rosenhof, D-37308 Heilbad Heiligenstadt, Germany
E-mail: holger.rothe@iba-heiligenstadt.de

[**] Acknowledgements, H. R. and B. F. were sponsored with the kind support of the BMBF Germany Pilot Program Campus PlasmaMed (subproject Plasmalmp, 13N9775). The GFP–vinculin plasmid was kindly provided by B. Geiger, Rehovot, Israel. The authors thank their technicians U. Kellner, U. Lindenmann, and G. Friedrichs for excellent assistance.

The cellular integration of implants plays a decisive role for the clinical success. In the last decade a lot of strategies in chemical modifications have been introduced to improve the cell–material interaction at the interface of an implant material.^{11–41} The cell attachment to the implant surface via the adhesion receptors, named integrins, is a key step in this process. Therefore, immobilized proteins and peptides (e.g., type I collagen, RGD peptides) that function as ligands for integrins are commonly used to improve the biomaterial's interface since a decade of years.¹⁵ Cell adhesion and spreading via integrins is required for the outcome of an orthopedic implant and further for the induction of regeneration of the tissue.^{16,71} The intracellular adhesion components involved in these processes are the actin cytoskeleton and the actin associated proteins like vinculin, paxillin, and focal adhesion kinase (FAK)^{18–101} (scheme in Fig. 1).

By functionalizing the surface of the implant material titanium using positively charged amino groups, the cell-adhesive characteristics can be significantly improved, as our previous studies with plasma polymerized allylamine (PPAAm) have shown.^{111,121} In this context, adhesion and migration are vitally important for the immediate occupation of an implant surface by osteoblasts. We demonstrated earlier

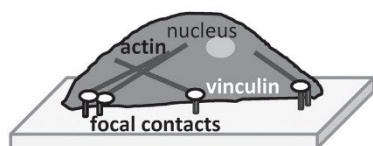


Fig. 1. Scheme of an adherent cell on the material surface. In principle, attachment is facilitated by the focal contacts which include integrins that bind extracellularly to ligands and are connected intracellularly to adapter proteins such as vinculin that bind to the actin cytoskeleton.

that MG-63 osteoblasts mediate the initial adhesion to a pure titanium surface by their pericellular hyaluronan matrix coat which facilitates a strong adhesion effect.^[13]

Hyaluronan is a large linear glycosaminoglycan (D-N-acetylglucosamine- β -D-glucuronic acid) of 10^6 – 10^7 Da, characterized by a highly negative charge due to the carboxyl group of the glucuronic acid and could therefore be responsible for the strong attachment of cells to positively charged surfaces.^[14] Hyaluronan is not only the first mediator of the initial adhesion which could also be demonstrated in epithelial cells,^[15] but is also responsible for the subsequent formation of the focal contact proteins paxillin, vinculin, and the activation of FAK. The formation and organization of these proteins in focal contacts of an adherent cell are the pre-condition for the integrin-mediated intracellular signaling via vinculin and the actin cytoskeleton.^[16,17]

Vinculin is an important intracellular adapter protein which is involved in the formation of focal adhesion (FA) complexes of adherent cells.^[18–20] FA contacts are of fundamental importance for attachment, survival, and growth of cells, since for adherent cells force transmission occurs exclusively at adhesion sites.^[21,22] It is known that these contacts, which enable the integrin signaling with the extracellular matrix, are not stationary.^[18,23] They move in order to enable the migration of cells and the formation of extracellular matrix. This migration is closely connected with the constant aggregation and separation of adhesion complexes, which demands a certain degree of mobility of the involved proteins.^[17,24] Our cellular investigations revealed an increase in the mobility of the vinculin contacts of osteoblasts on PPAAm-modified surfaces which may induce an increased cell spreading and enhanced cell migration.

This study highlights the role of dynamic cellular mechanisms, which can be controlled by positively charged carriers on implant surfaces and therefore contributes to an optimization of the fabrication of implants for bone regeneration.

Materials and Methods

Surface Functionalization

Plasma chemical modifications were carried out on glass surfaces because of the technical limitations of the confocal LSM with vital cells on opaque materials. The surfaces were functionalized with a thin layer of PPAAm. The method

has already been described in detail.^[11] Briefly, glass surfaces (Lab-Tek 4-well chambered cover glass, Nalge Nunc International) were decontaminated and activated by pulsed oxygen plasma (500 W, 50 Pa, 100 sccm O_2 /25 sccm Ar, 10 ms on/90 ms off, 15 s effective) and immediately coated by the plasma polymerization of the precursor allylamine (glass-PPAAm) using a pulsed low pressure microwave plasma (2.45 GHz, 500 W, 50 Pa, 50 sccm allylamine/50 sccm Ar, 300 ms on/1700 ms off, 144 s effective, plasma reactor V55G, Plasma Finish, Fig. 2).^[11,12,25,26] Cover glasses coated with collagen I (Col, rat, $20 \mu\text{g cm}^{-2}$, BD Biosciences) diluted to $200 \mu\text{g mL}^{-1}$ in 0.1% acetic acid (Mallinckrodt Baker) served as control (glass-Col). The Col solution was allowed to dry overnight under sterile conditions in the laminar flow box (LaminAir LB-48-C, Heraeus Med GmbH).

Surface Characterization

Water Contact Angle

The contact angle of native and treated glass surfaces was measured by the sessile drop method using the contact angle meter DIGIDROP (GBX Instrumentation Scientifique). The determination of the angle between the solid surface and the tangent of the drop was performed by computer control. Five measurements were performed on each surface, arithmetic means, and standard deviations were calculated with the software package Origin 6.1 (OriginLab).

XPS Analysis

The elemental surface composition and chemical binding properties of the glass surfaces were determined by high resolution scanning X-ray photoelectron spectroscopy (XPS) as previously described for titanium surfaces.^[11,12] Briefly, the Axis Ultra (Kratos) was run with the monochromatic Al K_{α} line at 1486 eV (150 W). Charge neutralization was implemented. Spectra were recorded at pass energy of 10 eV for highly resolved C1s and N1s peaks. The C–C/C–H component of the C1s spectrum was adjusted to 285.0 eV.^[27] C1s, O1s, N1s, and Si2p spectra were recorded at pass energy of 80 eV at three different sample positions for the quantification of surface composition. A chemical derivatization was applied for the quantification of amino groups, since amino groups do not lead to significant shifts in the binding energy of the C1s and N1s electrons. Amino groups were reacted with

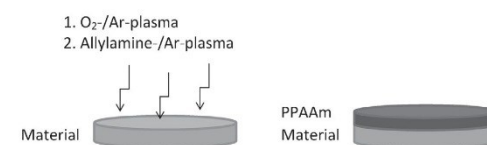


Fig. 2. Modification of material surfaces by amino functionalization. The material surface cleaned by oxygen plasma is coated with a PPAAm film (glass-PPAAm) of about ~ 50 nm thickness using pulsed low pressure microwave plasma (2.45 GHz, 960 s). Argon was used as carrier gas.

4-trifluoromethylbenzaldehyde (TFBA, Sigma–Aldrich) at 40 °C for 2 h in a saturated gas phase.

Zeta Potential

Zeta potential measurements were carried out by means of an Electrokinetic Analyzer (A. Paar KG). The measurements were performed in 0.001 M potassium chloride (KCl) solution at pH 6. A special borofloat glass B33 (10 mm × 20 mm) was used as substrate carrier.

Atomic Force Microscopy (AFM)

Surface roughness and film thickness were determined using the scanning probe microscope diCP2 (Veeco) in non-contact mode (cantilever MPP111, Veeco) with a tip radius of 10 nm before and after PPAAm film deposition as well as Col coating on silicon wafers (Universitywafers.com). The roughness R_a was calculated as the arithmetic average of measurements on a 4 μm × 4 μm wide area. For the determination of film thickness an uncoated stripe was prepared on a silicon wafer by masking with cellulose acetate, plasma- as well as Col-coating and removing the mask after the end of the process. The height of this trench was measured by AFM.

Cell Culture

The cultivation of human osteoblast like cells MG-63 (ATCC, CRL-1427) (passages 7–25) was done in 75 cm² bottles in Dulbecco's modified Eagle's medium (DMEM, Gibco) with 10% fetal calf serum (FCS Gold, PAA) and 1% gentamicin (Ratiopharm) at 37 °C with 5% CO₂.

Transfection

MG-63 cells were transfected with a green fluorescence protein (GFP)–vinculin construct (kindly provided by B. Geiger, Department of Molecular Cell Biology, Weizmann Institute of Science, Rehovot, Israel). For the transfection the cells were seeded (2 × 10⁴ cells overall) in a Petri dish

(Ø 3.5 cm) and transfected after 6 h of cultivation (Fig. 3). The transfection was done using the Effectene transfection reagent (Qiagen) according to the manufacturer's instructions as already described.^[28] We used 1 μg vector-DNA of GFP–vinculin for our osteoblasts in a mixture of 100 μL buffer, 6 μL enhancer, 6 μL effectene, and 600 μL serum-containing DMEM. A transfection efficiency of 30–40% was reached. After 24 h of culture the cells were detached with trypsin/EDTA (0.05% trypsin, 0.02% EDTA, Sigma) at 37 °C for 3 min and 1 × 10⁴ cells were disseminated on the various surfaces in serum-free medium. For these experiments serum-free medium was used to avoid masking of the positively charged amino groups.

Vinculin Mobility

For the microscopic analysis of the dynamics of vinculin-marked FAs, a confocal microscope (Leica TCS SP2 AOBS) equipped with an incubation chamber (TRZ 3700, Carl Zeiss) to maintain 37 °C and 5% CO₂ was used.

This method has already been described earlier.^[28] Single living cells were scanned in one optical plane and three images were recorded at intervals of 10 min (time points 0, 10, 20 min) in the time frame of 50–180 min after seeding the cells. To calculate the speed of the moving vinculin contacts, the images at the three time points were overlaid and the same contacts at different time points were visualized with different false colors [blue, green, red, Fig. 4(A)].

Analyses of the movement of vinculin in transfected MG-63 osteoblasts were done using the software UTHSCSA Image Tool 3.00 (University of Texas Health Science Center). For this analysis, the contacts at the three consecutive points in time of at least 17 cells per surface were evaluated, so that >500 contacts were measured for each material. To measure the distance that was covered by the contacts from time point 1 to 3, the total length for each contact in an overlay-image was measured and from this total length the mean length of a contact was subtracted [Fig. 4(B)]. The vinculin speed was obtained by dividing this value by the time of the measurement (i.e., 20 min) and expressed in nm min⁻¹.

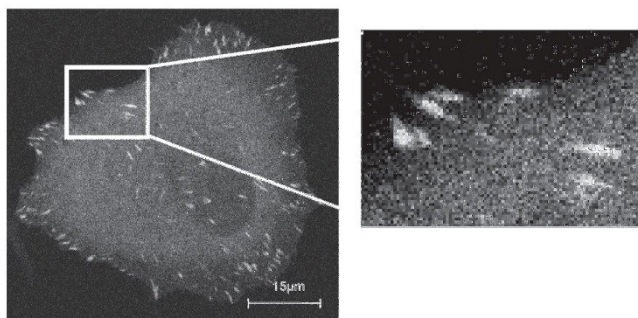


Fig. 3. GFP-labeled vinculin contacts of one MG-63 osteoblast on a Col coated surface (right: eight-fold magnification of the gate on the left, LSM 410).

Cell Migration

For migration analyses the cells were allowed to grow for 48 h on glass, glass-PPAAm, and glass-Col surfaces. Serum-free DMEM with 1% gentamicin was used to avoid masking of the amino groups on the surface. The cells were fixed with 4% PFA (10 min, Sigma), stained for 30 min with anti-fibronectin mAb (1:40, room temperature, Sigma) and labeled with anti-rabbit Cy3 mAb (1:100, at room temperature in the dark, Jackson Immuno Research) for further 30 min. The cells were then permeabilized with 0.1% Triton X-100 (10 min, room

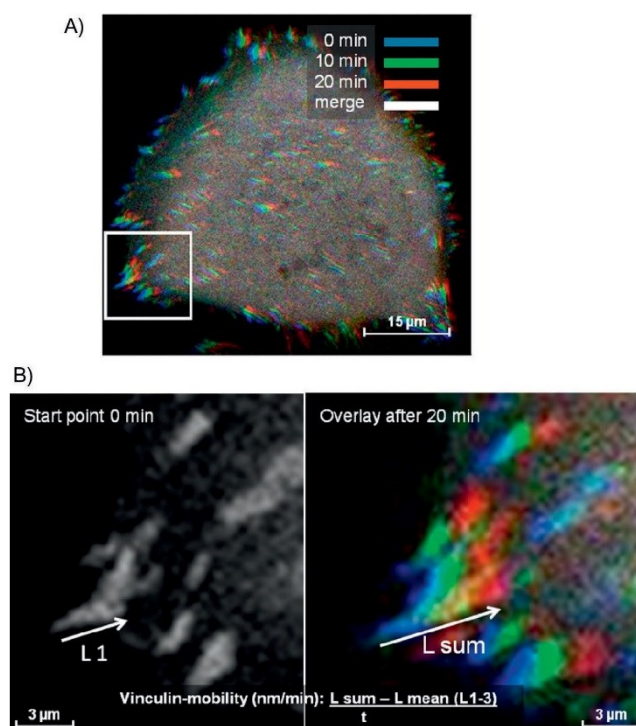


Fig. 4. Method to analyze vinculin mobility in MG-63 cells. (A) To calculate the speed of the moving vinculin contacts, the images at three time points (0, 10, 20 min) were overlaid and visualized with false colors in blue, green, and red (Leica TCS SP2 AOBBS). The frame is seen in the magnification in the next image. (B) To evaluate the distance that was covered by the vinculin contacts, the total length for each contact in an overlay image was measured and from this total length the mean contact length was subtracted.

temperature, Sigma) and the actin cytoskeleton was stained with BODIPY FL phalloidine (30 min, 1:40, room temperature, Molecular Probes). Finally the cells were embedded in mounting medium with a cover slip. The mounting medium was prepared using 30 g glycerine (Merck), 12 g polyvinylethanol (Sigma), 0.5 g phenol (Roth) in 30 mL aqua dest., and 60 mL of 0.1 M TRIS buffer solution at pH 8.5 (Roth). Briefly, glycerine, polyvinylethanol, and phenol were mixed for 12 h at room temperature. Then, TRIS was slowly added at 40–45 °C and finally, the mixture was stored at 4 °C in the dark. Cell and fibronectin area were measured with the tool “area measurement” (LSM 410 software, Carl Zeiss). The ratio of fibronectin area to cell area was calculated, so that a value of 1 represents equal size of fibronectin and cell size and a value >1 shows that fibronectin area is larger than cell area.

Microscopical Investigations

The BioStation IM (Nikon) was used to record “time lapse” images of living cells. The total recording time was 10 min. The

interval length was set to 20 s. Images were exported in the jpg format. The software ImageJ 1.41 (National Institute of Health) was used to measure the cell area.

The GFP-transfected osteoblasts were observed in a confocal microscope Leica TCS SP2 AOBBS equipped with an argon-ion laser (exc. 488 nm) and a 63× water objective (HCX OL APO CS 63.0 × 1.20 W corr).

Cell migration was analyzed with the inverted confocal laser scanning microscope LSM 410 (Carl Zeiss), equipped with an Ar-ion and He-Ne laser (excitation 488 nm for actin and 543 nm for fibronectin, respectively) and a 63× water objective (1.25/0.17, Carl Zeiss). The size of the images was 512 × 512 pixels.

Statistics

Statistical analyses were performed with the software SPSS Vers. 15.0 for Windows (SPSS Inc.) using Mann–Whitney U test. Data were presented as mean ± standard error of mean; (SEM) stand deviat (50) probability value of $p < 0.05$ considered as significant.

Results and Discussion

Plasma Functionalization with Allylamine Creates Positively Charged Surfaces due to Amino Groups

In order to evaluate the effect of positively charged amino groups on vinculin mobility, MG-63 osteoblasts were cultivated on surfaces which had been coated with thin PPAAm layers (Fig. 5). The PPAAm functionalization resulted in a higher hydrophilicity of the surface in comparison to the untreated glass but also to glass–Col. The water contact angle decreases from $\sim 65 \pm 0.8$ and $\sim 72 \pm 6$, respectively, to $\sim 50 \pm 1$ on glass–PPAAm [Fig. 6(A)] and seems to be optimal for cell responses.^[29]

In general, there is no difference in cell viability (MG-63) after 24 h as well as 3 d on glass–PPAAm compared to glass–Col surfaces (data not shown).

Zeta potential measurements verified a positive surface charge on glass–PPAAm (14 mV) whereas pure glass (−44 mV) as well as glass–Col (−3 mV) were negatively charged [Fig. 6(B)]. The nano-scaled roughness R_a was determined on a silicon wafer Si (0.14 nm) versus the PPAAm coated Si (0.25 nm) and versus the Col coated Si (2.65 nm). Whereas the average roughness values for Si versus PPAAm are nearly similar, the Col coated Si wafer has a slightly more structured surface in this pico-nano-scale range. The chemical composition of the PPAAm film on a glass surface was analyzed by XPS [Fig. 7(A)] [elemental content: 74% C, 15% N,

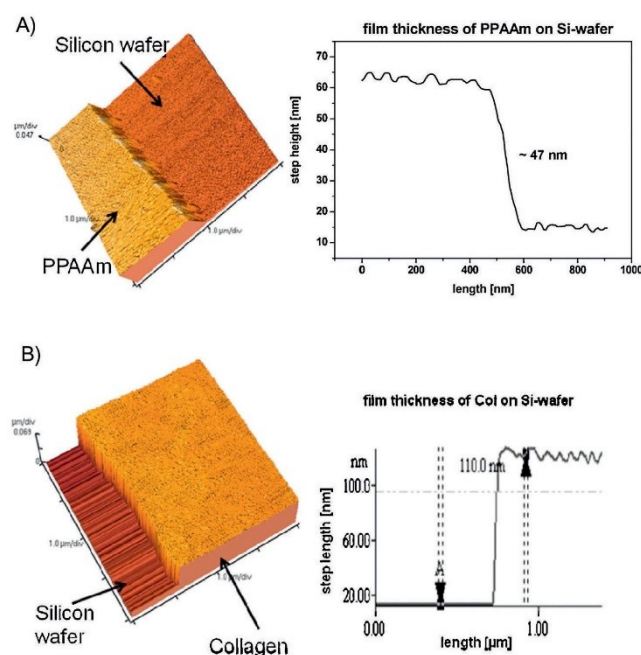


Fig. 5. Film thickness of the PPAAm- and the Col layer on the silicon wafer determined by AFM (diCP2).

8% O; elemental ratio: 20.3% N/C, 11% O/C (not shown)]. The density of amino groups NH_2/C was about 2–3%. The theoretical N/C value of polyallylamine is 33.3%. The O/C ratio of 11% is most probably due to oxygen uptake after plasma processing during air contact. The pure untreated glass surface consists of 25% silicon Si, 42% oxygen O, and ~5% of additional glass components such as boron B, potassium K, sodium Na, titanium Ti, zinc Zn (not shown). This composition differs considerably from a glass-PPAAm or glass-Col surface (elemental content: 65% C, 15% N, 17% O; elemental ratio: 23% N/C, 26% O/C. High resolution XPS C1s [Fig. 7(B)] spectra of glass-PPAAm and glass-Col verify the existence of different nitrogen and oxygen functional groups in terms of C–C, C–H, C–N, and C–O containing bonds. The relatively high content of C–N in the C1s spectrum confirms a good retention of the allylamine structure (glass-PPAAm), while the amide peak $\text{O}=\text{C}-\text{NH}$ for oxidation of the amine group is rather small. But there are differences in the C1s high resolution spectrum of glass-Col—the peak near 288 eV that stands for the peptide bond $\text{O}=\text{C}-\text{NH}$ in Col is especially pronounced. Highly resolved N1s spectra between 397–402 eV supported this interpretation. The broad peak at 398–400 eV for glass-PPAAm cannot be distinguished in single bonds therefore it was formally divided into C–N₍₁₎ and C–N₍₂₎. The first one includes amines, while the last one covers amides, imides, nitriles. Glass-PPAAm has a broader N1s high

resolution spectrum compared to glass-Col, due to the marginal fraction of primary amino groups in Col (Fig. 7B).

Initial Spreading is Enhanced on Positively Charged Surfaces

Time lapse recordings of vital MG-63 osteoblasts enabled the continuous monitoring of cell spreading. We could demonstrate that the vital osteoblasts on the positively charged glass-PPAAm surfaces spread significantly earlier and faster than on glass-Col surfaces (Fig. 8). Notably, the cells spread on glass-Col over an area of $1065 \pm 40 \mu\text{m}^2$ and $1530 \pm 70 \mu\text{m}^2$ after 5 and 30 min, respectively, whereas on glass-PPAAm the cells spread over $1708 \pm 37 \mu\text{m}^2$ and $5630 \pm 268 \mu\text{m}^2$ during the indicated times. The average size of MG-63 osteoblasts after their attachment stage (still rounded cells) is 10–20 μm in diameter. Thus, we could observe after 30 min a dramatically increase in cell area of nearly 280 times on glass-PPAAm compared to 75 times on glass-Col [Fig. 8(B)]. Our earlier results have demonstrated that functionalization of the material surface with PPAAm induced a strong initial cell adhesion (already after 5 min) and an enhanced formation of actin fibers in osteoblasts.^[12] This supports results demonstrating a higher fibroblast attachment and cell viability on allylamine-modified membranes and plasma polymer-treated substrates compared to untreated surfaces.^[30,31]

Although we observed differences in the pico-nano-scale roughness of glass-Col versus glass-PPAAm as described above the range of this surface topography between R_a 0.1 and 2 nm (pico-nano-topography) is outside and far from the surface landscape of genuine bone, ranging from $R_a < 50$ nm to $R_a \sim 1 \mu\text{m}$ (nano-micro-topography).^[32] We do not think that the “roughness” difference from PPAAm to Col in this pico-nano-range is responsible for our observed changes in vinculin mobility within one cell’s dimension and, in consequence, for the whole-cell spreading. It is discussed in the literature that interaction of integrins (adhesion receptors which also act in the focal complexes like vinculin) with the extracellular matrix occurs first on a scale of 100 nm ($=0.1 \mu\text{m}$).^[32] Concerning topography in the micrometer-scale we could present recently that actin re-organization in one cell’s dimension intensively occurs on cubic pillar structures with sizes of 3–5 μm ^[33] but not on smaller sizes of these geometrical structures (unpublished). Thus, we assume for our results that there exist strong chemical influencing factors such as positive surface charges as produced by physical plasma polymers^[11] which are dominant over the pico-nano-topography.

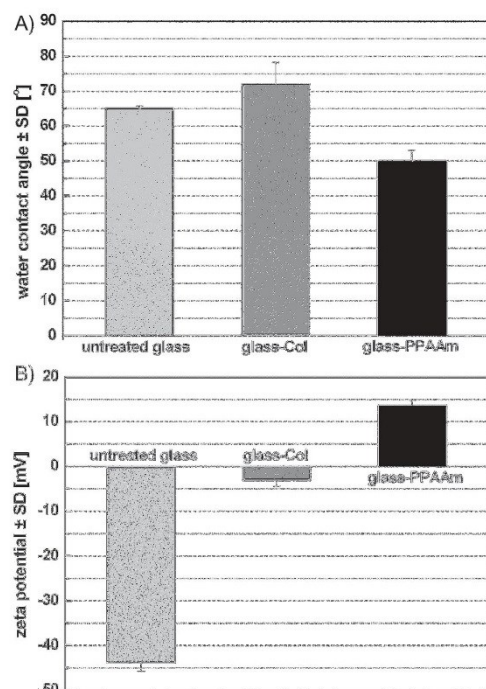


Fig. 6. Surface characterization of the functionalized surfaces. (A) Water contact angles measured on untreated and differently coated glasses ($n=5$). (B) Zeta potential determined on untreated and differently coated borofloat B33 glasses.

Vinculin Mobility is Reinforced on PPAAm

In order to investigate whether the increased spreading of cells is dependent on a superior mobility of FA contacts, the dynamic behavior of vinculin in living MG-63 osteoblasts was examined. The mobility of vinculin was measured during the first adhesion phase, i.e., up to a maximum of 3 h of cell adhesion (Fig. 9). Moving vinculin contacts appear in rainbow colors in the overlay images (false colored in blue, green, red). The results clearly demonstrate an increased mobility of vinculin in cells on glass-PPAAm. We could observe larger "rainbows" on these positively charged surfaces. The calculated mobility of the vinculin contacts was $100 \pm 9.1 \text{ nm min}^{-1}$ compared with $66 \pm 12.4 \text{ nm min}^{-1}$ on glass-Col.

We were not able to comparably measure the vinculin contacts on the pure glass surface because in the early adhesion phase $<1 \text{ h}$ cells adhered on uncoated glass, but did not spread out enough and therefore, no single FAs were visible in the confocal microscope. However, untreated glass was used as control in long term experiments (migration see Fig. 11).

While numerous studies have analyzed exchange dynamics of several FA proteins such as vinculin and paxillin

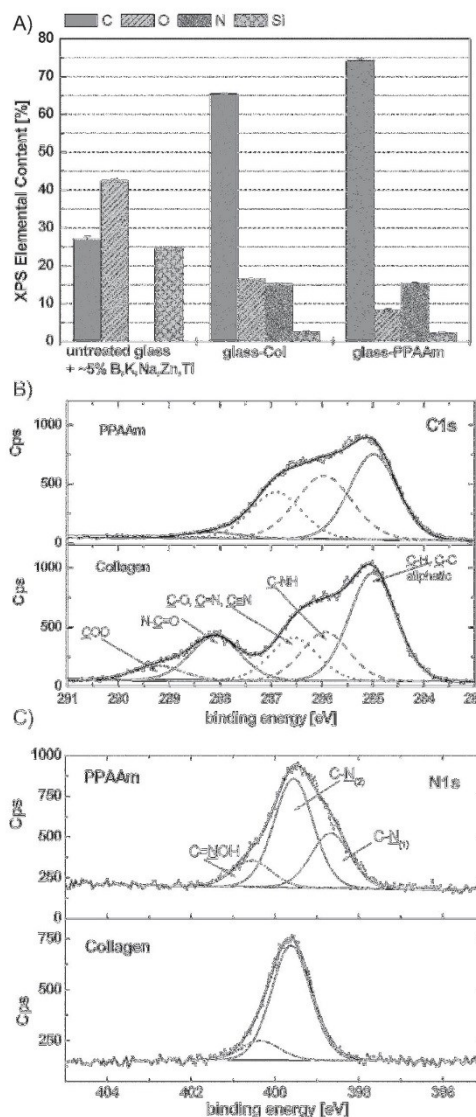


Fig. 7. (A) XPS measurement: chemical composition of untreated glass compared to collagen and PPAAm films on glass. The untreated glass contains traces up to 5% of B, K, Na, Ti, Zn. Note that the element content of glass-Col and glass-PPAAm is similar. (B) High resolution XPS analysis of C1s and N1s spectra of PPAAm and Col. The N1s peak fitted by different peaks signed by $-C-N_1$ and $-C-N_2$ for miscellaneous covalent $-C-N$ bonds, as $-C-NH_2$, $-C=N$, $=C=N$, $-C-N-C$, $O=C-NH_2$, $O=C-NH_2$.

by FRAP (fluorescence recovery after photobleaching),^{134–361} the mobility of these adhesions has rarely been studied in living cells. Examinations in living fibroblasts report a speed of 120 nm min^{-1} for FAs, measured by $\beta 1$ -integrin labeling in

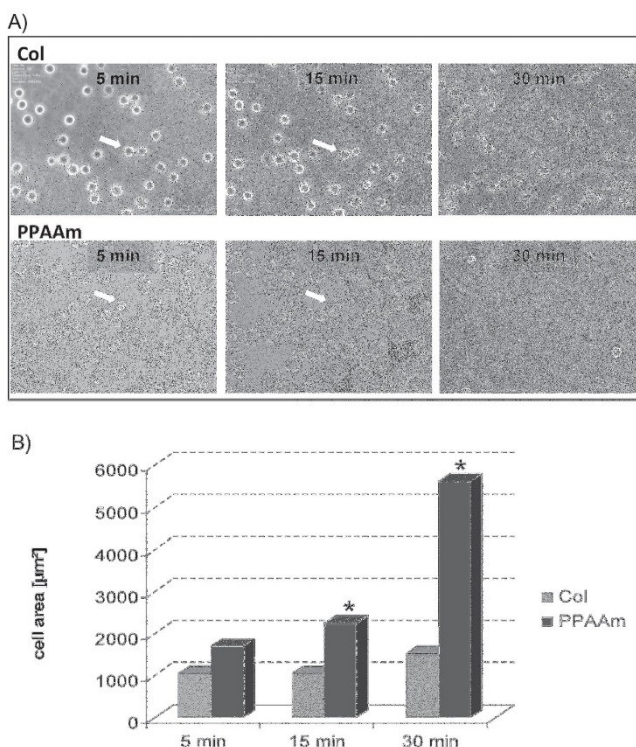


Fig. 8. (A) Excerpt from the time lapse recordings: time-dependent spreading of living MG-63 cells within the first 30 min. The same cells can be observed after 5 and 15 min (arrows, one cell example). (B) It is evident that already after the short time span of 15 min the cell spreading is significantly higher on PPAAm surfaces ($p < 0.05$, $n = 50$, BioStation IM).

well spread fibroblasts.^[23] Other groups showed that FA dynamics of adherent cells is strongly dependent on surface chemistry—a maximum velocity of 353 nm min^{-1} was detected on hydrophilic substrata, while on hydrophobic surfaces the speed was only 218 nm min^{-1} for $\beta 1$ -integrins

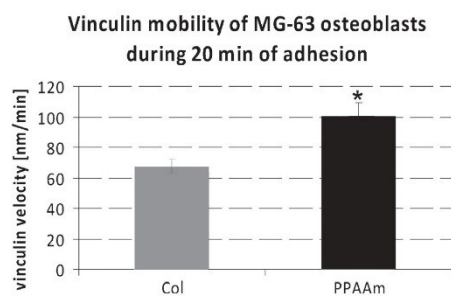


Fig. 9. Vinculin mobility of living MG-63 osteoblasts on chemically modified surfaces. Note that the speed of the vinculin contacts on PPAAm increased significantly in comparison to Col ($p < 0.05$, $n = 34$ for Col, $n = 17$ for PPAAm, \pm SEM).

in human fibroblasts.^[37] In human osteoblasts the mobility of FAs determined by vinculin measurements appeared to be significantly lower on polished titanium (40 nm min^{-1}) than on Col-coated glass surfaces (100 nm min^{-1}).^[28]

To our knowledge this is the first study reporting vinculin dynamics on plasma functionalized material surfaces during the initial phase of cell adhesion. We have demonstrated an increase in vinculin mobility, which is highly significant on PPAAm due to its positive charges. These results correlated with a faster spreading, observed in the time-lapse experiments during a time frame of 5–30 min. The initial speed of spreading supports earlier results which demonstrated an increased spreading on PPAAm-modified titanium surfaces up to 24 h.^[12] Our results suggest that increased spreading is facilitated by a higher mobility of adapter proteins in FA complexes. However, the mobility of FA components does not always correlate with the dynamic behavior of the whole cell. As reported by Smilenov *et al.*^[23] integrin contacts in migrating cells remained stationary in the cell center, whereas in stationary fibroblasts the contacts were highly motile resulting from a contraction of associated actin fibers.

FA Maturation Occurs Earlier on PPAAm

Maturation of FAs is a decisive factor of cell adhesion and migration.^[36] Although the FAs on Col are mature as well, we have observed an increased extension of vinculin containing FAs on the PPAAm surfaces (glass-PPAAm). After 1 h of adhesion the length of the contacts increased significantly from $1.8 \pm 0.1 \mu\text{m}$ on the reference glass-Col to $2.7 \pm 0.2 \mu\text{m}$ on glass-PPAAm (Fig. 10).

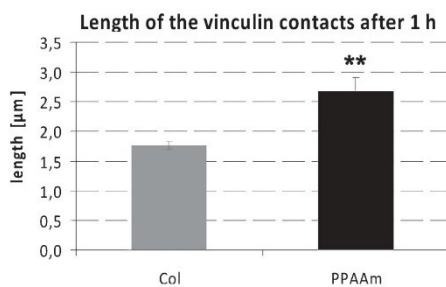


Fig. 10. Length of vinculin containing contacts after 1 h of cell adhesion on the different substrates. Note that on the PPAAm-modified surface the vinculin contacts are significantly longer than on Col ($p < 0.01$, $n = 5$, \pm SEM).

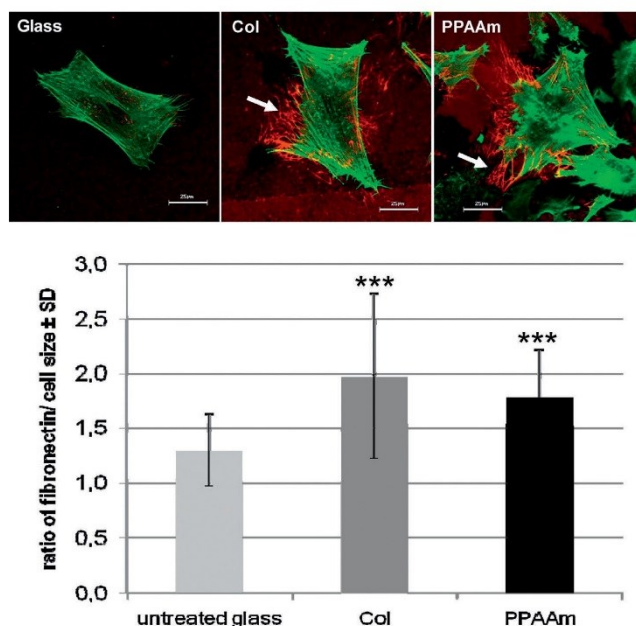


Fig. 11. Cell migration of MG-63 osteoblasts after 48 h on PPAAm functionalized glass surfaces compared to Col-coated and untreated glass. Secreted fibronectin (red) (arrow) marks the path that the cells (green) have covered (above). Note that on glass-PPAAm and on glass-Col the cells move intensively on the surface while cells on the untreated glass control remain stationary, which is statistically significant. The ratio of the fibronectin area to cell size is demonstrated below, whereas a value of 1 represents equal size of fibronectin and cell size (no migration) (***) $p < 0.001$, $n = 7$ for glass, $n = 34$ for Col and PPAAm).

Bershadsky *et al.*^[38] described two distinct morphological variants of FAs, the “dot” and “dash” variants.

“Dot,” or small initial, contacts are the predominant initial contact type, containing only vinculin, talin, and α -actinin^[39] with dimensions of 0.2–0.5 μm , and are mainly located at the active edge of the cell. “Dash” or elongated mature contacts differ due to their association with the cytoskeletal actin bundles. Dash contacts are 2–10 μm in length and 0.5 μm in width and are located centrally in parts of the lamellae, areas of the endoplasm and under the nucleus. During cell adhesion initial formation of dot contacts occurs followed by maturation into dash contacts.^[40] Our findings demonstrate that the length of the vinculin contacts is enlarged on amino functionalized surfaces. This could indicate a temporal advance in focal contact maturation and in consequence facilitating cell adhesion and subsequent biological responses such as proliferation and differentiation on PPAAm modified surfaces.

The influence of adhesion maturation on cell proliferation was examined by Slater and Frey, who discovered that larger adhesion sites promote proliferation in HUVEC cells.^[41] In this study, they compared variably sized fibronectin nanopattern surfaces to ascertain whether there is a correlation of nanopattern size, FA formation and, at later time points, cell

proliferation. As a result they identified significantly more dash adhesions on the larger patterns, what consequently resulted in a higher proliferation rate at these surfaces compared to smaller sized patterns. For adherent cells a correlation between adhesion strength and FA size is under discussion.^[42] Our osteoblasts adhere with a 2–3 times higher strength on PPAAm-modified titanium surfaces compared to untreated titanium (unpublished; personal communication).

It is noteworthy to mention that compared with Col coating, positive charges at the surface as detected by zeta potential measurements boost cell adhesion and spreading in the very first adhesion phase. This indicates a significant stimulation of the initial cell-surface contact solely by electrodynamic interactions.

PPAAm Promotes Cell Migration

We were able to demonstrate that cell migration after 48 h of cultivation was enhanced on our positively charged glass-PPAAm surfaces (Fig. 11). On these surfaces we could observe secreted fibronectin surrounding the cell body with “footprints” formed by the cells. In contrast, on untreated glass cells did not migrate and secreted fibronectin was only found beneath

the adherent cell. This indicates that the facilitation of the early adhesion phases due to amino functionalization, shown by faster vinculin maturation, strongly influences subsequent cell responses.

The deciding factor for the ingrowth of medical implants into human bones is their rapid acceptance by the cells. We suggest that implants could be optimized by these positive charge carriers. Our recent *in vivo* results revealed no local inflammations in the back musculature of rats.^[43]

The immediate adhesion, fast spreading and the migration of cells is essential for the settlement of biomaterials. Detailed analyses concerning the mechanisms during the initial adhesion of osteoblasts are required for the development of newly designed material surfaces.

Conclusion

Our investigations on the dynamics of vinculin contacts on plasma-modified surfaces demonstrated that a positively-charged surface due to amino groups promotes the initial spreading of vital cells, which presupposes increased mobility of the cells. Vinculin, a protein associated with the cytoskeleton, serves as a marker for the FAs. PPAAm-modified surfaces induced an increased mobility of the focal

contacts; detected by GFP–vinculin. It is likely that this dynamic behavior of FA components stimulated the early and rapid spreading of the cells on PPAAm-modified surfaces. We were able to demonstrate for the first time a more distinct dynamic behavior of FAs in living MG-63 osteoblasts on plasma polymerized surfaces. We suggest that the acceptance of implants in vivo could be optimized by positively charged carriers.

Received: December 16, 2009

Revised: May 3, 2010

Published online: July 7, 2010

- [1] H. F. Hildebrand, J. B. Nebe, J. San Roman, J. Amedec, *Biomol. Eng.* **2007**, *24*, 423.
- [2] N. Faucheux, R. Schweiss, K. Lutzow, C. Werner, T. Groth, *Biomaterials* **2004**, *25*, 2721.
- [3] T. A. Petrie, J. E. Raynor, C. D. Reyes, K. L. Burns, D. M. Collard, A. J. García, *Biomaterials* **2008**, *29*, 2849.
- [4] J. B. Nebe, L. Mueller, F. Luthen, A. Ewald, C. Bergemann, E. Conforto, F. A. Mueller, *Acta Biomater.* **2008**, *4*, 1985.
- [5] T. A. Petrie, J. E. Raynor, C. D. Reyes, K. L. Burns, D. M. Collard, A. J. García, *Biomaterials* **2008**, *29*(19), 2849.
- [6] M. Schuler, G. R. Owen, D. W. Hamilton, M. de Wild, M. Textor, D. M. Brunette, S. G. Tosatti, *Biomaterials* **2006**, *27*, 4003.
- [7] T. A. Petrie, J. R. Capadona, C. D. Reyes, A. J. Garcia, *Biomaterials* **2006**, *27*, 5459.
- [8] F. G. Giancotti, E. Ruoslahti, *Science* **1999**, *285*, 1028.
- [9] R. M. Ezzell, W. H. Goldmann, N. Wang, N. Parasharama, D. E. Ingber, *Exp. Cell Res.* **1997**, *231*, 14.
- [10] E. Ruoslahti, B. Öbrink, *Exp. Cell Res.* **1996**, *227*, 1.
- [11] B. Finke, F. Lüthen, K. Schröder, P. D. Müller, C. Bergemann, M. Frant, A. Ohl, J. B. Nebe, *Biomaterials* **2007**, *28*, 4521.
- [12] J. B. Nebe, B. Finke, F. Lüthen, C. Bergemann, K. Schröder, J. Rychly, K. Liefeth, A. Ohl, *Biomol. Eng.* **2007**, *24*, 447.
- [13] J. B. Nebe, F. Lüthen, in: *Metallic Biomaterial Interactions* (Eds.: J. Breme, C. J. Kirkpatrick, R. Thull), WILEY-VCH, Weinheim **2008**, p. 179.
- [14] T. C. Laurent, *Acta Otolaryngol. Suppl.* **1987**, *442*, 7.
- [15] D. Hanein, H. Sabanay, L. Addadi, B. Geiger, *J. Cell Sci.* **1993**, *104*, 275.
- [16] M. A. Schwartz, M. H. Ginsberg, *Nat. Cell Biol.* **2002**, *4*, 65.
- [17] R. Zaidel-Bar, M. Cohen, L. Addadi, B. Geiger, *Biochem. Soc. Trans.* **2004**, *32*, 416.
- [18] E. Cukierman, R. Pankov, D. R. Stevens, K. M. Yamada, *Science* **2001**, *294*, 1708.
- [19] S. Dedhar, G. E. Hannigan, *Curr. Opin. Cell Biol.* **1996**, *8*, 657.
- [20] C. Brakebusch, R. Faessler, *EMBO J.* **2003**, *22*, 2324.
- [21] D. E. Ingber, *J. Cell Sci.* **2003**, *116*, 1397.
- [22] N. Q. Balaban, U. S. Schwarz, D. Riveline, P. Goichberg, G. Tzur, I. Sabanay, D. Mahalu, S. Safran, A. Bershadsky, L. Addadi, B. Geiger, *Nat. Cell Biol.* **2001**, *3*(5), 466.
- [23] L. Smilenov, A. Mikhailov, R. Pelham, Jr., E. Marcantoni, G. Gundersen, *Science* **1999**, *286*, 1172.
- [24] N. Faucheux, R. Tzoneva, M. D. Nagel, T. Groth, *Biomaterials* **2006**, *27*, 234.
- [25] A. A. Meyer-Plath, K. Schröder, B. Finke, A. Ohl, *Vacuum* **2003**, *71*, 391.
- [26] A. Ohl, K. Schröder, in: *Low Temperature Plasma Physics* (Eds: R. Hippler, H. Kersten, M. Schmidt, K. H. Schoenbach), Wiley-VCH, Weinheim **2008**, p. 803.
- [27] G. Beamson, D. Briggs, *The scienta ESCA 300 database*, Wiley J & Sons, New York **1992**, p. 202.
- [28] A. Diener, J. B. Nebe, F. Lüthen, P. Becker, U. Beck, H.-G. Neumann, J. Rychly, *Biomaterials* **2005**, *26*, 383.
- [29] P. B. van Wachem, T. Beugeling, J. Feijen, A. Bantjes, J. P. Detmers, W. G. van Aken, *Biomaterials* **1985**, *6*, 403.
- [30] P. Hamerli, T. Weigel, T. Groth, D. Paul, *Biomaterials* **2003**, *24*, 3989.
- [31] M. Zelzer, R. Majani, J. W. Bradley, F. R. Rose, M. C. Davies, M. R. Alexander, *Biomaterials* **2008**, *29*, 172.
- [32] D. Geblinger, L. Addadi, B. Geiger, *J. Cell Sci.* **2010**, *123*, 1814.
- [33] C. Matschegewski, S. Staehlke, R. Loeffler, R. Lange, F. Chai, D. Kern, U. Beck, J. B. Nebe, *Biomaterials* **2010**, doi:10.1016/j.biomaterials.2010.03.073.
- [34] T. P. Lele, C. K. Thodeti, J. Pendse, D. E. Ingber, *Biochem. Biophys. Res. Commun.* **2008**, *369*, 929.
- [35] D. M. Cohen, B. Kutscher, H. Chen, D. B. Murphy, S. W. Craig, *J. Biol. Chem.* **2006**, *281*, 16006.
- [36] C. Möhl, N. Kirchgessner, C. Schäfer, K. Küpper, S. Born, G. Diez, W. H. Goldmann, R. Merkel, B. Hoffmann, *Cell Motil. Cytoskel.* **2009**, *66*, 350.
- [37] I. Zlatanov, T. Groth, A. Lendlein, G. Altankov, *Biophys. J.* **2005**, *89*, 3555.
- [38] A. D. Bershadsky, I. S. Tint, A. Neyfakh, J. M. Vasiliev, *Exp. Cell Res.* **1985**, *158*, 433.
- [39] L. Hemmings, D. J. Rees, V. Ohanian, S. J. Bolton, A. P. Gilmore, B. Patel, H. Priddle, J. E. Trevithick, R. O. Hynes, D. R. Critchley, *J. Cell Sci.* **1996**, *109*, 2715.
- [40] J. A. Cooper, *J. Cell Biol.* **1987**, *105*, 1473.
- [41] J. H. Slater, W. Frey, *J. Biomed. Mater. Res.* **2007**, *87*, 176.
- [42] A. D. Bershadsky, N. Q. Balaban, B. Geiger, *Annu. Rev. Cell Dev. Biol.* **2003**, *19*, 677.
- [43] A. Hoene, U. Walschus, B. Finke, S. Lucke, B. Nebe, K. Schroeder, A. Ohl, M. Schlosser, *Acta Biomater.* **2010**, *6*, 676.

2.3 Study III

Henrike Rebl, Birgit Finke, Regina Lange, Klaus-Dieter Weltmann, J. Barbara Nebe

Impact of plasma chemistry versus titanium surface topography on osteoblast orientation.

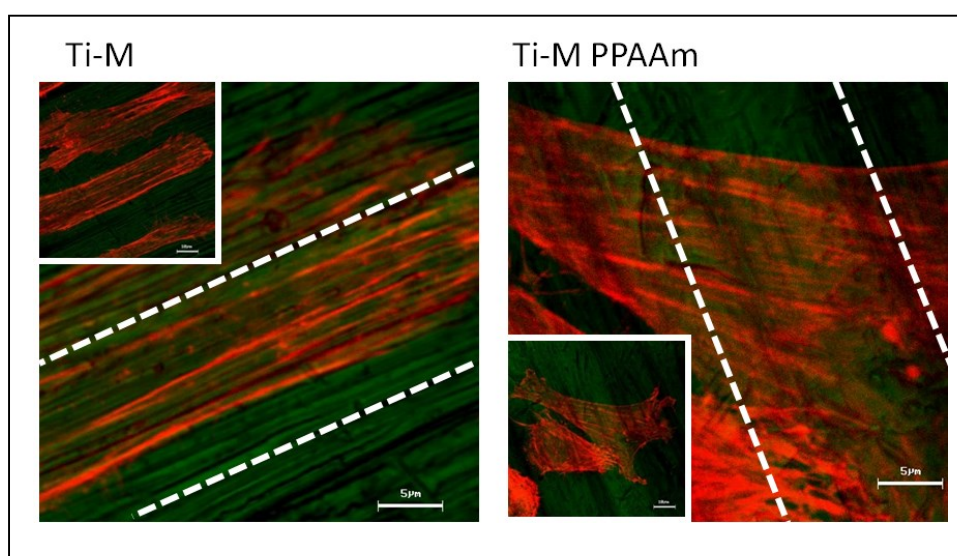
Acta Biomater, 2012; 8, 10, 3840-3851.

Abstract

In the third study we wanted to investigate whether there is a combinatory effect of topographical and chemical modifications of biomaterial surfaces and elucidate which of these properties is dominant.

Polished, machined and corundum-blasted titanium of increasing micro roughness was additionally coated with plasma polymerized allylamine (PPAAm). On all of these allylamine-plasma-modified surfaces (i) adhesion of human MG-63 osteoblastic cells increased significantly in combination with roughness, (ii) cells resembled the underlying structure and melted with the surface, (iii) cells overcame the topographical restrictions of a grooved surface and spread out over a large surface area. We could find out that the cellular effects of the plasma-chemical surface modification are predominant over surface topography. This is even more distinct in the initial phase. If collagen I was immobilized using different spacers, it did not improve surface adhesion features comparably, although collagen I is the “gold standard” in cell adhesion studies with osteoblasts.

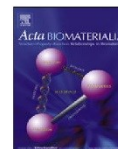
Graphical abstract:





Contents lists available at SciVerse ScienceDirect

Acta Biomaterialia

journal homepage: www.elsevier.com/locate/actabiomat

Impact of plasma chemistry versus titanium surface topography on osteoblast orientation

Henrike Rebl^a, Birgit Finke^b, Regina Lange^c, Klaus-Dieter Weltmann^b, J. Barbara Nebe^{a,*}

^a Department of Cell Biology, Biomedical Research Centre, University of Rostock, Rostock 18057, Germany

^b Leibniz Institute for Plasma Science and Technology (INP), Greifswald 17489, Germany

^c Department of Electrical Engineering and Information Technology, University of Rostock, Rostock 18119, Germany

ARTICLE INFO

Article history:

Received 23 March 2012

Received in revised form 4 June 2012

Accepted 8 June 2012

Available online 15 June 2012

Keywords:

Actin cytoskeleton

Osteoblast

Plasma polymerization

Surface topography

Allylamine

ABSTRACT

Topographical and chemical modifications of biomaterial surfaces both influence tissue physiology, but unfortunately little knowledge exists as to their combined effect. There are many indications that rough surfaces positively influence osteoblast behavior. Having determined previously that a positively charged, smooth titanium surface boosts osteoblast adhesion, we wanted to investigate the combined effects of topography and chemistry and elucidate which of these properties is dominant. Polished, machined and corundum-blasted titanium of increasing microroughness was additionally coated with plasma-polymerized allylamine (PPAAm). Collagen I was then immobilized using polyethylene glycol diacid and glutar dialdehyde. On all PPAAm-modified surfaces (i) adhesion of human MG-63 osteoblastic cells increased significantly in combination with roughness, (ii) cells resemble the underlying structure and melt with the surface, and (iii) cells overcome the restrictions of a grooved surface and spread out over a large area as indicated by actin staining. Interestingly, the cellular effects of the plasma-chemical surface modification are predominant over surface topography, especially in the initial phase. Collagen I, although it is the gold standard, does not improve surface adhesion features comparably.

© 2012 Acta Materialia Inc. Published by Elsevier Ltd. All rights reserved.

1. Introduction

The metallic implants used in orthopedic surgery or oral implantology can be regarded as bone-replacing and bone-contacting applications, and include joint and tooth replacement, fracture healing and reconstruction of skeletal abnormalities. For these implants, the ultimate goal is to obtain a lifelong secure anchorage in the native surrounding bone. Due to its excellent mechanical properties, biocompatibility as well as corrosion resistance, commercially pure titanium has been widely used as an implant material in various dental and orthopedic applications [1–4]. For the efficacy of these implants, it is essential to establish a mechanically solid interface with complete fusion between the material's surface and the bone tissue without fibrous tissue interface [5].

Although it is well established that titanium is an osteoconductive material, little precise knowledge has been established to ascertain whether titanium chemistry or topography is the more crucial factor in determining the level of osteoconductive capacity; it is a big challenge to change only one factor without changing the other because the surface chemistry and topography of titanium are interrelated [6]. The influence of surface topography has been widely reported and plays an important role in cell behavior [6–

8]. Osteoblast-like cells cultured in vitro on rough surfaces show stronger cell adhesion and spreading [7,9] and high production of both differentiation-associated growth factors and extracellular matrix proteins [10–12]. Surface modifications which alter the topography of the titanium surface mainly include mechanical methods, such as machining, grinding, polishing and blasting, and chemical methods, such as etching and anodization [7,8,13–16].

Another approach towards the creation of a biologically active implant surface involves the application of an additional layer onto the titanium surface by means of physicochemical and biochemical deposition techniques [17,18]. One main focus concerning the chemical modification of material surfaces involves coating with proteins. Because collagen is a ligand which facilitates the cell adhesion via integrins, coating with adhesion proteins or peptides (especially RGD) and/or growth factors is of great interest [19,20]. Another strategy utilizes the net negative charge of eukaryotic cells by providing the surface with positive charge carriers, e.g. NH₂ groups [21–24]. Plasma modification of titanium surfaces with allylamine renders the surface more hydrophilic and generates positively charged amine groups [23,24]. Allylamine is widely used as a precursor for providing materials with a net positive surface charge and for allowing further covalent coupling of proteins or peptides via suitable linkers [17,25–27]. However, previous research has merely tested the influence of the plasma-polymerized

* Corresponding author. Tel.: +49 381 4947771; fax: +49 381 4947764.
E-mail address: barbara.nebe@med.uni-rostock.de (J.B. Nebe).

Author's personal copy

H. Rebl et al./Acta Biomaterialia 8 (2012) 3840–3851

3841

allylamine (PPAAm)-modified surface chemistry on smooth polyethylene terephthalate, silicon, polysiloxane and titanium surfaces.

This is, to our knowledge, the first paper to report the cellular effects caused by a combination of topography (microstructured titanium surfaces) and a well-directed surface chemistry by PPAAm as well as collagen coupling via different linkers. In particular, we wanted to answer the question of whether surface topography or chemistry is dominant. We hypothesized that a positively charged plasma polymer layer has enormous power, sufficient for cells to overcome the restrictions of a grooved microtopography.

2. Materials and methods

2.1. Surface characteristics

2.1.1. Roughness

Titanium of technical purity (Ti, cp, grade 2, DOT GmbH, Rostock, Germany) was used in the form of discs or plates (30 and 11 mm in diameter, with a height of 5 and 2 mm, respectively). The physical structure of the surface was modified by the following techniques: Polishing (Ti-P) with SiC wet grinding paper (grit P4000); machining (Ti-M) and blasting with corundum (aluminum

oxide) particles (500–600 μm) at 6 bar (Ti-CB). The characterization of surface roughness has been described previously [7]. Briefly, for measurement of the roughness, a surface profiler HOMMEL-Tester T8000 (Hommel, Schwenningen, Germany) was used. Before their use in the experiments, non-modified materials were ultrasonically cleaned and sterilized with 70% ethanol overnight. Scanning electron microscopy (DSM 910A, Carl Zeiss, Oberkochen, Germany) and stereomicroscopy (Axiovert 200M, Carl Zeiss, Oberkochen, Germany) were used to display the material surface (Fig. 1).

2.1.2. Profilometry

A DEKTAK 3ST profiler (Veeco, Santa Barbara, CA, USA) was used to record the surface profile (Fig. 2). The radius of the standard diamond stylus was 2.5 μm , the stylus force 30 mg, and the scan length 8 mm.

2.1.3. Water contact angle

The contact angle of the titanium surfaces was measured by the sessile drop method using a DIGIDROP contact angle meter (GBX Instrumentation Scientifique, Romance, France). The determination of the angle between the solid surface and the tangent of

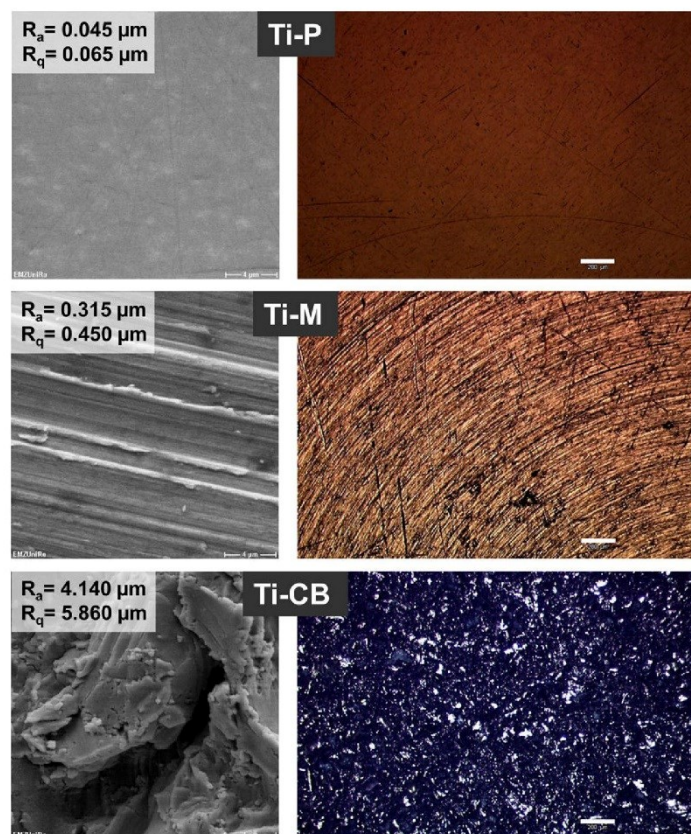


Fig. 1. SEM and stereomicroscopic images of cp Ti with increasing roughness: SEM magnification $\times 5,000$, bar = 4 μm (DSM 910A), stereomicroscopy magnification $\times 200$, bar = 200 μm (Axiovert 200M). Differences in the surface structure have been found depending on the roughening technique used. While corundum blasting of the surface resulted in a rock-like stochastic topography with sharp ridges and edges, machining created grooves and striations.

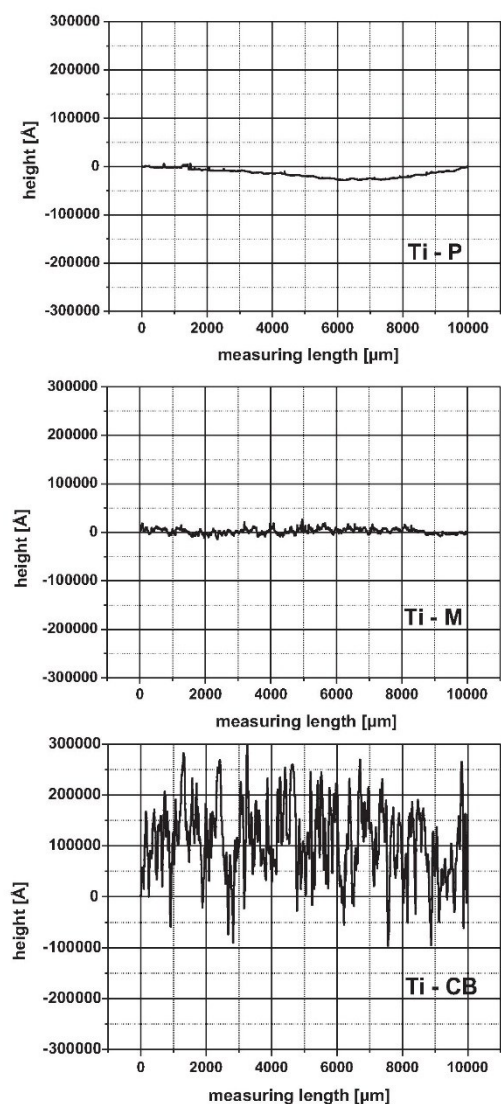


Fig. 2. Profilometry of structured titanium surfaces: Ti-P, polished; Ti-M, machined; and Ti-CB, corundum blasted. Note that the surface profiles are characteristic for the particular surface treatment. Ti-P surface shows certain waviness within the scan length due to the polishing process. Ti-M reflects the regularity of the turning lathe feed, whereas Ti-CB shows the highest roughness.

the drop was performed by computer control. Three measurements were performed on each surface, and arithmetic means and standard deviations were calculated using the software package Origin 6.1 (OriginLab Corp., Northampton, USA).

2.1.4. Surface energy

The polar and disperse components of surface energy were calculated from measurements of contact angles with different liq-

uids, namely water, ethylene glycol and methylene iodide. The contact angles were determined using the OCA 30 contact angle measuring system (Data Physics Instruments GmbH, Filderstadt, Germany) with the sessile drop method (using software SCA20). The surface energy was calculated using the methods of Owens, Wendt and Rabel [28,29]. These measurements were always performed within 30 min after sample preparation [30].

2.1.5. XPS analysis

The elemental surface composition and chemical binding properties of the glass surfaces were determined by high-resolution scanning X-ray photoelectron spectroscopy (XPS) as previously described for titanium surfaces [23,24]. Briefly, the Axis Ultra (Kratos, Manchester, GB) was run with the monochromatic Al K_{α} line at 1486 eV (150 W). Charge neutralization was implemented. Spectra were recorded at pass energy of 10 eV for highly resolved C1s and N1s peaks. The C-C/C-H component of the C1s spectrum was adjusted to 285.0 eV [31]. C1s, O1s and N1s spectra were recorded at a pass energy of 80 eV at three different sample positions for quantification of surface composition. A chemical derivatization was applied for the quantification of amino groups, since amino groups do not lead to significant shifts in the binding energy of the C1s and N1s electrons. Amino groups were reacted with 4-trifluoromethylbenzaldehyde (TFBA, Sigma-Aldrich, Steinheim, Germany) at 40 °C for 2 h in a saturated gas phase.

2.2. Chemical functionalization of titanium

Amino functionalization was performed in a low-pressure plasma process reactor V55G (plasma finish, Schwedt, Germany, V = 60 l) in a two-step procedure. First, the titanium samples were decontaminated and activated by continuous wave (cw) oxygen-plasma (500 W, 50 Pa, 100 sccm O₂/25 sccm Ar). Then, the plasma polymerization of the precursor allylamine was carried out using a microwave-excited (2.45 GHz, 500 W), pulsed (duty cycle of 0.15 at a pulse length of 2 s), low pressure (P = 50 Pa) gas-discharge plasma [24] for a treatment duration of 960 s (Ti PPAAM = plasma-polymerized allylamine on titanium). Allylamine was fed from a liquid handling system, which was carefully purified of air by evacuating and purging with N₂ prior to use. Argon was applied as a carrier gas (50 sccm Ar). The substrate was located in a downstream plasma position.

The immobilization of collagen I (Col) (Sigma-Aldrich) was performed immediately after the PPAAM coating with a wet-chemical process. Covalent coupling reactions of the plasma-generated amino groups [24] with Col (scheme shown in Fig. 3A) were performed via the bifunctional linker molecule polyethylene glycol diacid (PEG DA, VWR International GmbH, Darmstadt, Germany) or glutar dialdehyde (GDA, Sigma-Aldrich). The coupling process with Col via PEG DA has already been described in detail [23,32]. The coupling procedure via GDA was carried out as subsequently specified by a two-step wet-chemical grafting process immediately after PPAAM film preparation: the PPAAM coated disks were placed into 6-well chambers (Becton Dickinson, Franklin Lakes, USA) and treated with 5 ml 2% GDA solution for 3 h. Then the disks were rinsed with sterilized water and subsequently treated overnight with 5 ml of a 0.003% Col solution in a Ca²⁺, Mg²⁺-free phosphate-buffered solution (PBS, Life Technologies GmbH, Darmstadt, Germany). After rinsing with sterilized water, the disks were dried for 24 h in air. All the wet-chemical work was done under a laminar flowbox in a clean room.

All four different chemical modifications (untreated, PPAAM, PEG DA-Col and GDA-Col) were combined with the three different topographies (Ti-P, Ti-M, Ti-CB); thus 12 distinct different specimens were compared.

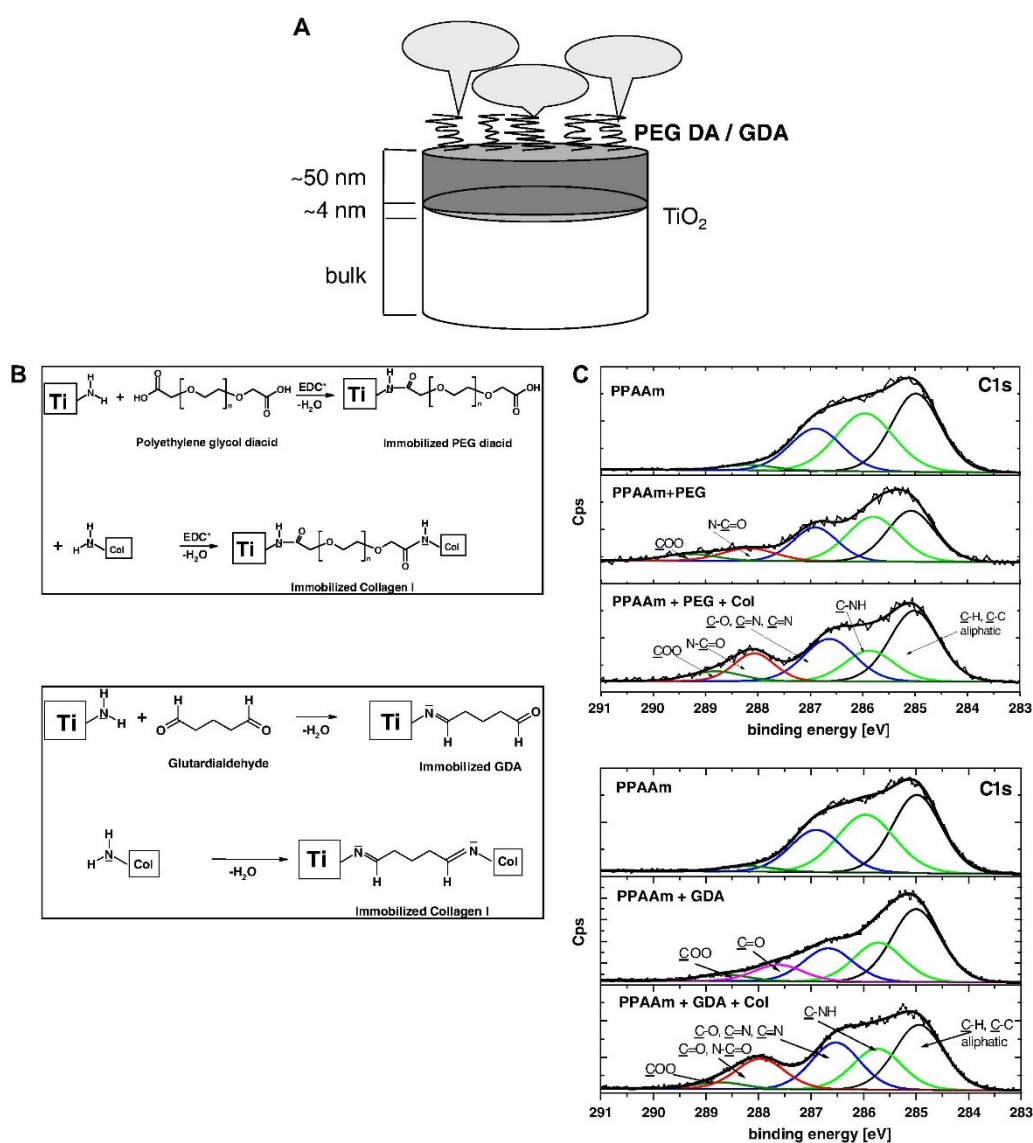


Fig. 3. (A) Layer configuration of coated titanium disks: the plasma-cleaned titanium oxide layer is covered with a thin film of PPAAm or, in addition, with a following wet-chemical coupling of Col via PEG DA or GDA. (B) Chemical coupling schemes of Col to PPAAm-coated Ti via the linkers PEG DA (above) and GDA (below). Note that the used linker molecules have different chain lengths (PEG DA: ~3.8 nm/GDA: ~1.2 nm). (C) XPS analysis of the high-resolution C1s peak—coupling of Col to PPAAm via the linker PEG DA (above) and GDA (below). In the first step the peptide bond formation $-N-C=O$ at 288.1 eV and the remaining $-COO$ bond from PEG DA at 289.2 eV, functioning as the linker group for Col in the next coupling step, can be verified. In contrast to this, GDA has two aldehyde groups for the reactions. The $-C=O$ signal at 287.7 eV corresponds to the free aldehyde functionality. After the Col immobilization the formation of the characteristic peptide $-N-C=O$ bond with a share of about 25 or 20% for PEG DA-Col and GDA-Col, respectively, can be observed [24].

2.3. Cell culture

The human osteoblast-like cell line MG-63 (ATCC, CRL-1427, LGC Promochem, Wesel, Germany) was used for all experiments.

The cells were cultured in 75 cm² flasks in Dulbecco's modified Eagle's medium (DMEM) with 10% fetal calf serum (FCS, PAA), and 1% gentamicin (Ratiopharm GmbH, Ulm, Germany) at 37 °C in a humidified atmosphere with 5% CO₂. In general, MG-63 cells were

cultured under serum-free conditions to avoid masking of the amino-functionalized Ti surface with adsorbed proteins, e.g. soluble fibronectin [23].

2.4. Scanning electron microscopy (SEM)

The material surfaces were investigated by scanning electron microscopy (SEM) using DSM 960A and FE-SEM Supra 25 microscopes (both Carl Zeiss, Oberkochen, Germany). For cell analyses, 4×10^4 cells were grown on titanium plates for 24 h, fixed with 4% glutaraldehyde (1 h), dehydrated through a graded series of acetone, dried in a critical point dryer (K 850, EMITECH, Taunusstein, Germany) and sputtered with a coater (SCD 004, BAL-TEC, Balzers, Lichtenstein). To make the osteoblast-like cells clearly visible on PPAAm (Ti-M) the circumference of the cells was pigmented in false color using Adobe Photoshop® 7.0 (Adobe Systems Inc.).

2.5. Cell adhesion

Suspended MG-63 cells in serum-free DMEM were seeded onto the discs for 5 min at a density of 1×10^5 per specimen, and non-adherent cells in the supernatant were counted and analyzed by flow cytometry (FACSCalibur, BD Biosciences). The software CellQuest Pro 4.0.1 was used for data acquisition. Cell adhesion was then calculated as a percentage of the cell number at 0 min.

2.6. Cell spreading

Human MG-63 cells were trypsinated, washed in PBS (PAA Laboratories GmbH, Pasching, Austria) and the cell membrane stained with the red fluorescent linker PKH26 (PKH26 General Cell Linker Kit, Sigma) for 5 min in suspension. 4×10^4 cells were then seeded onto the plates and cultured for 30 min, 1 and 3 h. After fixation with 4% paraformaldehyde (PFA, Merck) the cells were embedded on a coverslip. Microscopic examinations were performed using an inverted confocal laser scanning microscope LSM 410 (Carl Zeiss). Spreading (cell area in μm^2) of 40 cells per specimen was measured using the "area measurement" software of the LSM 410. Finally, cell spreading was calculated relative to the corresponding chemically untreated surface.

2.7. Actin and nucleoli staining

For actin staining 4×10^4 cells were cultivated on the plates for 24 h, washed three times with PBS, fixed with PFA (4%, 10 min, Merck) and permeabilized with Triton X-100 (0.1%, 10 min, Sigma). Actin staining was performed using Alexa Fluor 546 Phalloidin (1:100, 30 min, Invitrogen). For staining of the nucleoli, 4×10^4 cells were seeded on collagen-coated coverslips. In brief, cover glasses (Menzel GmbH, Braunschweig, Germany) were coated with collagen I (Col, rat, 20 mg cm^{-2} , BD Biosciences) and were allowed to dry overnight under sterile conditions in the laminar flowbox [32]. After 24 h the cells were fixed with methanol for 10 min, stained with Syto® RNASelect™ (1:2,000, Invitrogen) for 20 min and counterstained with DAPI (1:20,000, Boehringer-Mannheim GmbH) for a further 20 min. Finally cells were embedded and analyzed with the LSM 410 and the AxioScope A1 (both Carl Zeiss). Cell orientation was quantified using the software ImageJ (v. 1.41o, NIH).

3. Results

3.1. Surface characteristics

The average roughness (R_a) and the corresponding root mean squared roughness (R_q) values of the samples are indicated in Fig. 1, and the profilometry is shown in Fig. 2.

The covalent coupling of Col to Ti-PPAAm via the linker PEG-DA or GDA can be described by the chemical reactions in Fig. 3B. In the first step the PEG-DA immobilization to Ti-PPAAm can be verified via XPS analysis by the peptide bond formation $-\text{N}-\text{C}=\text{O}$ at 288.1 eV, with the remaining $-\text{COO}$ bond from PEG-DA at 289.2 eV functioning as the linker group for Col in the next coupling step. After Col immobilization a significant increase in peptide bond share can be observed (Fig. 3C). The area of this specific peak correlates with the attached amount of Col ($\sim 25\%$). In contrast to PEG-DA, GDA offers two reactive aldehyde groups for the subsequent immobilization step. Efficient derivatization of the PPAAs amino groups with GDA can be verified by the characteristic $-\text{C}=\text{O}$ signal at 287.7 eV, corresponding to the free remaining aldehyde functionality of the linker. After successive immobilization of Col the formation of the specific $-\text{N}-\text{C}=\text{O}$ bond with a share of about 20% is observed.

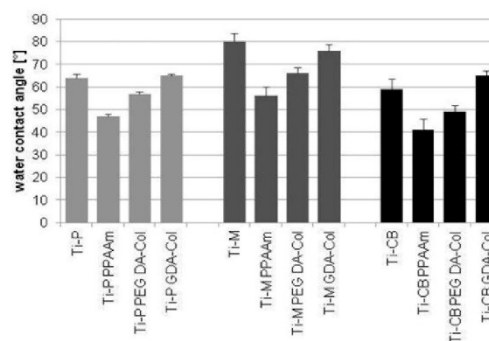


Fig. 4. Water contact angle: the functionalization with PPAAm leads to decreasing water contact angles which are between 40° and 55° in comparison to the untreated surfaces of identical roughness. Coatings with Col result in successive increase of the water contact angle values compared to PPAAm. $n = 3$.

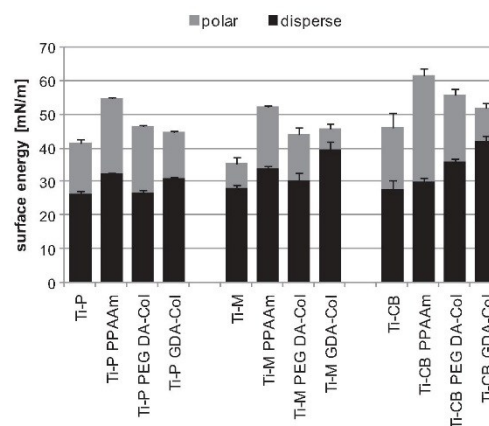


Fig. 5. Surface energy: functionalization with PPAAm strongly increases the surface energy mainly in the polar part in comparison to the untreated surfaces of identical roughness. Additional coatings with Col results in a decreasing polar and increasing dispersed part of the surface energy. $n = 3$.

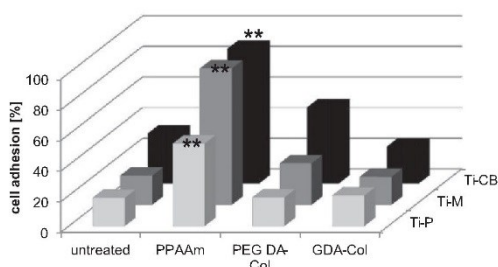


Fig. 6. Short-term adhesion (5 min) of MG-63 cells on topographically and chemically modified titanium surfaces; note that surface charges due to amino functionalization on the structured Ti-M and Ti-CB increase initial cell adhesion significantly 3- to 5-fold. The effect of additional Col immobilization is not comparable. Flow cytometry, $n=3 \times 50,000$ cells, Student's *t*-test, $^{**}P \leq 0.01$ compared to all modifications of the corresponding topography.

Measurements of surface wettability (Fig. 4) revealed a significant decrease in the water contact angle after modification with PPAAm. On untreated surfaces an angle of 64° , 80° and 59° was determined for the Ti-P, Ti-M and Ti-CB surfaces, respectively. After PPAAm treatment these values were decreased to 47° , 56° and 41° for the Ti-P, Ti-M and Ti-CB surfaces, respectively. This represents an average decrease of approximately 30%. Collagen coating resulted in a successive increase of the water contact angle compared to PPAAm.

In analogy to these results, the surface energy (Fig. 5) was increased slightly by coating the surfaces with Col. Overall surface energy of the untreated surfaces was increased from 41.3, 35.5

and 46.3 mN m^{-1} for the Ti-P, Ti-M and Ti-CB surfaces, respectively. The highest increase was observed on the PPAAm samples regardless of the topography. On the PPAAm-treated surfaces the values changed to 54.8 , 50.0 and 57.4 mN m^{-1} for the Ti-P, Ti-M and Ti-CB surfaces, respectively.

3.2. Initial cell-surface contact

The initial cell contact with the surfaces was examined using cell adhesion experiments (Fig. 6). We observed cell adhesion of $18 \pm 2\%$ on the untreated smooth surface (Ti-P) after 5 min. Plasma chemical modification of Ti-P with PPAAm resulted in $54 \pm 5\%$ attached cells (Ti-P PPAAm). This represents a 2.9-fold increase in cell adhesion due to a modified surface chemistry.

On the untreated rough surfaces (Ti-M and Ti-CB) $19 \pm 8\%$ and $33 \pm 16\%$ of the cells were attached after 5 min, respectively. In this case modification with PPAAm resulted in $89 \pm 2\%$ and $88 \pm 2\%$ attached cells for Ti-M and Ti-CB, respectively, representing a 4.7-fold and 2.7-fold increase. This reveals that the positive effect is not only additive, but it is likely that a synergistic role is played by topography and chemical modification with PPAAm.

Additional coupling of Col did not lead to increased adhesion values either on the polished or the machined surfaces. Only cell adhesion on Ti-CB surfaces functionalized with PEG DA-Col was visibly but not significantly enhanced.

Spreading was observed on the modified surfaces to obtain results in the medium-term timeframe of minutes–hours after cell-surface contact. Spreading was examined 30, 60 and 180 min after cell seeding (Fig. 7). The cell size could not be validated on corundum-blasted samples due to the extremely rough topography which did not allow the monitoring of the cells with the confocal

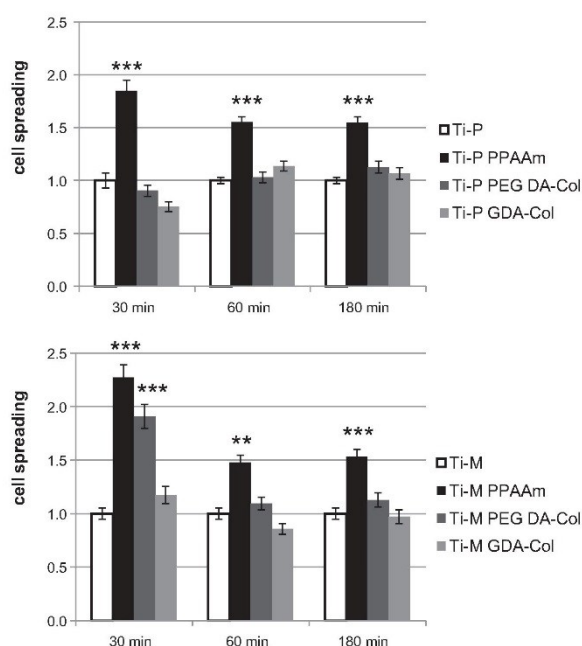


Fig. 7. Spreading of MG-63 cells after 30, 60 and 180 min on Ti-P and Ti-M surfaces; it is noteworthy that modification with PPAAm boosts the initial spreading. LSM 410, $n=40$ ($n=80$ for Ti-P; 60, 180 min), ANOVA post hoc Bonferroni, $^{**}P \leq 0.01$, $^{***}P \leq 0.001$ compared to untreated Ti-P and Ti-M.

Author's personal copy

3846

H. Rebl et al./Acta Biomaterialia 8 (2012) 3840–3851

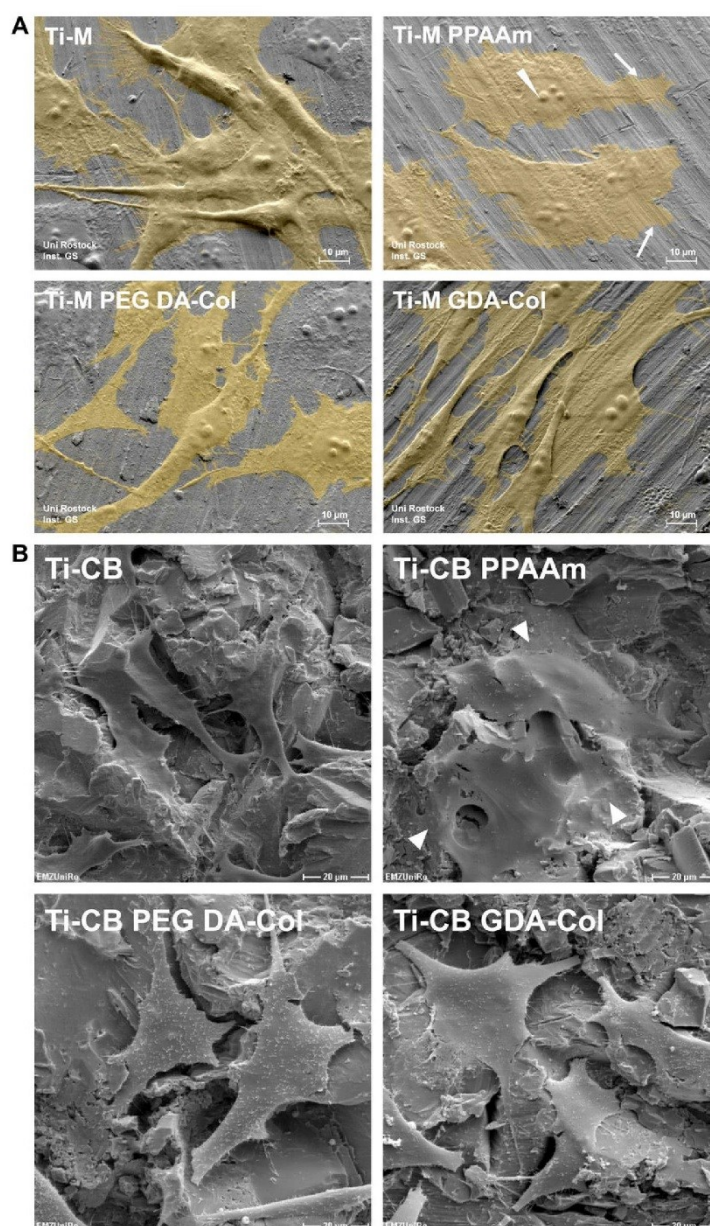


Fig. 8. (A) Morphology of MG-63 cells on untreated and chemically modified Ti-M: note that the positively charged groups (Ti-M PPAAm) allow the cells literally to melt into the groove structure, and the edges of the cells can hardly be distinguished from the surface (arrows). The only convex cellular structures are the nucleoli (arrowhead). FE-SEM (Supra 25, Carl Zeiss); false color with Adobe Photoshop 7.0. (B) Morphology of MG-63 cells on rough untreated and chemically modified Ti-CB: note that cells on the untreated and on both Col-coated Ti-CB surfaces preferentially span the ridges and craters but cells on Ti-CB PPAAm stick to the crater walls and melt with the surface. Thus partial cells on PPAAm can hardly be distinguished from the surface structure (arrowheads). SEM, DSM 960A.

microscope in one horizontal optical plane. Because the cells spanned the craters and spread into the holes of the structure,

the optical error would have been too high to correctly compare the results.



Fig. 9. Nucleoli of MG-63 cells (arrow) stained with SytoRNAgreen: the nucleus is seen in blue (DAPI). Fluorescence microscope AxioScope A1. The insert shows a SEM image of a cell on Ti-M. DSM 960A, bars = 20 μm .

On Ti-P and Ti-M, we observed that there was no significant change in cell area on the Col-coated surfaces compared to the control. However, we found that modification with PPAAm boosts the initial spreading of the osteoblastic cells. Cell area after 30 min was nearly doubled (1.8 for Ti-P, 2.3 for Ti-M). After 60 min the cell area on Ti-M PPAAm was increased by 48% compared to unmodified Ti-M. Comparison of both amino-functionalized surfaces displayed that cell area on Ti-M PPAAm surfaces exceeded the Ti-P PPAAm surface by 10% after 60 min.

3.3. Cell morphology and orientation

In order to detect effects at later time points, cell morphology was observed after 24 h of cell culture (Fig. 8A). Cells on untreated Ti-M seemed to be elongated along the grooved structure and were clearly visible at their extensions. In contrast, on Ti-M chemically modified with PPAAm the edges of the cells could hardly be distinguished from the surface. For this reason we have colored the cells to visualize their entire cell area. The positively charged amino groups of PPAAm allowed the cells literally to melt into the groove structure of the surface. Cells on the surfaces coated with Col mainly expressed the same shape as the control cells, and thus the edges were slightly raised.

We could also observe an impressive effect of the PPAAm-modification on the rough corundum-blasted surfaces (Fig. 8B). Cells on the untreated Ti-CB and the Ti-CB PEG DA-Col surfaces preferentially spanned the craters. When functionalized with amino groups, the surface exhibited an underlayer where the cells stuck to the crater walls and melted with the surface topography. Thus the cells on Ti-CB PPAAm could in part hardly be distinguished from the very rough surface structure.

Only few convex cellular structures could be seen on plasma-functionalized surfaces. We stained the nucleoli and the nucleus to illustrate the distribution of these structures in our MG-63 cells (Fig. 9). From these images we could conclude that the cell morphological structures observed in the SEM images were the nucleoli.

3.4. Actin cytoskeleton

Our observations of the actin cytoskeleton shed light on how chemical modifications can influence the orientation of cells and the alignment of their actin filaments. The actin fibers followed the direction of the grooves on the untreated Ti-M surface and on Ti-M PEG DA-Col and Ti-M GDA-Col (Fig. 10A). In comparison,

on Ti-M functionalized with PPAAm the actin filaments were much thinner and often stretched over the grooves and ridges, and thus proceeded at an angle of 90° to the machined structure. This phenomenon was even more obvious in the overview images (Fig. 10B).

We have quantified the orientation of the cells relative to the grooves (Fig. 11A). The deviation between the cells' orientation and the machined structure accounts for 6° , 11° and 15° on the untreated, PEG DA-Col and GDA-Col surface, respectively.

Having observed that the mean angle between the cells and the surface on the PPAAm-coated surface is 41° , we can conclude that the cells do not follow the direction of the grooves with this amino-modification. This quantification is further proof that the cells can overcome the restrictions of the grooved surface.

The shape index (calculated from actin images) supported this assumption (Fig. 11B). A shape index of 1 represents a perfectly rounded cell. Whereas the cells on the untreated surfaces and the Col-coated surfaces adapted to the underlying structure of the surface and displayed an elongated morphology (shape index of $2.90 \pm 1.0\%$ for Ti-M), the cells on the surfaces chemically modified with PPAAm spread well in all directions and imitated the relief of the structured surface. The shape index for the cells on Ti-M PPAAm was $1.97 \pm 0.8\%$. Thus the cells were less elongated due to the plasma modification.

4. Discussion

Improved hard-tissue repair or replacement has become a very significant challenge for orthopedic biomaterials and orthopedic surgery [34,35]. Meeting these challenges depends on establishing firm relationships between implant success and biomaterial properties that can guide the implant design process [36]. In this paper we present short-term cell adhesion experiments performed to measure the earliest stages of cell–interface interactions as well as medium- to long-term studies (morphology characterization, spreading, actin filament arrangement) regarding the effects on cell behavior on the different substrates.

Of course, a distinction has to be made between macro (above cell size) and micro (below cell size) surface features [37]. It is important to keep in mind that here only the microroughness of the topography is considered. Atomic force microscopy measurements revealed a surface layer thickness of $0.052 \mu\text{m}$ and an average roughness $R_a = 0.25 \text{ nm}$ (i.e. $R_a = 0.00025 \mu\text{m}$) for PPAAm [33]. This layer is nearly negligible if a microroughness of $R_a = 0.315 \mu\text{m}$ for machined and $R_a = 4.140 \mu\text{m}$ for corundum-blasted surfaces is considered.

A very general rule concerning material properties and cell–surface compatibility emerging from decades of focused research is that adherent mammalian cells favor modestly hydrophilic surfaces exhibiting a water contact angle of 40° – 60° [38–40]. The water contact angle of pure titanium used in our experiments is in the range of 60° – 80° . The functionalization of the surface with PPAAm results in a water contact angle of 40° – 55° , thus moving the specified surfaces into the aforementioned “biocompatibility window”.

The surface free energy is highest on the allylamine-coated surfaces of one roughness. The main increase can be seen in the polar part. Polar groups created by plasma polymerization of allylamine include amino groups and a small amount oxygen groups that carry charges and thus induce a certain polarity. The well-directed deposition of amino groups was shown to increase cell adhesion, spreading and proliferation [41,42].

It has been reported that cell adhesion and proliferation depend on surface chemistry and vary with individual functional groups rather than general surface properties such as surface wettability

3848

H. Rebel et al./Acta Biomaterialia 8 (2012) 3840–3851

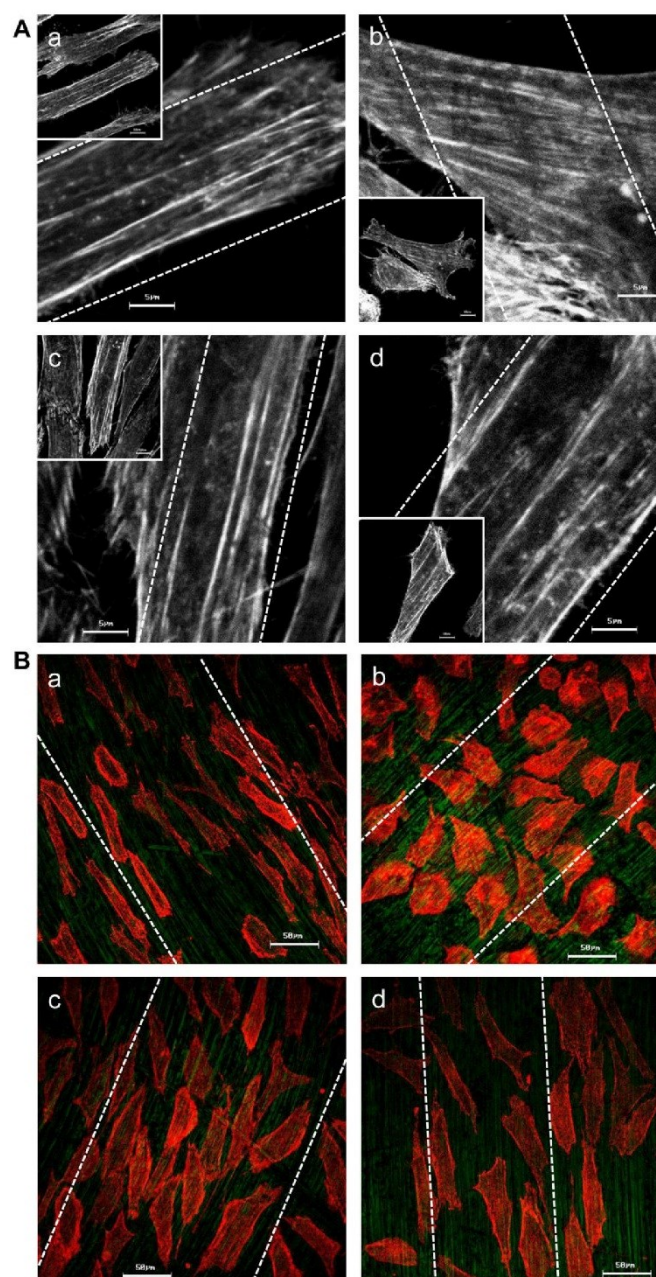


Fig. 10. (A) Actin cytoskeleton of MG-63 cells after 24 h on untreated Ti-M (a), Ti-M PPAAm (b), Ti-M PEG DA-Col (c) and Ti-M GDA-Col (d): It can clearly be seen that not only the cells but also the actin fibers are aligned (a, c, d). However, it is important to note that the actin fibers on Ti-M PPAAm (b) are not arranged likewise. Here, the cells and their actin fibers can overcome the grooved structure. The insert shows an overview of the whole cell; direction of grooves of the machined surface in white dotted lines. LSM 410; bars = 5 μm, bars insert = 10 μm. (B) Alignment of MG-63 cells after 24 h on untreated Ti-M (a), Ti-M PPAAm (b), Ti-M PEG DA-Col (c) and Ti-M GDA-Col (d). Actin is stained in red; Ti surface is false colored in green. The direction of the grooves of the machined surface is indicated with white dotted lines. It is clearly visible that the cells are elongated along the grooves and ridges (a, c, d) except for PPAAm (b). Here, cell growth is not oriented due to the dominance of the plasma chemistry. LSM 410, bar = 50 μm.

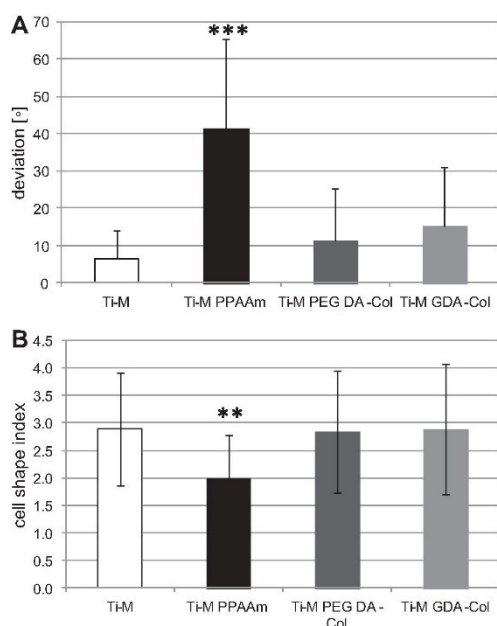


Fig. 11. (A) Mean deviation of the cells' orientation in relation to the grooved surface Ti-M. It is clearly visible that the cells follow the surface features very strictly except for PPAAm-coated surfaces. Here a high deviation could be found, indicating that the cells overcome the restrictions of the surface and spread out in all directions. \pm SD, $n = 90$ –110, ANOVA post hoc Bonferroni, *** $P \leq 0.001$. (B) Cell shape index of MG-63 cells on Ti-M: a cell shape index = 1 represents a rounded cell; higher values indicate that the cell is elongated. Note the significantly lower cell shape index on PPAAm, indicating that the cells are not aligned but spread in all directions (see Fig. 10). $n = 40$, ANOVA post hoc Bonferroni, ** $P \leq 0.01$.

[22]. We used two different collagen-coated surfaces and a surface coated with PPAAm to elucidate the adhesion behavior of osteoblastic cells. It is of primary importance to find out how the modification of an implant surface by chemical means can play a role in bone tissue engineering. In our experiments we demonstrate that increasing roughness alone results in an elevated cell attachment. Our results are in agreement with Keller et al. [43], who report that in their in vitro experiments the highest level of rat osteoblast cell attachment was obtained with rough, sandblasted Ti-6Al-4V surfaces compared to grooved ones. According to Anselme et al. [44], cells prefer surfaces with a relatively high microroughness amplitude ($R_a = 0.37 \mu\text{m}$ and $R_z = 4.13 \mu\text{m}$) and with a low level of repeatability (order $\sim 10\%$) in their in vitro experiments. Thus, the greater attachment of the osteoblastic cells on the corundum-blasted samples determined in our experiments might be due to the greater roughness and the random structure of the blasted surface.

We determined that cell adhesion is significantly enhanced on the positively charged PPAAm-coated surfaces, irrespective of the topography. However, the increase is highest on the microstructured surfaces (Ti-M PPAAm ~ 5 -fold). Hence the effect of roughness and chemical modification combine, and yield an enormous increase in cell adhesion. In contrast, additional coupling of collagen I to the different roughnesses does not enhance cell adhesion in a similar fashion. This makes clear that the choice of chemical functionalization used is crucial. A general conclusion drawn from data at hand is that positive charges alone are more significant

than cell matrix components for facilitating and enhancing osteoblastic cell attachment to a biomaterial surface.

Enhancing directed cell attachment is pivotal, especially if the situation after an implantation or operation is considered: cells, including osteoblasts, fibroblasts etc., and bacteria are in a crucial race to the surface [45], and for a positive outcome of the operation it is essential that there is complete fusion between the implant surface and bone tissue without any infection or fibrous tissue surrounding the implant [39,46–48].

We determined cell spreading at different time points and could clearly show that, again, the PPAAm surface displays clear advantages over both the collagen-coated and the untreated surfaces. These strong positive effects of PPAAm on cell spreading could be verified with human bone marrow stem cells [49]. At the early time points it is even more obvious that cells can spread faster and exhibit more extensions.

In contrast, the cells on the collagen-coated surfaces do not spread faster than on the untreated control. We used two different linkers for collagen I coupling. We assume that the chain length of the linker influences the stiffness of the collagen bonding—the shorter the chain length, the more inflexible is the bonding and the worse is the cell growth. PEG-DA has a chain length of about 3.8 nm and GDA of about 1.2 nm. We considered whether cells grown on Col bonded via the longer-chain PEG-DA grow better than cells bonded via the shorter GDA chain, because the self-adjustment of cells onto Col could be better realized by bonding via PEG-DA. This might explain why the cells tend to adhere better to PEG DA-Col surfaces than to GDA-Col. In analogy to this, the cell spreading on the machined surfaces is also better on the PEG DA-Col surface.

After 24 h the increase of cell spreading on PPAAm is still visible but the cells on the collagen-coated surfaces have caught up. This might be due to the fact that there is a maximum size the cells can reach. Liu et al. postulated a time–cell–substratum compatibility principle in which similar bioadhesive outcomes can be achieved on all surfaces, but the time required to arrive at this outcome increases with decreasing cell–substratum compatibility [36].

SEM images reveal that cells on PPAAm are spread out very flatly. On the rough PPAAm surfaces it becomes evident that the cells can really adapt to the surface structure. In contrast, on chemically untreated surfaces the cells would span over the craters. This shows that the cells can overcome the hurdles of the grooves and hills because of the chemical modification with amino groups. We hypothesize that a better distribution of the cells over the implant surface and a closer cell–surface contact due to the higher contact area could result in a faster ingrowth of the implant into the bone. We have shown earlier that the cells' metabolism is not affected although the cells are flattened and stick close to the surface [33,50]. In this paper we are able to show that the cells are flattened but the nucleoli are still visible as convex structures. As they are the sites of rRNA synthesis, this is further proof that there is no obvious impairment, although the cell profile is extremely flattened on the PPAAm-modified surfaces.

Several authors have shown that osteoblast-like cells cultured on materials with micron-scale grooves or channels become elongated parallel to the direction of the grooves [7,44,51,52]. We could also observe this effect on our unmodified and on both collagen-coated Ti-M surfaces. The cells are oriented in the direction of the grooves and also their actin cytoskeleton is aligned in this direction. However, on PPAAm-coated surfaces the cells can overcome the lined structure and grow diagonally to the grooves and hills. The cytoskeleton is not oriented in an particular direction, although it sometimes follows the grooves.

Indeed, the observation that a plasma-chemical surface modification allows the cells to overcome the restrictions of the surface topography has not previously been elucidated in the literature.

Here we are able to demonstrate for the first time that the altered alignment behavior of the cells on plasma-functionalized surfaces (PPAAm) is only due to the chemical modification with amino groups. We find this striking because it is very clear that the plasma chemical functionalization of a surface is dominant over its topography.

We believe that the combination of topography and chemical modifications results in truly bone-resembling coatings and that, as Dowling et al. [53] suggested, the interactions of the phenomena taking place in cell–material interactions can only be elucidated if both surface roughness and chemistry are optimized to design new biomaterial surfaces.

5. Conclusion

The cell response in the initial phase can be significantly enhanced by the combined effect of topographical and plasma-chemical modification if positive charges are used. In contrast, collagen I via PEG DA or GDA linker on structured Ti surfaces does not comparably improve osteoblast adhesion, although collagen is a ligand for the cell adhesion receptors.

In this paper we describe how short-term cell adhesion experiments, performed to measure the earliest stages of cell–interface interactions, reveal an additional significant increase in cell adhesion on PPAAm-modified rough surfaces. SEM images show a flattened phenotype and cells which seemingly melt into the grooved structure of Ti–M PPAAm. Morphological images and staining of the actin cytoskeleton reveal that the cells can overcome the restrictions of the grooved topography and adapt to the surface structure when grown on PPAAm-coated Ti–M surfaces. Here we are able to demonstrate that cell orientation and alignment due to topography can be overcome if a surface is well-directed plasma-chemically modified.

Acknowledgements

The authors thank E. Pauthe (University of Cergy-Pontoise, France) and T. Vorhaben (INP) for fruitful discussions. The excellent technical assistance of A. Schella, U. Kellner U. Lindemann, R. Ihrke, M. Brüser and G. Friedrichs (INP) is kindly acknowledged. We kindly thank Dr. A. Weidmann (formerly University of Rostock) for excellent support. This work was realized within the framework of the multidisciplinary research cooperation "Campus PlasmaMed", particularly within the project "Plasmalmp". The financial support of the German Ministry of Education and Research (BMBF, Grant Nos. 13N9779, 13N11188) for H.R. and B.F. is gratefully acknowledged. We appreciate the technical assistance of the EMZ at University of Rostock.

References

- Brånemark PI, Adell R, Albrektsson T, Lekholm U, Lundkvist S, Rockler B. Osseointegrated titanium fixtures in the treatment of edentulousness. *Biomaterials* 1983;4:25–8.
- Balazic M, Kopac J, Jackson JM, Ahmed W. Titanium and titanium alloys in medicine. *Int J Nano Biomater* 2007;1:3–34.
- Liu X, Chu PK, Ding C. Surface modification of titanium, titanium alloys, and related materials for biomedical applications. *Mater Sci Eng* 2004;R47:49–121.
- Niinomi M. Mechanical biocompatibilities of titanium alloys for biomedical applications. *J Mech Behav Biomed Mater* 2008;1:30–42.
- Anselme K. Osteoblast adhesion on biomaterials. *Biomaterials* 2000;21:667–81.
- Tsukimura N et al. The effect of superficial chemistry of titanium on osteoblastic function. *J Biomed Mater Res A* 2008;84(1):108–16.
- Lüthen F, Lange R, Becker P, Rychly J, Beck U, Nebe JB. The influence of surface roughness of titanium on beta1- and beta3-integrin adhesion and the organization of fibronectin in human osteoblastic cells. *Biomaterials* 2005;26(15):2423–40.
- Lange R, Lüthen F, Beck U, Rychly J, Baumann A, Nebe B. Cell-extracellular matrix interaction and physico-chemical characteristics of titanium surfaces depend on the roughness of the material. *Biomol Eng* 2002;19:255–61.
- Ranucci CS, Moghe PV. Substrate microtopography can enhance cell adhesive and migratory responsiveness to matrix ligand density. *J Biomed Mater Res* 2001;54:149–61.
- Mendonca DBS, Miguez PA, Mendonca G, Yamauchi M, Aragao FJL, Cooper LF. Titanium surface topography affects collagen biosynthesis of adherent cells. *Bone* 2011;49(3):463–72.
- Hatano K, Inoue H, Kojo T, Matsunaga T, Tsujisawa T, Uchiyama C, et al. Effect of surface roughness on proliferation and alkaline phosphatase expression of rat calvarial cells cultured on polystyrene. *Bone* 1999;25:439–45.
- Boyan BD, Hummert TW, Dean DD, Schwartz Z. Role of material surfaces in regulating bone and cartilage cell response. *Biomaterials* 1996;17:137–46.
- Barbour ME, O'Sullivan DJ, Jenkinson HF, Jagger DC. The effects of polishing methods on surface morphology, roughness and bacterial colonisation of titanium abutments. *J Mater Sci: Mater Med* 2007;18:1439–47.
- Szmukler-Moncler S, Perrin D, Ahoissi V, Magnin G, Bernard JP. Biological properties of acid etched titanium implants: effect of sandblasting on bone anchorage. *J Biomed Mater Res B: Appl Biomater* 2004;68:149–59.
- Park KH, Heo SJ, Koak JY, Kim SK, Lee JB, Kim SH, et al. Osseointegration of anodized titanium implants under different current voltages: a rabbit study. *J Oral Rehabil* 2007;34:517–27.
- Anselme K, Bigerelle M. Role of materials surface topography on mammalian cell response. *Int Mater Rev* 2011;56(4):243–66.
- Morra M. Biomolecular modification of implant surfaces. *Expert Rev Med Devices* 2007;4:361–72.
- Narayanan R, Seshadri SK, Kwon TY, Kim KH. Calcium phosphate-based coatings on titanium and its alloys: a review. *J Biomed Mater Res B: Appl Biomater* 2008;85:279–99.
- Schuler M, Trentin D, Textor M, Tosatti SG. Biomedical interfaces: titanium surface technology for implants and cell carriers. *Nanomedicine* 2006;1:449–63.
- García AJ, Collard DM, Keselowsky BG, Cutler SM, Gallant ND, Byers BA, et al. Engineering of integrin-specific biomimetic surfaces to control cell adhesion and function. In: Dillow AK, Lowman AM, editors. *Biomimetic materials and design*. New York: Dekker; 2000. p. 29–55.
- Fauchoux N, Tzoneva R, Nagel MD, Groth T. The dependence of fibrillar adhesions in human fibroblasts on substratum chemistry. *Biomaterials* 2006;27:234–45.
- Schweiki H, Müller R, Englert C, Hiller KA, Kujat R, Nerlich M, et al. Proliferation of osteoblasts and fibroblasts on model surfaces of varying roughness and surface chemistry. *J Mater Sci: Mater Med* 2007;18:1895–905.
- Nebe B et al. Improved initial osteoblast functions on amino-functionalized titanium surfaces. *Biomol Eng* 2007;24(5):447–54.
- Finke B et al. The effect of positively charged plasma polymerization on initial osteoblastic focal adhesion on titanium surfaces. *Biomaterials* 2007;28(30):4521–34.
- Hamerli P, Weigel T, Groth T, Paul D. Surface properties of and cell adhesion onto allylamine-plasma coated polyethyleneterephthalate membranes. *Biomaterials* 2003;24:3989–99.
- Ren TB, Weigel T, Groth T, Lendlein A. Microwave plasma surface modification of silicone elastomer with Allylamine for improvement of biocompatibility. *J Biomed Mater Res A* 2008;86(1):209–19.
- Harsch A, Calderon J, Timmons RB, Gross GW. Pulsed plasma deposition of allylamine on polysiloxane: a stable surface for neuronal cell adhesion. *J Neurosci Methods* 2000;98:135–44.
- Owens DK, Wendt RC. Estimation of surface free energy of polymers. *J Appl Polym Sci* 1969;13:1741–7.
- Rabel W. Einige Aspekte der Benetzungstheorie und ihre Anwendungen auf die Untersuchung und Veränderung der Oberflächeneigenschaften von Polymeren. *Farbe und Lack* 1971;77:997–1005.
- Schröder K et al. Similarities between plasma amino functionalized PEEK and titanium surfaces concerning enhancement of osteoblast cell adhesion. *J Adhes Sci Technol* 2010;24(5):905–23.
- Beamson G, Briggs D. The scientia ESCA 300 database. New York: John Wiley; 1992. p. 202.
- Wende K, Schroder K, Lindequist U, Ohl A. Plasma-based modification of polystyrene surfaces for serum-free culture of osteoblastic cell lines. *Plasma Process Polym* 2006;3:524–31.
- Rebl H, Finke B, Ihrke R, Rothe H, Rychly J, Schroeder K, et al. Positively charged material surfaces generated by plasma polymerized allylamine enhance vinculin mobility in vital human osteoblasts. *Adv Eng Mater* 2010;12:B356–64.
- Kiberstis P, Smith O, Norman C. Bone health in the balance. *Science* 2000;289:1497.
- Rodan GA, Martin TJ. Therapeutic approaches to bone diseases. *Science* 2000;289:1508–14.
- Liu X, Lim JY, Donahue HJ, Dhurjati R, Mastro AM, Vogler EA. Influence of substratum surface chemistry/energy and topography on the human fetal osteoblastic cell line hFOB 1.19: phenotypic and genotypic responses observed in vitro. *Biomaterials* 2007;28:4535–50.
- Vercaigne S, Wolke JGC, Naert I, Jansen JA. Histomorphometrical and mechanical evaluation of titanium plasma-spray-coated implants placed in the cortical bone of goats. *J Biomed Mater Res* 1998;41:41–8.

Author's personal copy

H. Rebl et al./Acta Biomaterialia 8 (2012) 3840–3851

3851

- [38] Vogler EA, Bussian RW. Short-term cell-attachment rates: a surface sensitive test of cell-substrate compatibility. *J Biomed Mater Res* 1987;21:1197–211.
- [39] Donahue HJ, Siedlecki CA, Vogler E. Osteoblastic and osteocytic biology and bone tissue engineering. In: Hollinger JO, Einhorn TA, Doll B, Sfeir C, editors. *Bone tissue engineering*. Boca Raton, FL: CRC Press; 2004. p. 44–54.
- [40] Lim JY, Liu X, Vogler EA, Donahue HJ. Systematic variation in osteoblast adhesion and phenotype with substratum surface characteristics. *J Biomed Mater Res* 2004;68A:504–12.
- [41] Nebe JB, Jesswein H, Weidmann A, Finke B, Lange R, Beck U, et al. Osteoblast sensitivity to topographical and chemical features of titanium. *Mater Sci Forum* 2010;638–642:652–7.
- [42] Kubies D et al. The interaction of osteoblasts with bone-implant materials: 1. The effect of physicochemical surface properties of implant materials. *Physiol Res* 2011;60:95–111.
- [43] Keller JC, Stanford CM, Wightman JP, Draughn RA, Zaharias R. Characterizations of titanium implant surfaces.3. *J Biomed Mater Res* 1994;28:939–46.
- [44] Anselme K, Biggerelle M, Noël B, Lost A, Hardouin P. Effect of grooved titanium substratum on human osteoblastic cell growth. *J Biomed Mater Res* 2002;60(4):529–40.
- [45] Gristina AG. Biomaterial-centered infection – microbial adhesion versus tissue integration. *Science* 1987;237(4822):1588–95.
- [46] Anselme K, Noel B, Hardouin P. Human osteoblast adhesion on titanium alloy, stainless steel, glass and plastic substrates with same surface topography. *J Mater Sci Mater Med* 1999;10:815–9.
- [47] Keller JC, Collins JG, Niederauer GG, McGee TD. In vitro attachment of osteoblast-like cells to osteoceramic materials. *Dent Mater* 1997;13:62–8.
- [48] Zinger O et al. Time-dependent morphology and adhesion of osteoblastic cells on titanium model surfaces featuring scale-resolved topography. *Biomaterials* 2004;25:2695–711.
- [49] Schröder K et al. Capability of differently charged plasma polymer coatings for control of tissue interactions with titanium surfaces. *JAST* 2010;24:1191–205.
- [50] Rebl H, Finke B, Schroeder K, Nebe JB. Time-dependent metabolic activity and adhesion of human osteoblast-like cells on sensor chips with a plasma polymer nanolayer. *Int J Artif Organs* 2010;33:738–48.
- [51] Chesmel KD, Clark CC, Brighton CT, Black J. Cellular responses to chemical and morphologic aspects of biomaterial surfaces.2. The biosynthetic and migratory response of bone cell-populations. *J Biomed Mater Res* 1995;29:1101–10.
- [52] Lange R et al. Titanium surfaces structured with regular geometry – material investigations and cell morphology. *Surf Interface Anal* 2010;42(6–7):497–501.
- [53] Dowling DP, Miller IS, Ardhaoui M, Gallagher WM. Effect of surface wettability and topography on the adhesion of osteosarcoma cells on plasma-modified polystyrene. *J Biomater Appl* 2011;26(3):327–47.

2.4 Study IV

Holger Testrich, Henrike Rebl, Birgit Finke, Frank Hempel, Barbara Nebe, Jürgen Meichsner

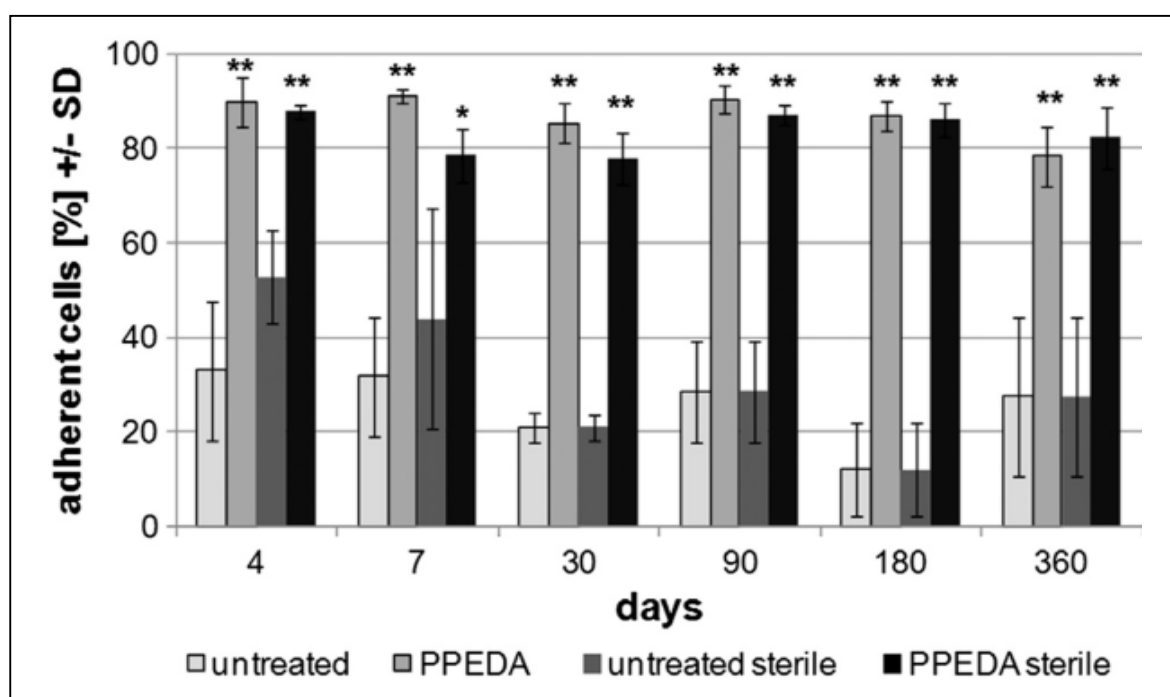
Aging effects of plasma polymerized ethylenediamine (PPEDA) thin films on cell-adhesive implant coatings.

Mater. Sci. Eng., C C 33 (2013) 3875–3880.

Abstract

This article deals with the characterization of a plasma polymer layer using the precursor ethylenediamine (PPEDA). Thin films with a thickness of 50-100 nm were deposited on biomedical titanium substrates. Layer characterization and optimization was attended by surface characterization techniques e.g. x-ray photoelectron spectroscopy (XPS), water contact angle measurements (WCA), fourier transform infrared spectroscopy (FTIR). Cellular behavior was analyzed by flow cytometry (cell adhesion) and scanning electron microscopy (cell shape). All Samples coated with PPEDA were biocompatible and the cells showed a well spread phenotype after 24h. This positive effect of PPEDA on cell adhesion and spreading could be observed even when the samples were sterilized and stored for 360 days. This makes these surfaces highly attractive for the clinical application.

Graphical abstract:





Aging effects of plasma polymerized ethylenediamine (PPEDA) thin films on cell-adhesive implant coatings

H. Testrich^{a,*}, H. Rebl^b, B. Finke^c, F. Hempel^c, B. Nebe^b, J. Meichsner^a

^a University of Greifswald, Institute of Physics, Felix-Hausdorff Str. 6, 17489 Greifswald, Germany

^b University of Rostock, Biomedical Research Center, Department of Cell Biology, Schillingallee 69, 18057 Rostock, Germany

^c Leibniz Institute for Plasma Science and Technology, Felix-Hausdorff Str. 2, 17489 Greifswald, Germany

ARTICLE INFO

Article history:

Received 30 October 2012

Received in revised form 27 March 2013

Accepted 10 May 2013

Available online 18 May 2013

Keywords:

RF plasma

Ethylenediamine

Plasma polymerization

Implant coating

Aging effects

Osteoblast adhesion

ABSTRACT

Thin plasma polymer films from ethylenediamine were deposited on planar substrates placed on the powered electrode of a low pressure capacitively coupled 13.56 MHz discharge. The chemical composition of the plasma polymer films was analyzed by Fourier Transform Infrared Reflection Absorption Spectroscopy (FT-IRRAS) as well as by X-ray photoelectron spectroscopy (XPS) after derivatization of the primary amino groups. The PPEDA films undergo an alteration during the storage in ambient air, particularly, due to reactions with oxygen. The molecular changes in PPEDA films were studied over a long-time period of 360 days. Simultaneously, the adhesion of human osteoblast-like cells MG-63 (ATCC) was investigated on PPEDA coated corundum blasted titanium alloy (Ti-6Al-4V), which is applied as implant material in orthopedic surgery. The cell adhesion was determined by flow cytometry and the cell shape was analyzed by scanning electron microscopy. Compared to uncoated reference samples a significantly enhanced cell adhesion and proliferation were measured for PPEDA coated samples, which have been maintained after long-time storage in ambient air and additional sterilization by γ -irradiation.

© 2013 Elsevier B.V. All rights reserved.

1. Introduction

The development of novel bioactive surfaces for the improvement of orthopedic implant materials is in the focus of biomedical research. The fast and permanent attachment of osteoblast cells on the implant material is an essential point to achieve a stable bone-implant interface. Bioactive coatings have to fulfill specific requirements which are important for subsequent use, such as mechanical stability and adequate density of functional groups, e.g., primary amino groups and other nitrogen functionalities, or surface charge. Different techniques can be used to deposit thin films with various functional groups. Compared to other techniques in surface modification, the non-thermal plasma technology offers the advantages that it is an energy efficient and dry technique whereby only the top layer of the material is modified, whereas the bulk material remains unchanged [1,2]. This is highly desired in the field of orthopedic surgery, because it enables the modification of existent, commercially available implant materials [3]. The cell functions can be improved by deposition of plasma polymer films containing positively charged functional groups [4–6]. Different plasma processes and precursors were already investigated, for example allylamine [7–10], ethylenediamine [11,12], propylamine [13] or cyclopropylamine [14] as well as mixtures of hydrocarbons with nitrogen or ammonia [15,16]. Here, the preparation of nitrogen-rich surfaces has

been demonstrated an efficient way to improve the cell attachment, spreading proliferation and occupation via migration capacity.

In this work, the deposition of cell-adhesive thin plasma polymer films from ethylenediamine (EDA, $\text{H}_2\text{N}-\text{CH}_2-\text{CH}_2-\text{NH}_2$) was investigated using low pressure capacitively coupled radio-frequency (RF) plasma at 13.56 MHz [17]. The ethylenediamine is of special interest concerning the high N/C ratio of 1:1 and two primary amino groups in the precursor molecule. The paper reports on the aging of plasma polymerized ethylenediamine (PPEDA) films during storage under ambient air up to 360 days. In particular, the chemical modification of the PPEDA films and their influence on the initial adhesion and proliferation of osteoblast cells are discussed.

2. Materials and methods

2.1. Substrate materials

The PPEDA films were deposited on different substrate materials. Planar circular samples from Ti-6Al-4V alloy were coated for cell adhesion tests. These samples with a diameter of 11 mm have been corundum blasted (CB) to achieve a surface roughness of $R_a = 20 \pm 5 \mu\text{m}$. Furthermore, glass plates ($20 \times 60 \text{ mm}^2$) with highly reflective aluminum layer and silicon wafer were applied as substrate material for thin film analysis by FT-IRRAS and ellipsometry, respectively.

* Corresponding author. Tel.: +49 3834 86 4743; fax: +49 3834 86 4701.
E-mail address: holger.testrich@uni-greifswald.de (H. Testrich).

2.2. Deposition of plasma polymerized ethylenediamine (PPEDA) thin films

Fig. 1 shows a sketch of the experimental set-up used for the synthesis of thin nitrogen-rich organic films by ethylenediamine (EDA) plasma polymerization. The stainless steel vacuum chamber with the diameter and height of 400 mm, respectively, was pumped by a turbo pump to a base pressure of 10^{-5} Pa. A stage rotary pump ensured a total processing gas pressure of between 20 and 200 Pa. The processing gas was a mixture of the carrier gas argon and the precursor ethylenediamine (ETHYLENDIAMIN ROTIPURAN®, $\geq 99.5\%$, p.a., Carl Roth GmbH + Co. KG, Germany). The liquid precursor EDA in the storage vessel was held on a temperature of about 30 °C to ensure a constant vapor pressure. The gas flow rate could be varied between 4 and 60 sccm for argon by mass flow controller and between 4 and 20 sccm for EDA, which was adjusted manually by a needle valve. Thereby, the EDA gas supply system including the needle valve was heated to avoid condensation. The discharge configuration consists of a planar water cooled electrode (diameter 100 mm), which was powered by an RF generator at 13.56 MHz via matching network. The shielding of the powered electrode and the chamber wall were grounded. The asymmetric RF discharge operated in pulsed mode using a combination of a pulse-delay generator with the RF power generator. A typical set of plasma processing parameter was 60 W forward RF power, 10 Hz pulse frequency at 50% duty cycle, 60 Pa total pressure of an argon to EDA mixture of 5:1, and 24 sccm total gas flow rate.

The PPEDA thin film thickness was determined by spectroscopic ellipsometry taking into account a single layer Cauchy dispersion model for PPEDA on silicon substrate. The typical PPEDA film thickness ranged between 50 and 80 nm. Immediately after the deposition the coated samples were stored under ambient conditions in plastic boxes. Subsequently, the thin film aging and its influence on the cell adhesion were tested on independent samples after different storage times up to 360 days.

2.3. Thin film analysis by Fourier Transform Infrared Reflection Absorption Spectroscopy (FT-IRRAS)

The chemical composition and the molecular structure of PPEDA thin films and their changes were analyzed by FT-IRRAS. Here, the classical IRRAS arrangement, [18], was applied by means of a vacuum FTIR spectrometer Vertex 80v (Bruker) with a specific reflection unit in the sample compartment providing parallel-polarized light at grazing incidence of 75°. The thin film absorption was measured in the wave number range of between 3500 and 800 cm^{-1} at a spectral resolution of 0.3 cm^{-1} by the MCT detector. The data acquisition and processing software OPUS was applied to generate the thin film absorption spectrum.

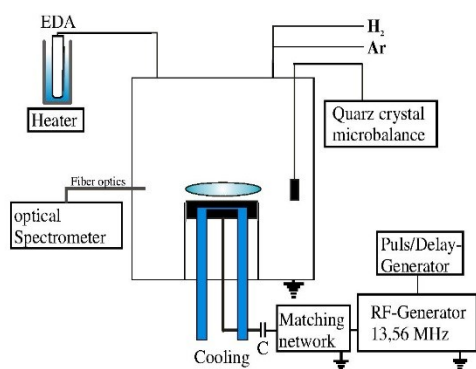


Fig. 1. Sketch of the experimental set-up with low pressure RF discharge configuration.

2.4. Surface analysis by X-ray Photoelectron Spectroscopy (XPS)

The XPS measurements were performed using an AXIS Ultra DLD electron spectrometer (Kratos Analytical, GB) equipped with a monochromatic aluminum K_{α} X-ray source (1486 eV; 150 W), implemented charge neutralization, and pass energy of 80 eV for the determination of the chemical elemental composition, or 10 eV for highly resolved C1s spectra. N(C, H) moieties in different configurations and conformations, e.g., amines, imines and nitriles exhibit only very small shifts in N1s binding energy and, therefore, it could not be quantified by highly resolved XPS measurements. Chemical derivatization reactions have to be applied for the quantification of a specific functional group in mixture of different moieties typical for plasma functionalization processes. Gas phase processes are advantageous in this case. In particular, the primary amino groups were quantified by a vapor phase reaction with 4-trifluoromethylbenzaldehyde (TFBA, Sigma-Aldrich, Germany) at 40 °C for 2 h, which was sufficient for the complete derivatization reaction of the surface. The elemental fluorine content was determined by XPS. Three fluorine atoms mark one primary amino group via the following reaction:



Data acquisition and processing was performed with the vision 2.1.3 software (operating software Kratos). The peak fitting was processed with the help of CasaXPS software version 2.2 (Casa Software Ltd., UK) using the Gauss-Lorentz (30% Lorentz) distribution, linear baseline and a fixed FWHM between 1.1 and 1.5 eV. All values are presented in at.-% and corresponding element ratio, [19–22].

2.5. Cell adhesion and morphology tests

The human osteoblast cell line MG-63 (ATCC, CRL-1427, LGC Promochem, Wesel, Germany) was applied for the cell adhesion experiments. The cells were cultured in 75 cm^2 flasks in Dulbecco's modified Eagle's medium (DMEM) with 10% fetal calf serum (FCS, PAA), and 1% gentamicin (Ratiopharm GmbH, Ulm, Germany) at 37 °C in a humidified atmosphere with 5% CO_2 . Suspended MG-63 cells were seeded onto the samples for 10 min at a density of 5×10^4 /specimen, and non-adherent cells in the supernatant were counted and analyzed by flow cytometry (FACSCalibur, BD Biosciences). The software CellQuest Pro 4.0.1 was used for data acquisition. Cell adhesion was then calculated in percent to the initial cell number.

After 24 h the cells on the material surface were investigated by the scanning electron microscope (SEM) DSM 960A (Carl Zeiss, Oberkochen, Germany). Thereby, the grown cells on the samples were fixed with 4% glutaraldehyde (1 h), dehydrated through a graded series of acetone, dried in a critical point dryer (K 850, EMITECH, Taunusstein, Germany) and sputtered with a coater (SCD 004, BAL-TEC, Balzers, Lichtenstein). The prepared samples for cell adhesion tests were partly sterilized by γ -irradiation with a dose of 25.0–30.0 kGy at GAMMA-SERVICE Produktbestrahlung GmbH, Radeberg, Germany.

3. Results and discussion

3.1. Absorption spectrum and molecular structure of thin PPEDA films

In Fig. 2 three thin film absorption spectra are shown which were taken from three PPEDA films at a thickness of about 50 nm immediately after the deposition, and after storage over 30 and 360 days under ambient air, respectively. In particular, the PPEDA absorption spectrum immediately after the deposition (day 0) is characterized by absorption bands of the N-H stretching vibrations broadened due to hydrogen bridge bonds ($3500\text{--}3000 \text{ cm}^{-1}$), the C-H symm/asymm. stretching

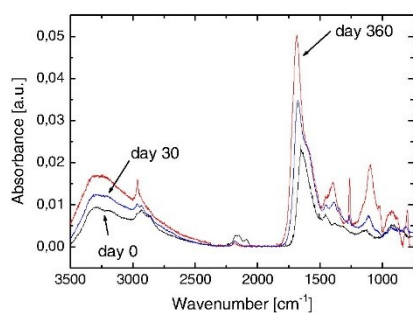


Fig. 2. Thin film IR absorption spectra of PPEDA taken after preparation (day 0, black) and storage in ambient air over 30 (blue) and 360 (red) days, respectively.

vibrations ($2980\text{--}2880\text{ cm}^{-1}$), the stretching vibrations of nitrile $\text{C}\equiv\text{N}$ and carbon-carbon triple bonds $\text{C}\equiv\text{C}$ ($2200\text{--}2150\text{ cm}^{-1}$), the imine group $\text{C}=\text{N}$ and carbon-carbon double bond $\text{C}=\text{C}$ vibrations ($1690\text{--}1650\text{ cm}^{-1}$), as well as the deformation vibrations of the amine group N-H ($1650\text{--}1510\text{ cm}^{-1}$) [12]. The comparison of this absorption spectrum with that taken after 30 and 360 days storage under ambient air reveals significant molecular changes in the PPEDA film. These changes become clearly visible in the difference of the spectra from day 360 and day 0, see Fig. 3. The difference spectrum provides important information about the formation and degradation of molecular groups as well as the broadening and shifting of absorption bands. In particular, the identified characteristic molecular changes are assigned to the formation of O-H groups (stretching vibrations at $3500\text{--}3000\text{ cm}^{-1}$) and carbonyl groups $\text{C}=\text{O}$ (stretching vibrations at $1700\text{--}1680\text{ cm}^{-1}$) which is combined with acid amide formation. In the fingerprint region the observed absorptions can be assigned to the deformation vibrations of C-H and O-H groups at $1465\text{--}1375\text{ cm}^{-1}$ as well as to the stretching vibrations C-N and C-O at about 1250 cm^{-1} and 1100 cm^{-1} , respectively. These absorptions in the fingerprint region are strongly pronounced after 360 days of storage, compare Figs. 2 and 3. This might also be interpreted by a more ordered molecular surrounding due to chemical reactions and relaxation processes inside the cross-linked amorphous plasma polymer film. Furthermore, a loss of the triple bonded $\text{C}\equiv\text{N}$ and $\text{C}\equiv\text{C}$ molecular structures is found. The temporal development of the peak absorbance at selected wave numbers is shown in Figs. 4 and 5.

Over the complete storage time of 360 days a considerable increase of the absorbance is observed in the wave number range between 1700 and 1680 cm^{-1} due to rising content of carbonyl groups in acid amine [10], see Fig. 4. A weaker increase is found for the stretching vibrations

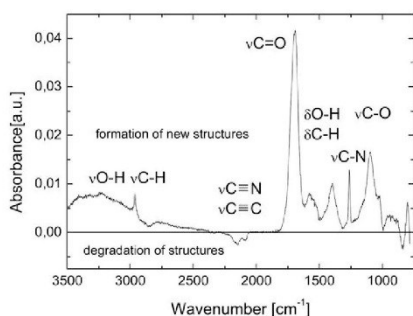


Fig. 3. The difference of the spectra from day 360 and day 0 in Fig. 2 reveals important information about the formation and degradation of characteristic molecular groups.

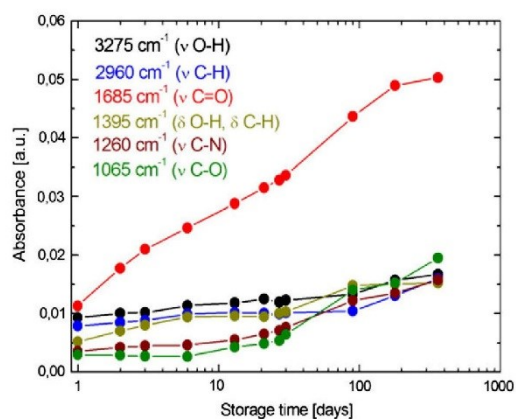


Fig. 4. Temporal evolution of the FTIR peak absorbance from different molecular structures during long-time storage in ambient air over 360 days. In particular, the rising peak absorbance at 1685 cm^{-1} reflects the formation of carbonyl groups ($\text{C}=\text{O}$).

assigned to C-N and C-O in the fingerprint region. On the other hand, the content of the nitrile groups $\text{C}\equiv\text{N}$ decreases continuously over 360 days (logarithmic time scale), whereas the carbon-carbon triple bonds $\text{C}\equiv\text{C}$ are already strongly reduced after 2 days and remain on low level as shown in Fig. 5. Therefore, the alteration of the triple bonded $\text{C}\equiv\text{N}$ and $\text{C}\equiv\text{C}$ in the PPEDA film was investigated more detailed on a short-time scale over 3 h immediately after film deposition. In Fig. 6 the $\text{C}\equiv\text{N}$ and $\text{C}\equiv\text{C}$ peak absorbance is plotted over time during storage of the PPEDA film in vacuum and in contact with atmospheric oxygen from ambient air in the sample compartment of the FTIR-spectrometer, respectively. The storage in vacuum shows no significant effects, whereas the storage in air results in significant decreasing absorbance of the triple bonded carbon ($\text{C}\equiv\text{C}$), see Fig. 6. The absorbance of other molecular structures in PPEDA increases slightly in air at this short time scale, only.

Generally, the plasma polymerization process at low pressure is described by radical reactions on the surface due to adsorption of neutral transient reactive species from precursor fragmentation in the plasma and the plasma-surface interaction (ion bombardment, $(\text{V})\text{UV}$ photons). Following, the plasma polymerization is a plasma-initiated process leading to crosslinked amorphous organic thin film with high content of free radicals as well as more or less concentration of functional groups from the precursor molecule. Free radicals

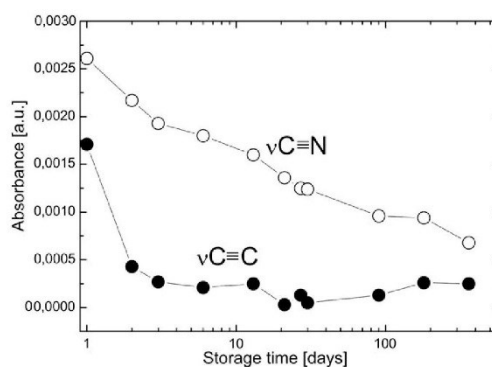


Fig. 5. Temporal evolution of the $\text{C}\equiv\text{N}$ and $\text{C}\equiv\text{C}$ peak absorbance during long-time storage in ambient air over 360 days.

3878

H. Testrich et al. / Materials Science and Engineering C 33 (2013) 3875–3880

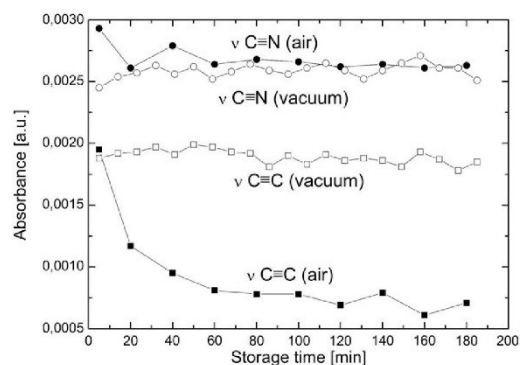


Fig. 6. Temporal evolution of the $C \equiv N$ and $C \equiv C$ peak absorbance immediately after the film deposition. In comparison to the storage of PPEDA in vacuum, the PPEDA film in contact with atmospheric oxygen from ambient air shows a fast loss of the triple bonded carbon over the first 3 h.

remain on the surface and in the film which are able to react immediately with free oxygen from the air by the so-called auto-oxidation processes. Generally, post oxidation of all surface functional groups and carbon itself but also hydration (shown in Figs. 2 and 3) take place during the PPEDA storage on air:

1. An initial bounded carbon radical reacts with oxygen from air to a peroxy radical. In a series of reactions different products can be formed, e.g., carbonyls, carboxyls, new carbon radicals.
2. Furthermore, it is suspected that motile polymer radicals localize at the carbon atom anchor of the electron rich primary amino group and promote their oxidation to acid amide groups and partially into imides [23]. These reactions are very quick. About 60% of the primary amino groups in PPEDA are converted into acid amides in the first 30 days of storage on air, (shown in Figs. 7 and 8) [17].
3. Following, acid amides can be hydrolyzed to carboxylic acid groups and ammonia. Also nitrile hydrolyzes to the same end products. The decreasing curve progression in the FTIR spectra (shown in Figs. 2 and 5) could be explained in this way.

3.2. Elemental composition of the PPEDA surface

X-ray photoelectron spectroscopy (XPS) was applied to investigate the chemical surface composition and the density of amino groups on the surface. The XPS elemental analysis of PPEDA films on Ti-6Al-4V (Ti-CB) substrate revealed pinhole-free films. No titanium signal from

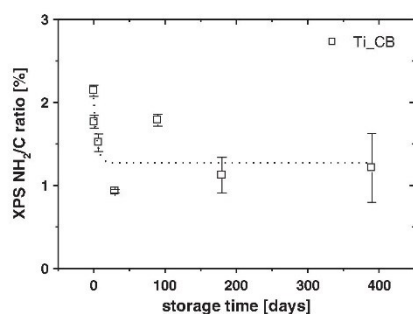


Fig. 7. NH_2/C ratio on PPEDA surface as a function of storage time measured by XPS. The NH_2/C ratio was determined after derivatization of the PPEDA surface with TFBA.

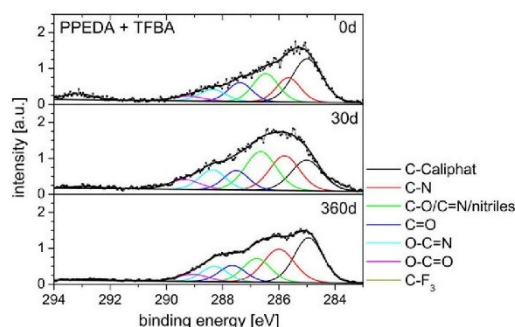


Fig. 8. XPS $C1s$ high resolution spectra of PPEDA after 0, 30 and 360 days storage in ambient air.

the substrate was observed. The aging of the PPEDA on Ti-CB was investigated for one year, respectively. The $C-C/C-H$ component of the $C1s$ peak was adjusted to 285.0 eV. The other components of the $C1s$ peak were assigned to known values [10]: $C-NH$ at 285.8 ± 0.1 eV; $C-O$, $C-O-C$, $C=N$, nitriles at 286.6 ± 0.2 eV, $C=O$ at 287.0 ± 0.3 eV, $O=C-N$ at 288.0 ± 0.3 eV, $O-C=O$ at 289.2 ± 0.2 eV, and CF_3 at 292.7 ± 0.2 eV.

The surface analysis confirms the fast oxidation of the plasma polymerized film by subsiding post plasma processes initiated by the reaction of surface free radicals with atmospheric oxygen after sample storage on air as observed in the FTIR analysis of PPEDA films, see 3.1.

The N/C ratios at the PPEDA surface after plasma polymerization and the following storage for one month as well as one year, respectively, show only a minor change (see Table 1). Since the precursor EDA features a N/C ratio of 1:1 and no oxygen, the measured N/C and O/C elemental ratios on the PPEDA surface prove the instantaneous impact of contact with air to the deposited layers. Whereas no obvious trend is found for O/C , an increase of N/C in the first month is noticeable, followed by constant value during the rest of the aging period. Amino group densities are found to be about 2.2 ± 0.1 % after preparation and with 1.2 ± 0.4 % after 360 days. The aging process causes a loss of about 45–60% of primary amino groups within the first 15 days of storage and a constant level of amino groups of 1.3 ± 0.4 % remains afterwards, shown in Fig. 7, whereas the relative change of the nitrogen content N/C is in the percentage range only (see Table 1).

Fig. 8 compares the high resolution $C1s$ spectra of the PPEDA surface after the preparation and the following aging on ambient air for 30 and 360 days, respectively. Bond changes after 30 and 360 days are clearly visible. The loss of primary amino groups (labeled by the CF_3 -peak at 292.7 eV due to derivatization reaction with TFBA) is obviously accompanied by an oxidation to acid amides at 288.2 eV, increasing $C-O$, $C=N$, nitrile bonds at 286.6 eV and $C=O$ bonds at 287.5 eV in relation to the $C-C$ bond peak at 285.0 eV. Primary amino groups are lost while amide $N-C=O$ and carboxyl $O-C=O$ bonds are increased. The oxidation process causes predominantly an oxidation of carbon atoms with an attached amino group leading to the formation of amides.

Table 1

Elemental ratios at the surface of PPEDA thin film on Ti-6Al-4V for various storage times, analyzed by XPS.

PPEDA (Ti-CB)			
	N/C [%]	O/C [%]	NH_2/C [%]
0 day	30.1 ± 0.7	18.3 ± 1.7	2.2 ± 0.1
30 days	35.9 ± 0.6	27.7 ± 1.4	0.9 ± 0.1
360 days	36.9 ± 2.1	19.1 ± 0.7	1.2 ± 0.4

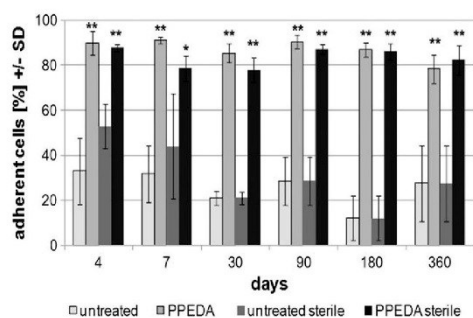


Fig. 9. Initial adhesion (10 min) of MG-63 cells is significantly increased on PPEDA coated compared to uncoated corundum blasted Ti-6Al-4V samples. The enhanced cell adhesion is not influenced by PPEDA film aging over 360 days and an additional sterilization by γ -irradiation. ($n = 5$, Flow Cytometry, FACSCalibur, BD).

3.3. Cell adhesion and morphology

Independent of the storage time of up to one year it was found that the initial cell adhesion after 10 min was significantly increased on Ti-CB samples functionalized with PPEDA, see Fig. 9. Although the PPEDA thin film was already chemically modified within 0–30 days after deposition as shown in Figs. 4–6, the cell adhesion was still increased by approximately 55% at day 360. These results are in good agreement with investigations from other groups using allylamine as precursor [8,10]. High cell adhesion was also found on heptylamine-modified titanium surfaces [24].

Furthermore, our experiments revealed that an additional sterilization process of the PPEDA functionalized samples with γ -irradiation, which is necessary for medical applications, did not influence the improved adhesion behavior of the osteoblast cells.

The same long term stability of the cell attracting capacity of PPEDA was observed by scanning electron microscopy. On the untreated sample the cells are spanned over the craters and developed only few connections to the surface. However, on PPEDA the cells are melted into the rough surface structure and the cell morphology is flattened and well spread, shown in Fig. 10. We assume that this behavior results in an increased contact area between cells and surface and thus most likely to a higher bonding of the implant in the human body.

It seems that nitrogen-containing groups facilitate this spreading behavior of the cells and enable them to melt into the steep and rough terrain. This was also observed on rough titanium substrate coated with a plasma polymerized allylamine layer [5].

4. Summary and conclusions

Nitrogen-rich thin films from plasma polymerization of ethylenediamine in low pressure capacitively coupled RF plasma at 13.56 MHz were studied for cell adhesive implant coatings. At optimized plasma processing parameters the deposited thin PPEDA films on Ti-6Al-4V implant material are mechanical stable and exhibit a significantly enhanced initial adhesion of human osteoblast cells (MG-63) compared to uncoated samples. In particular, the aging of PPEDA thin films was investigated due to storage in ambient air over 360 days. The FT-IRRAS and XPS analysis reveal the reactions with atmospheric oxygen resulting in, e.g., amide, carbonyl and carboxyl groups. The content of primary amine groups is rather low (1–2%). The aging of PPEDA thin films in ambient air as well as an additional

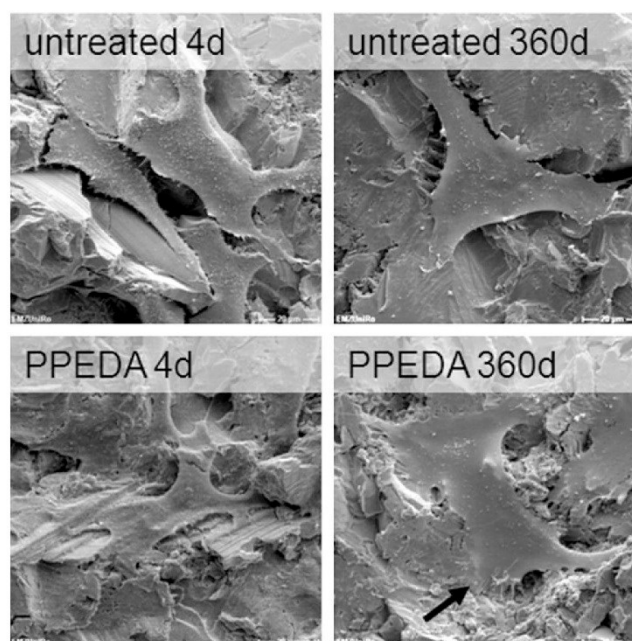


Fig. 10. Morphology of adherent cells on PPEDA thin films observed with scanning electron microscopy (magnification: $\times 1000$). Cells were cultured on the samples for 24 h. Note that cells on PPEDA seem to melt into the rough topography of the corundum blasted Ti-6Al-4V samples also on day 360 (arrow).

sterilization process by γ -irradiation have no influence on the improved cell adhesion and proliferation. Obviously, the high N/C ratio of about 35% and an effective positive surface charge significantly contribute to the enhanced attraction of the osteoblast cells.

Acknowledgements

The authors express their gratitude to V. Danilov for support in IRRAS measurement as well as J. Wenzel and K. Duske for their excellent cell biological support. The investigations were funded by the Federal Ministry of Education and Research (Germany) within the research association "Campus PlasmaMed", Plasmalmp, grant no. 13 N11182, 13 N9775, 13 N9779, and 13 N11188.

References

- [1] R. d'Agostino, Plasma deposition, Treatment and Etching of Polymers, Academic Press, Boston, 1990.
- [2] J. Meichsner, M. Schmidt, R. Schneider, H.-E. Wagner, Nonthermal Plasma Chemistry and Physics, CRC Press, Taylor and Francis Group, 2012.
- [3] F.S. Denes, S. Manolache, Prog. Polym. Sci. 29 (8) (2004) 815–885, <http://dx.doi.org/10.1016/j.progpolymsci.2004.05.001>.
- [4] H. Rebl, B. Finke, J. Rychly, K. Schröder, J.B. Nebe, Adv. Biomater. 12 (2010) 356–364, <http://dx.doi.org/10.1002/adbi.200900070>.
- [5] H. Rebl, B. Finke, R. Lange, K.-D. Weltmann, B. Nebe, Adv. Biomater. 8 (10) (2012) 3840–3851, <http://dx.doi.org/10.1016/j.actbio.2012.06.015>.
- [6] J.B. Nebe, H. Jesswein, A. Weidmann, B. Finke, R. Lange, U. Beck, K. Schroeder, Mater. Sci. Forum vols. 638–642 (2010) 652–657, <http://dx.doi.org/10.4028/www.scientific.net/MSF.638-642.652>.
- [7] J. Friedrich, G. Kühn, R. Mix, A. Fritz, A. Schönhals, J. Adhes. Sci. Technol. 17 (2003) 1591, <http://dx.doi.org/10.1163/156856103322396695>.
- [8] P. Hamerli, T. Weigel, T. Groth, D. Paul, Biomaterials 24 (2003) 3989, [http://dx.doi.org/10.1016/S0142-9612\(03\)00312-0](http://dx.doi.org/10.1016/S0142-9612(03)00312-0).
- [9] R. Förch, Z. Zhang, W. Knoll, Plasma Process. Polym. 2 (2005) 351, <http://dx.doi.org/10.1002/ppap.200400083>.
- [10] B. Finke, F. Luethen, K. Schroeder, P.D. Mueller, C. Bergemann, M. Frant, A. Ohl, J.B. Nebe, Biomaterials 28 (2007) 4521–4534, <http://dx.doi.org/10.1016/j.biomaterials.2007.06.028>.
- [11] T.R. Gengenbach, R.C. Chatelier, H.J. Griesser, Surf. Interface Anal. 24 (1996) 611, [http://dx.doi.org/10.1002/\(SICI\)1096-9918\(19960916\)24:9<611::AID-SIA169>3.0.CO;2-7](http://dx.doi.org/10.1002/(SICI)1096-9918(19960916)24:9<611::AID-SIA169>3.0.CO;2-7).
- [12] J. Kim, D. Jung, Y. Park, Y. Kim, D.W. Moon, T.G. Lee, Appl. Surf. Sci. 253 (2007) 4112–4118, <http://dx.doi.org/10.1016/j.apsusc.2006.09.011>.
- [13] F. Fally, C. Doneux, J. Riga, J.J. Verbist, J. Appl. Polym. Sci. 56 (1995) 597, <http://dx.doi.org/10.1002/app.1995.070560509>.
- [14] L. Denis, P. Marsal, Y. Olivier, T. Gogfroid, R. Lazzaroni, M. Hecc, J. Cornil, R. Snyders, Plasma Process. Polym. 7 (2010) 172, <http://dx.doi.org/10.1002/ppap.200900131>.
- [15] F. Mwal, A. Petit, H. Tian Wang, L.M. Epure, P.L. Girard-Lauriault, J.A. Ouellet, M.R. Wertheimer, J. Antoniou, The Open Orthopaedics Journal 2 (2008) 137–144, <http://dx.doi.org/10.2174/1874325000802010137>.
- [16] A. Gigout, S. Levasseur, P.L. Girard-Lauriault, M.D. Buschmann, M.R. Wertheimer, M. Jolicoeur, Macromol. Biosci. 9 (10) (2009) 979–988, <http://dx.doi.org/10.1002/mabi.200900079>.
- [17] B. Finke, F. Hempel, H. Testrich, A. Artemenko, H. Rebl, O. Kylián, J. Meichsner, H. Biederman, B. Nebe, K.-D. Weltmann, K. Schröder, Surf. Coat. Technol. 205 (2011) S520–S524, <http://dx.doi.org/10.1016/j.surfcoat.2010.12.044>.
- [18] R. Greenler, J. Chem. Phys. 44 (1966) 310, <http://dx.doi.org/10.1063/1.1726462>.
- [19] D.E. Everhart, C.N. Reilly, Anal. Chem. 53 (1981) 665, <http://dx.doi.org/10.1021/ac00227a022>.
- [20] A. Chilkoti, B. Ratner, D. Briggs, Chem. Mater. 3 (1991) 51–61, <http://dx.doi.org/10.1021/cm00013a016>.
- [21] P. Favia, M.V. Stendardo, R. d'Agostino, Plasmas Polym. 1 (1996) 91–112, <http://dx.doi.org/10.1007/BF02532821>.
- [22] K. Schröder, A. Meyer-Plath, D. Keller, W. Besch, G. Babucke, A. Ohl, Contrib. Phys. 41 (2001) 562–572, [http://dx.doi.org/10.1002/1521-3986\(200111\)41:6<562::AID-CTPP562>3.0.CO;2-Y](http://dx.doi.org/10.1002/1521-3986(200111)41:6<562::AID-CTPP562>3.0.CO;2-Y).
- [23] H.J. Griesser, R.C. Chatelier, T.R. Gengenbach, G. Johnson, J.G. Steele, J. Biomat. Sci. Polymer Edn. 5 (1994) 531, <http://dx.doi.org/10.1163/156856294X000194>.
- [24] J.H. Zhao, W.P. Michalski, C. Williams, L. Li, H.S. Xu, P.R. Lamb, S. Jones, Y.M. Zhou, X.J. Dai, J. Biomed. Mater. Res. Part A 97A (2) (2011) 127–134, <http://dx.doi.org/10.1002/jbm.a.33035>.

3. Discussion

The hypothesis of this project was that a positively charged layer with amino groups would promote cell adhesion due to the fact, that human osteoblastic cells are surrounded by a negatively charged hyaluronan coat. This is why we have attempted to use plasma polymerization of the monomers allylamine and ethylenediamine for surface coatings. Our approach was to use a positively charged surface to enhance cell adhesion in a stage before the cell starts to secrete matrix proteins and builds up the essential focal contacts. Due to the generally negative charge of cells and many proteins we hypothesized that an oppositely charged surface would promote cell adhesion.

Generally, there exist a lot of papers dealing with different techniques for surface coating with amino groups. Nevertheless, there are only few comparative studies and so far no research to elucidate the mechanisms of how cell adhesion is promoted by these surfaces. Mostly the biomaterials research is driven by the applied research that has the aim to generate a surface for the endoprosthesis market. With our cell-biological techniques we attempted to identify differences in the cellular behavior on different plasma polymer layers and investigate the main sequences of cell adhesion and growth on plasma modified surfaces.

A representative polished titanium surface has a negative surface charge of approximately -3.4 mV [KOKUBO *et al.* 2010, LI *et al.* 2004, NEBE *et al.* 2007]. Likewise human cells possess a net negative charge due to the hyaluronic acid and the lipid composition of the pericellular glycocalyx [M. COHEN *et al.* 2006, SCHNITZER 1988, ZIMMERMAN *et al.* 2002] as described in section 1.3 (Molecular mechanisms of the initial cell adhesion). Recent measurements of the zeta potential revealed, that the cells used in these studies (MG-63 osteoblastic cells) have a negative surface potential of -15.5 mV (measurement of the suspended cells in DMEM; ZetaSizer, Malvern, Dr. M. Hammer, INP Greifswald). However, if the binding partners, both cells and surface, would possess a negative charge this would lead to a retraction due to electrostatic reasons (Coulomb's-law) [COULOMB 1785]. To overcome this problem, many researchers have focused on the possibility to coat a surface with a positively charged layer, for example by attaching NH₂ groups [FAUCHEUX *et al.* 2006, GARCIA *et al.* 2002, MEYER-PLATH *et al.* 2003, NEBE *et al.* 2007, SCHWEIKL *et al.* 2007]. In our case cold plasma processes with low pressure and microwave excitation were used at the INP Greifswald to generate allylamine plasma polymer (PPAAm) layers [FINKE *et al.* 2007]. Ethylenediamine layers (PPEDA) were generated by the University of Greifswald using low pressure and rf-excitation [TESTRICH *et al.* 2013].

Overview of the discussion section

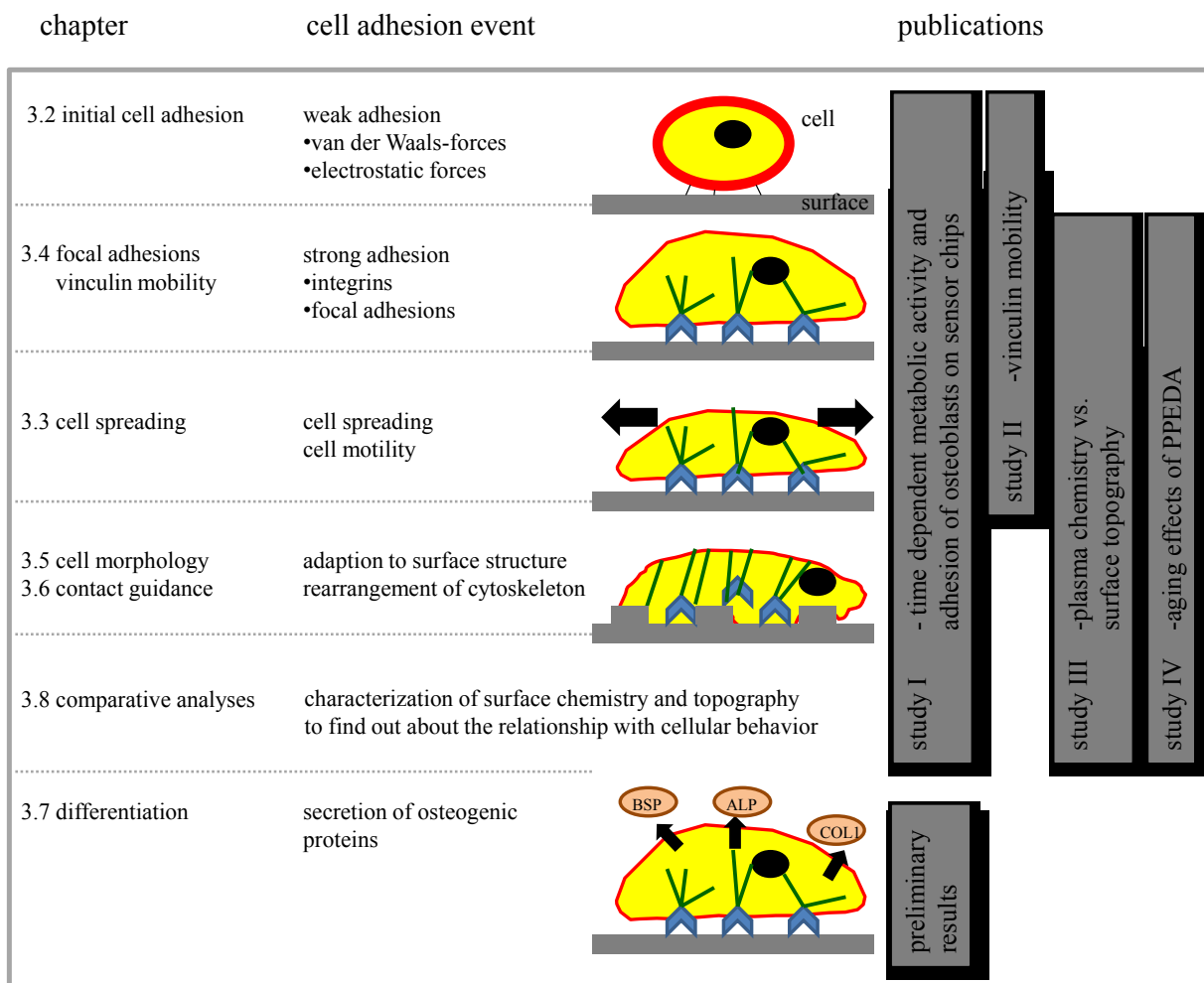


Figure 4: The scheme gives an overview over the discussion section. The chapters of this thesis and the studies I-IV are listed according to the events of cell adhesion.

3.1 Introduction of a new method for monitoring cells on nano-surface coatings

To evaluate the cell adhesion, spreading and growth on the surface layer PPAAm we first decided to use a chip-based system to monitor the cell adhesion of vital cells during the time span of one day. Biochips offer an ideal noninvasive online measurement platform to obtain precise and reproducible data on basic functional parameters such as metabolic activities of living, adherent cells over long time_periods [THEDINGA *et al.* 2007]. However, they have not been used for the evaluation of a surface coating so far. In order to determine reasonable time points for more precise testing methods, chip-based assays are widely applied. Cell adhesion, morphological changes, cellular metabolic activity or the rate of mitochondrial oxygen consumption are typically investigated [WIEST *et al.* 2005]. This makes these assays extremely useful for monitoring drug effects and dosage influence [THEDINGA *et al.* 2007].

The main advantage is that cellular effects can be monitored noninvasively over a long period of time. Conventional cell-based assays often require a larger number of cells, and seldom provide information

about the dynamics of the cells. Nonetheless, they do yield more detailed information. The evaluation of functional layers with these sensor-based systems has not been the center of interest so far. To our knowledge, our paper “Time-dependent metabolic activity and adhesion of human osteoblast-like cells on sensor chips with a plasma polymer nanolayer” (study I) is the first study reporting the effect of a surface coating with a continuous adhesion measurement method, monitoring metabolic activity in the same time frame (for method see Appendix II; Method Bionas Analyzer 1500®).

The *in vitro* method we introduced is thought to get additional long term information about vital cells for these special parameters adhesion and metabolism. Although not performed by us, it is possible to additionally observe the cell reaction immediately after an addition of substances in the medium flow [THEDINGA *et al.* 2007]. Thus, one can observe the vital cell behavior on a functionalized chip surface in combination with e.g. growth stimulating factors. This will help to gain a better understanding of cell adhesion processes at the material interface.

Our continuous adhesion measurements revealed that osteoblast attachment is highly increased in the first adhesion phase on the chip surface with PPAAm (nearly 2-fold compared to the control). Subsequently, this increase is minor but still significantly different between the control and the plasma functionalized PPAAm surface. The changes in metabolic activity, i.e. oxygen consumption and medium acidification are not significant over the whole time span of 24 h. This is indicating that the osteoblasts are not stressed on the PPAAm surface. Moreover the nano-scaled layer of PPAAm is stable and not cytotoxic. Taken together, these results point out that the MG-63 cells are supported in their adhesion and spreading activities by the surface charges due to PPAAm but without disturbing, affecting or stimulating the metabolic activity. From these investigations we found that the main benefit of the coating is the promotion of the initial adhesion phase. We therefore decided to analyze this process in more detail.

3.2 Initial cell adhesion is significantly improved on plasma-modified surfaces

There are different possibilities to monitor the first minutes of cell adhesion. On the one hand we have used cell counting *via* flow cytometry (FACS) to obtain information about the number of cells attached to a surface after a certain time. On the other hand we have used time lapse imaging to get additional information about the dynamics of the cell adhesion process on the PPAAm- and collagen I layer. Time lapse recordings of MG-63 osteoblasts enabled the continuous monitoring of cell spreading. We could demonstrate that the vital osteoblasts on the positively charged PPAAm surfaces spread significantly earlier and faster than on collagen I surfaces.

Different collagen I-coated surfaces served as control for all experiments. Collagenous proteins are the main protein component (90%) in the human bone and therefore good ligands for osteoblast adhesion. The major part (97%) of the collagenous proteins consists of collagen I [ANSELME 2000]. However, we observed, that additional coupling of collagen I to the different roughnesses did not enhance cell adhesion and spreading comparatively. This makes clear that it is crucial which chemical functionalization is used for surface coating. We have used two different spacers, polyethylene glycol-diacid (PEG-DA) and glutardialdehyde (GDA) for the coupling of collagen I. We assumed that the chain length of the linker influences the stiffness of the collagen bonding - the shorter the chain length the less flexible is the bonding. This in turn should lead to low cell spreading and growth. PEG-DA has a chain length of about 3.8 nm and GDA of about 1.2 nm. We were wondering whether cells on PEG-DA Col I grow better than cells settled on GDA Col I. Potentially, the rearrangement of the cells can be better realized on the longer PEG-DA chain. Indeed, we observed a slightly better cell spreading on the PEG-DA Col I surfaces. However, we could not observe such a strong increase as on the PPAAm surfaces. In general, adhesion of osteoblasts is significantly increased on all titanium surfaces in combination with chemical features of positively charged amino groups (+ PPAAm or PPEDA). However, this chemical effect of the amino groups could be enhanced more on structured titanium. We used grooved titanium (machined, M) with an average roughness (Ra: mean of the peak-to-valley measurements of a surface) of 0.3 μm and very rough corundum-blasted (CB) titanium with irregular craters and sharp edges with a Ra of 4.1 μm .

The initial cell adhesion on structured Ti-M and Ti-CB functionalized with amino groups increased nearly twice compared to amino-functionalized polished Ti. Reconfirming the results of other authors [KELLER *et al.* 1994], we demonstrated that increasing roughness alone resulted in an elevated cell attachment. In 2002, Anselme *et al.* reported that osteoblastic cells prefer surfaces with a relatively high micro-roughness amplitude and with a low level of repeatability [ANSELME *et al.* 2002]. Thus the increased attachment of the osteoblastic cells on the corundum-blasted samples determined in our experiments might be due to the greater roughness and the random structure of the blasted surface. We determined that cell adhesion is significantly enhanced on the positively charged PPAAm-coated surfaces, especially on the micro-structured surfaces (Ti-M PPAAm ~5-fold). This means that the effect of roughness and chemical modification add up to and yield an enormous increase in cell adhesion.

3.3 Initial cell spreading is promoted on PPAAm

After the cells adhered to a materials surface, they have to spread in order to build up a strong contact to the surface. Spreading is an essential event for all adherent cells and a prerequisite for further steps, as there are proliferation, migration, and differentiation. We determined cell spreading at different time points and we could clearly show that the PPAAm-surface displays clear advantages over both the collagen-coated and the untreated titanium surfaces. These strong positive effects of PPAAm on cell spreading could be verified with human bone marrow stem cells [SCHRÖDER *et al.* 2010a, SCHRÖDER *et al.* 2010b]. At the early time points, it was even more obvious that cells can spread faster and exhibit more extensions (Appendix II; supplementary data: A).

After 24 h, the increase of cell spreading on PPAAm is still visible but the cells on the collagen I surfaces have caught up. The reason for this might be that all cells are limited in their maximum size. Liu *et al.* postulated a time-cell substratum-compatibility principle, in which similar bioadhesive outcomes can be achieved on all surfaces, but the time required to arrive at this outcome increases with decreasing cell–substratum compatibility [LIU *et al.* 2007]. So the main advantage of the PPAAm surfaces can be seen in the fast occupation by human cells. For the occupation of an implant surface, it is important that the surface is coated with vital bone cells immediately, so the possibly occurring bacteria cannot bind to the implant surface. This process is called “race to the surface” and it is assumed, that those cells who bind to the surface first will dictate the fate of the ingrowth and stability of an orthopedic implant [GRISTINA 1987]. To design a surface that will preferentially attract distinct cell types (stem cells and osteoblastic cells for orthopedic implants, fibroblasts and muscle cells for implants in inner medicine e.g. hernia meshes) and drive their spreading, proliferation, migration and differentiation is one of the top goals in implant development.

3.4 Mobility and length of vinculin contacts is enhanced on positively charged surfaces

In order to investigate the underlying mechanisms of the increased spreading process the dynamic behavior of vinculin in living MG-63 osteoblasts was examined. We wanted to find out whether the increased spreading of cells is dependent on a superior mobility of focal adhesion contacts.

A lot of effort of the scientific community was based on analyzing exchange dynamics of several focal adhesion proteins such as vinculin and paxillin by FRAP (fluorescence recovery after photobleaching) [D.M. COHEN *et al.* 2006, LELE *et al.* 2008, MOHL *et al.* 2009]. However, the mobility of these adhesions has rarely been studied in living cells. To our knowledge study II was the first article reporting vinculin dynamics on plasma functionalized material surfaces during the initial phase of cell adhesion. We could show a significant increase of vinculin mobility and focal contact length on PPAAm, suggesting that the increased spreading is facilitated by a higher mobility of proteins in focal adhesion complexes. The

higher mobility of the focal adhesion proteins might result from the interaction with the positively charged amino groups on the surface. The cell is tethered to the surface *via* numerous weak electrostatic bonds and thus the focal adhesions do not need to be so tight and stiff. Consequentially, this might enable the focal contacts to be more mobile and thus allowing the cell to occupy a larger surface area. Moreover we could show that the higher vinculin mobility leads to faster cell migration on the amino-functionalized surfaces. This might enable the cell to reorganize itself in the context of the whole cell population, leading to a complete coverage of the materials surface.

It is well known that maturation of focal adhesions is determining cell adhesion and migration [LELE *et al.* 2008]. Two morphological variants of focal adhesions, the ‘dot’ and ‘dash’ variants, are described in the literature [BERSHADSKY *et al.* 1985]. First, ‘dot’ contacts form during initial adhesion, which later mature into ‘dash’ contacts [COOPER 1987]. The enlarged length of the vinculin contacts on amino-functionalized surfaces measured in our experiments could indicate a temporal advance in focal contact maturation. Subsequent biological responses such as proliferation and differentiation might consequently be promoted on PPAAM-modified surfaces, since it was proven, that larger focal adhesions lead to higher proliferation rates *in vitro* [SLATER *et al.* 2008].

Another aspect might be considered when analyzing the vinculin protein in focal adhesions. It is known that the role of vinculin is to stabilize focal adhesions [ZIEGLER *et al.* 2006]. Decreased expression of vinculin might thus lead to increased cell motility. In our experiments we have analyzed the number and motility of vinculin containing focal adhesions, but not the amount of vinculin protein that is present in the FAs and other compartments of the cell at these time points. It is up to future research to shed more light on the role of vinculin in the process of cell mobility. Gene expression studies might also explore other candidate genes that are involved in this process.

3.5 Morphology of osteoblastic cells is flattened on PPAAM

When applying the PPAAM layer to structured titanium surfaces (grooved or stochastically blasted surfaces), we observed that the cells spread out very flatly. In contrast, on the pure titanium surfaces, the cells span over the craters. Also on the sensor chips, used for the time dependent monitoring of the cells, we observed that the morphology of the osteoblasts was extremely flattened on allylamine-modified chip-surfaces. The cells seemed to merge with the sensor-relief of the surface. Unfortunately we could not find any report about this phenomenon of “cell-flattening” on plasma polymer layers in the literature. Possibly this is due to the fact that many researchers focus on the aspect of cell toxicity when investigating a novel plasma layer. To investigate whether this close cell-surface contact might influence the cells’ metabolism we carried out metabolic analyses of the cell on these sensor chips.

The overall oxygen consumption and the acidification of the cell culture medium was measured over a time-span of 24 h [EHRET *et al.* 2001]. We could demonstrate that the metabolism is not affected

although the cells are flattened and stick close to the surface [REBL *et al.* 2010a, REBL *et al.* 2010b]. This proved that there is no obvious impairment although the cell's profile is extremely flattened on the PPAAm-modified surfaces. We hypothesize that a better distribution of the cells over the implant surface and a closer cell-surface contact due to the higher contact area could result in a faster ingrowth of the implant into the bone.

3.6 Contact guidance along grooves is abrogated on plasma-modified surfaces

The adaption of cells to different surface structures is called 'contact guidance'. There are a lot of observations that osteoblast-like cells cultured on materials with micron scale grooves or channels become elongated parallel to the direction of the grooves [ANSELME *et al.* 2002, CHESMEL *et al.* 1995, LANGE *et al.* 2010, LUETHEN *et al.* 2005, MATSCHEGEWSKI *et al.* 2012]. We could also observe this effect on our grooved machined surfaces. The cells were oriented in the direction of the grooves and also their actin cytoskeleton was aligned in this direction. In contrast, on the plasma-modified allylamine surfaces the cells grew diagonally to the grooves and hills. The cytoskeleton was not oriented in a special direction, although it sometimes followed the grooves.

Indeed, the observation that a plasma-chemical surface modification allows the cells to overcome the restrictions of the surface-topography has not been described in the literature up to now. Here we were able to demonstrate for the first time that the altered alignment behavior of the cells on plasma functionalized surfaces (PPAAm) was only due to the chemical modification with amino groups. The modification of the surfaces with collagen I did not induce this random spreading behavior. So we could demonstrate that the plasma chemical functionalization of a surface is dominant over its topography. We assume that the difference in quantity and conformation of protein adhesion is responsible for the altered cell behavior.

3.7 Differentiation of osteoblastic cells is promoted on structured PPAAm surfaces

To analyze whether the last step of implant integration, namely the differentiation of osteoblastic cells into mature osteoblasts, is altered by the investigated surfaces, we performed gene expression analyses. We found that the expression of early osteogenic markers like alkaline phosphatase (ALP) and collagen I (Col I) are not influenced by the plasma-functionalized surfaces. When analyzing a late marker, bone sialoprotein (BSP), we found an increase on the PPAAm surfaces on smooth and rough topographies (Appendix II; supplementary data: B). This means that the secretion of the late osteogenic marker is enhanced also on surfaces that are relevant for implants in the orthopedic sector.

The increase in BSP gene expression was also observed by other colleagues, when culturing MG-63 cells or primary osteoblastic cells on polished PPAAm surfaces for 3 days [NEBE *et al.* 2007, SCHRÖDER *et al.* 2010a, SCHRÖDER *et al.* 2010b]. This positive effect on gene expression could be verified by protein analyses. BSP protein was increased on polished PPAAm surfaces, after 24h of culture [FINKE *et al.* 2007]. However, the influence of topography was not studied there.

3.8 Comparative analyses with PPEDA and stored surfaces show that the amino group density is not deciding for the elevated cell adhesion

Similar results with reference to increased cell adhesion, growth and morphology could be observed on surfaces plasma-functionalized with ethylenediamine (study IV). The theoretical amino group density of these layers is very high due to the N/C ratio of 1:1. The layers investigated in our study were composed of 4.3% amino groups. This is 1.8% more than the PPAAm layer, but when producing PPEDA layers with possibly higher amino group density, the layers delaminated in water, maybe due to the lower degree of crosslinking.

	PPAAm	PPEDA
Precursor	allylamine	ethylenediamine
molecular formula	C ₃ H ₇ N	C ₂ H ₈ N ₂
N/C ratio - theoretical	33.3 %	100 %
N/C ratio - measured by XPS	25 %	49 %
amino group density (NH₂)	2.5 %	4.3 %
cell adhesion after 10 min	86.6 ± 1.8 %	84.3 ± 2.8 %

Table 1: Comparison of the plasma layers investigated in our studies. The N/C ratio and the amino group density was measured by X-ray photoelectron spectroscopy (XPS, n=3, for detailed methods see study III and IV) after derivatization with trifluormethylbenzaldehyd (TFBA). Cell adhesion was measured *via* flow cytometry (n=4)

Despite the increased amino group density we could not find a different cellular behavior. We also investigated surfaces generated from sputtered nylon with even higher amino group density of 7.2%, but we could not observe a further increase in cell adhesion or spreading [FINKE *et al.* 2011]. So we came to the conclusion that the amino group density is not the deciding factor for the enhanced cell attachment. Regarding the amino group density it can be speculated that there is a certain threshold value that has to

be reached to facilitate cell adhesion. A further increase over this value does not lead to a further increase in cell adhesion.

So far it was not possible for us to completely distinguish if the strong positive influence on cell adhesion, spreading, motility and differentiation, observed on the PPAAm and PPEDA surfaces, is an effect of the positive charges or the amino- or other chemical groups on the surface. Due to the fact that plasma processes create a mixture of chemical groups, thereunder amino groups, amides or imides, the connection of the results of cell experiments and chemical analyses is rather difficult. We found that amino-group density decreases with time. We examined cell adhesion on freshly prepared and one year old plasma-functionalized PPAAm and PPEDA surfaces [FINKE *et al.*, submitted, TESTRICH *et al.* 2013]. Over the whole time of one year the cell attachment and spreading behavior was significantly enhanced on the plasma coated surfaces. The overall content of nitrogen was relatively stable over the investigated period. In contrast, the chemical analyses revealed that only 10% of the original primary amino groups were left after 180 days of storage [FINKE *et al.*, paper submitted]. Amino groups are converted into amides, imines, and nitriles mainly by oxidation processes. We assume that the amide groups, which are the oxidation products of amino groups, can also promote cell attachment. In fact, surface charge was still enhanced over a timeframe of 200 days [FINKE *et al.*, paper submitted]. Even after 4 years of storage the zeta potential of the surface is higher than on the uncoated surfaces (personal communication with Dr. Finke). This leads us to the opinion, that not the primary amino groups but the general positive charge of the surface is highly likely the reason for the superior cell behavior. This would confirm our hypothesis that the cell adhesion can be promoted by a generally positively charged surface and not by defined chemical groups.

3.9 *In vivo results*

Of course we are aware that in the *in vivo* application in the human body, cells would not directly interact with the amino groups of the plasma polymer. Proteins would immediately bind to the surface and mask the amino groups. However, differences in surface charge or hydrophilicity influence protein adsorption. Thus quantity and quality, i.e. conformation and degree of unfolding, of the adsorbed proteins can be influenced by altering the surface chemistry. This is leading to different density and or availability of cell binding sites. In conclusion, also cell adhesion processes can be triggered indirectly *via* changing the surface charge or elemental composition [MOLINO *et al.* 2012, PANOS *et al.* 2012]. For better comparison with future *in vivo* experiments we repeated some of our *in vitro* experiments using cell culture medium containing 10% serum. These experiments showed that there was only little difference between experiments performed with and without serum. We concluded that most of the effects described here can be transferred to the *in vivo* situation. Before analyzing the layers *in vivo*, their

mechanical stability and resistance to sterilization was proven [FINKE *et al.*, paper submitted, TESTRICH *et al.* 2013].

Subsequent *in vivo* investigations in a rat model revealed that the local inflammatory response to the PPAAm coated specimens was as low as to the uncoated control [HOENE *et al.* 2010]. When investigating the PPAAm and PPEDA layers *in vivo* in bone, our *in vitro* results regarding the cell adhesive potential of the surface were confirmed. The bone-to-implant contact was evaluated *in vivo* after six weeks in the medial tibia of rats. Uncoated titanium implants had a contact area of 40%. Implants functionalized with PPAAm showed an increased contact area of 58%, and PPEDA-modified implants revealed even a significantly increased area of 63% [GABLER *et al.* 2014]. These results indicate that the modification of implant surfaces with PPAAm or PPEDA layers improve the osseointegration and could therefore be well-suited for the orthopedic market.

4. *Conclusions and future prospects*

A central question in bone tissue engineering is how an implant surface can be modified by chemical means to modulate its suitability for interacting with bone cells. The immediate adhesion, fast spreading and the migration of cells is essential for the settlement of biomaterials. A general conclusion drawn from data at hand is that positive charges alone are in advance of cell matrix components to facilitate and enhance osteoblastic cell attachment to a biomaterial surface.

We showed that the techniques used in the present studies were well-taken to shed some light on the major steps of osteoblast adhesion to the plasma modified surfaces. Some of those techniques were in part developed to investigate the cellular behavior on the novel plasma layers. We found that not the primary amino groups *per se* but rather the general positive charge of the surface is responsible for the superior cell behavior. This supports our hypothesis that the cell adhesion can be promoted by a generally positively charged surface and not by defined chemical groups.

Unfortunately, the cellular mechanisms that lead to the higher cell attachment and spreading remain unclear. Future work should characterize the underlying cellular mechanisms that lead to the promoted cellular occupation of the surfaces.

This could include the following working packages to answer basic questions of the cell adhesion process.

I) Single protein adhesion studies:

Can atomic force microscopy (AFM) analyses shed light on altered protein adhesion or conformational changes on the plasma modified surface?

II) Studies on the influence of the actin and microtubule network on the spreading of cells grown on functionalized surfaces:

Does the supported spreading behavior compensate for a disrupted cytoskeleton or signaling cascade in morbid cell types, e.g. osteoporotic cells?

III) Holistic gene expression studies on differently modified surfaces:

Is a modified vinculin expression or availability the reason for the higher cell motility? Which genes or proteins are differentially regulated due to the fast adhesion process on these surfaces? Which regulatory factors control and/or induce those candidate genes and represent therefore crucial target proteins in biomedicine?

In part, the research on these aspects has already started. Investigations with the actin-disrupting agent cytochalasin D revealed that cells can compensate the loss in cell area when they are grown on PPAAM surfaces, even though the actin cytoskeleton is fragmented [KUNZ *et al.*, submitted]. Additionally,

Matschegewski *et al.* could show that cell adhesion is not impaired on statistically oriented pillars, even though the cells cannot build up stabilizing actin fibers [MATSCHEGEWSKI *et al.* 2010, MATSCHEGEWSKI *et al.* 2012]. It seemed that also dot-like actin is sufficient to mediate proper cell spreading on PPAAm coated surfaces.

The combination of mechanically stable and storable positively charged surfaces (PPAAm or PPEDA) developed in the project “Campus PlasmaMed” with or without additional defined ligands for bone cells, e.g. peptide sequences, might increase the bonding of bone cells to the implant surface. Detailed analyses concerning the mechanisms during the initial adhesion of osteoblasts are required for the development of newly designed material surfaces. This might lead to faster implant integration and higher bone-implant contact area which in turn would lead to longer standing times of implants and less revision operations.

5. *Summary*

Titanium surfaces of different topographies were plasma-chemically functionalized with allylamine (study I-III) or ethylenediamine (study IV). First, we have analyzed the adhesion process of vital cells (study I) and the mobility of focal adhesions on the plasma-polymerized allylamine surfaces (study II). Second, we have observed a positive effect on the initial cell adhesion, spreading, as well as on the cell morphology and the osteogenic differentiation (study III). Third, comparative studies of cell adhesion and spreading were performed on surfaces plasma-functionalized with ethylenediamine (study IV).

In order to understand the process of cell adhesion on plasma-polymerized allylamine surfaces, we have decided for a novel approach to investigate the cell adhesion and metabolism non-stop over a time span of 24h on plasma polymer layers (study I). We wanted to elucidate the time-dependency of the adhesion process and find out whether the faster cell spreading, observed on the PPAAm layers, would lead to changes in the cell's metabolism. Interestingly, the fast adhesion and also the very flat cell morphology did not alter the cells acidification and respiration rates.

To shed light on the underlying mechanisms of the spreading process, the vinculin-containing focal adhesions were analyzed (study II). The expression, the average length and the mobility of vinculin was clearly enhanced on PPAAm during the first hours of cell-surface contact. Thus we concluded that the faster maturation and higher mobility of the vinculin containing focal adhesions leads to the faster cell spreading of cells on plasma-polymerized allylamine surfaces.

In a subsequent approach, we have used structured materials for the detailed analyses of cell adhesion, cytoskeleton formation and cell morphology (study III). For the first time we could demonstrate the dominance of a chemical surface modification over surface topography. The contact guidance of the grooved surfaces was abrogated by the plasma polymer layer. The cells express a very flat cell morphology and spread out over the grooves and hills. Also the actin cytoskeleton is no longer expressed parallel to the grooves when the cells are grown on the PPAAm layer. The differentiation of the osteoblastic cells was enhanced as indicated by the higher expression of bone sialoprotein (BSP).

Similar results with reference to increased cell adhesion, growth and morphology could be observed on surfaces plasma-functionalized with ethylenediamine (study IV). Although the amino group density decreased over the storage period of one year, the increase of cell attachment was stable. Moreover we could demonstrate that a higher amount of amino groups in the PPEDA layer, compared to the PPAAm surface, does not lead to increased values of adherent cells. We came to the conclusion that not the amino group density but rather the general surface charge is the deciding factor for the enhanced cell attachment.

6. Zusammenfassung

Titanoberflächen mit verschiedenen Rauigkeiten wurden mittels plasmachemischer Verfahren mit Allylamin (Studie I-III) oder Ethylendiamin (Studie IV) funktionalisiert. Zunächst wurde der Adhäsionsprozess auf plasma-funktionalisierten Allylaminschichten (PPAAm) an vitalen Osteoblastenzellen untersucht (Studie I). Darauf folgte die Analyse der Mobilität der Fokalen Kontakte anhand des Adapterproteins Vinkulin (Studie II). In weiterführenden Untersuchungen konnten wir einen positiven Effekt auf die initiale Zelladhäsion, Zellausbreitung, Morphologie und die osteogene Differenzierung feststellen (Studie III). Vergleichende Analysen der Zelladhäsion und Zellausbreitung wurden auf plasma-funktionalisierten Ethylendiaminschichten (PPEDA) durchgeführt (Studie IV).

Um den zeitlichen Ablauf des Adhäsionsprozesses auf PPAAm-Schichten zu untersuchen wurde ein neuer Ansatz gewählt in dem über einen Zeitraum von 24 h eine kontinuierliche Messung der Zelladhäsion, sowie der Respiration und Azidifikation erfolgte (Studie I). Dadurch sollte untersucht werden ob die schnelle Zellausbreitung, die auf den PPAAm-Schichten beobachtet wurde, den Zellmetabolismus beeinflusst. Interessanterweise wirken sich die schnelle Ausbreitung der Zellen und auch die extrem flache Morphologie nicht auf die Zellatmung und die Ansäuerung des Zellmediums aus und stellen somit keinen Stress für die Osteoblastenzellen dar.

Um den Adhäsionsprozess genauer zu beleuchten wurden Analysen zur Mobilität von Vinkulin-enthaltenden Fokalen Adhäsionskontakten durchgeführt (Studie II). Die Anzahl, Länge und Mobilität der Vinkulinkontakte war während des Ausbreitungsprozesses auf PPAAm wesentlich erhöht. Die Ergebnisse lassen vermuten, dass die erhöhte Mobilität und das schnellere Wachstum der Vinkulinkontakte wesentlich zu einer schnelleren Zellausbreitung auf plasma-funktionalisierten Allylaminschichten beitragen.

Unterschiedlich strukturierte Oberflächen wurden in einem weiteren Ansatz funktionalisiert und hinsichtlich ihres Einflusses auf die Zelladhäsion, Morphologie und das Zytoskelett untersucht (Studie III). Erstmals konnte gezeigt werden, dass eine chemische Modifikation der Oberfläche einen größeren Einfluss ausübt als deren Topographie. Die Ausrichtung der Zelle und auch des Aktinzytoskeletts entlang der Grabenstruktur der Oberfläche wurde durch die Plasmabeschichtung aufgehoben.

Auf plasmachemisch abgeschiedenen Ethylendiaminschichten wurde ein ähnliches Zellverhalten in Bezug auf Zelladhäsion und Spreading beobachtet (Studie IV). Es konnte gezeigt werden, dass die gesteigerte Zelladhäsion auch auf einjährig gelagerten Proben erhalten bleibt, obwohl die Aminogruppendichte drastisch absinkt. Darüber hinaus haben die Analysen ergeben, dass die höhere Aminogruppendichte der PPEDA Schicht nicht zu einer weiteren Steigerung der Zelladhäsion führt. Daraus lässt sich ableiten, dass nicht die Aminogruppendichte sondern eher die generelle Ladung der Oberfläche entscheidend für die erhöhte Zelladhäsion ist.

7. *References*

- Anselme, K.; Osteoblast adhesion on biomaterials. *Biomaterials*, 2000; 21, 7, 667-681.
- Anselme, K., Bigerelle, M., Noel, B., Iost, A., Hardouin, P.; Effect of grooved titanium substratum on human osteoblastic cell growth. *J. Biomed. Mater. Res.*, 2002; 60, 4, 529-540.
- Barbour, M.E., O'Sullivan, D.J., Jenkinson, H.F., Jagger, D.C.; The effects of polishing methods on surface morphology, roughness and bacterial colonisation of titanium abutments. *J. Mater. Sci.-Mater. Med.*, 2007; 18, 7, 1439-1447.
- Bershadsky, A.D., Tint, I.S., Neyfakh, A.A., Vasiliev, J.M.; Focal contacts of normal and rsv-transformed quail cells - hypothesis of the transformation-induced deficient maturation of focal contacts. *Exp. Cell Res.*, 1985; 158, 2, 433-444.
- Boyan, B.D., Hummert, T.W., Dean, D.D., Schwartz, Z.; Role of material surfaces in regulating bone and cartilage cell response. *Biomaterials*, 1996; 17, 2, 137-146.
- Chen, H., Cohen, D.M., Choudhury, D.M., Kioka, N., Craig, S.W.; Spatial distribution and functional significance of activated vinculin in living cells. *J. Cell Biol.* 2005: 169, 459-470.
- Chesmel, K.D., Clark, C.C., Brighton, C.T., Black, J.; Cellular responses to chemical and morphologic aspects of biomaterial surfaces. 2. The biosynthetic and migratory response of bone cell populations. *J. Biomed. Mater. Res.*, 1995; 29, 9, 1101-1110.
- Clover, J., Dodds, R.A., Gowen, M.; Integrin subunit expression by human osteoblasts and osteoclasts in situ and in culture. *J Cell Sci.* 1992; 103, 267-71.
- Cohen, D.M., Kutscher, B., Chen, H., Murphy, D.B., Craig, S.W.; A conformational switch in vinculin drives formation and dynamics of a talin-vinculin complex at focal adhesions. *J. Biol. Chem.*, 2006; 281, 23, 16006-16015.
- Cohen, M., Klein, E., Geiger, B., Addadi, L.; Organization and adhesive properties of the hyaluronan pericellular coat of chondrocytes and epithelial cells. *Biophys. J.*, 2003; 85, 3, 1996-2005.
- Cohen, M., Joester, D., Geiger, B., Addadi, L.; Spatial and temporal sequence of events in cell adhesion: From molecular recognition to focal adhesion assembly. *Chembiochem*, 2004; 5, 10, 1393-1399.
- Cohen, M., Kam, Z., Addadi, L., Geiger, B.; Dynamic study of the transition from hyaluronan- to integrin-mediated adhesion in chondrocytes. *Embo J.*, 2006; 25, 2, 302-311.
- Collier, J.H., Segura, T.; Evolving the use of peptides as components of biomaterials. *Biomaterials*, 2011; 32, 18, 4198-4204.
- Compston, J.E., Papapoulos, S.E., Blanchard, F.; Report on osteoporosis in the European community: Current status and recommendations for the future. *Osteoporosis Int.*, 1998; 8, 6, 531-534.
- Cooper, J.A.; Effects of cytochalasin and phalloidin on actin. *J Cell Biol.*, 1987; 105, 4, 1473-1478.
- Coulomb, C.A.; Premier mémoire sur l'électricité et le magnétisme, in *Histoire de l'Académie royale des sciences*, Académie royale des sciences Paris, eds, De l'imprimerie royale, Gent, 1785; 569-577.
- Critchley, D.R.; Cytoskeletal proteins talin and vinculin in integrin-mediated adhesion. *Biochem. Soc. Trans.*, 2004; 32, 5, 831-836.

- Czekanska, E.M., Stoddart, M.J., Richards, R.G., Hayes, J.S.; In search of an osteoblast cell model for in vitro research. *Eur. Cell.Mater.*, 2012; 24, 1-17.
- Delmas, P.D., Anderson, M.; Launch of the Bone and Joint Decade 2000-2010. *Osteoporosis Int.*, 2000; 11, 2, 95-97.
- Denes, F.S., Manolache, S.; Macromolecular plasma-chemistry: an emerging field of polymer science. *Prog. Polym. Sci.*, 2004; 29, 8, 815-885.
- Diener, A., Nebe, B., Lüthen, F., Becker, P., Beck, U., Neumann, H.G., Rychly, J.; Control of focal adhesion dynamics by material surface characteristics. *Biomaterials*, 2005; 26, 4, 383-392.
- Ducheyne, P., Beight, J., Cuckler, J., Evans, B., Radin, S.; Effect of calcium-phosphate coating characteristics on early postoperative bone tissue ingrowth. *Biomaterials*, 1990; 11, 8, 531-540.
- Ehret, R., Baumann, W., Brischwein, M., Lehmann, M., Henning, T., Freund, I., Drechsler, S., Friedrich, U., Hubert, M.L., Motrescu, E., Kob, A., Palzer, H., Grothe, H., Wolf, B.; Multiparametric microsensor chips for screening applications. *Fresenius J. Anal. Chem.*, 2001; 369, 30-5.
- Faucheux, N., Schweiss, R., Lutzow, K., Werner, C., Groth, T.; Self-assembled monolayers with different terminating groups as model substrates for cell adhesion studies. *Biomaterials*, 2004; 25, 14, 2721-2730.
- Faucheux, N., Tzoneva, R., Nagel, M.D., Groth, T.; The dependence of fibrillar adhesions in human fibroblasts on substratum chemistry. *Biomaterials*, 2006; 27, 2, 234-245.
- Finke, B., Luethen, F., Schroeder, K., Mueller, P.D., Bergemann, C., Frant, M., Ohl, A., Nebe, B.J.; The effect of positively charged plasma polymerization on initial osteoblastic focal adhesion on titanium surfaces. *Biomaterials*, 2007; 28, 30, 4521-4534.
- Finke, B., Hempel, F., Testrich, H., Artemenko, A., Rebl, H., Kylián, O., Biederman, H., Nebe, B., Weltmann, K.-D., Schröder, K.; Plasma processes for cell-adhesive titanium surfaces based on nitrogen-containing coatings. *Surf. Coat. Tech.*, 2011; 205, 520-524.
- Finke, B., Rebl, H., Hempel, F., Schäfer, J., Liefeth, K., Weltmann, K.-D., Nebe, J.B., Ageing of plasma-polymerised allylamine nanofilms and the maintenance of their cell adhesion capacity. submitted to *Acta Biomaterialia*.
- Gabler, C., Zietz, C., Göhler, R., Fritsche, A., Lindner, T., Haenle, M., Finke, B., Meichsner, J., Lenz, S., Frerich, B., Lüthen, F., Nebe, J.B., Bader, R.; Evaluation of osseointegration of titanium alloyed implants modified by plasma polymerization. *Int. J. Mol. Sci.*, 2014; 15, 2, 2454-64.
- Garcia, A.J., Collard, D.M., Keselowsky, B.G., Cutler, S.M., Gallant, N.D., Byers, B.A., Stephansson, S.N.; Engineering of integrin-specific biomimetic surfaces to control cell adhesion and function, in *Biomimetic materials and design*, L. A. Dillow AK, eds, New York, 2002, 29-55.
- Geiger, B., Bershadsky, A.; Assembly and mechanosensory function of focal contacts. *Curr. Opin. Cell Biol.*, 2001; 13, 5, 584-592.
- Geiger, B., Yamada, K.M.; Molecular Architecture and Function of Matrix Adhesions. 2011; 3, 5, Giancotti, F.G., Ruoslahti, E.; Transduction - Integrin signaling. *Science*, 1999; 285, 5430, 1028-1032.
- Grausova, L., Bacakova, L., Kromka, A., Vanecek, M., Rezek, B., Lisa, V.; Molecular markers of adhesion, maturation and immune activation of human osteoblast-like MG 63 cells on nanocrystalline diamond films. *Diam. Relat. Mat.*, 2009; 18, 2-3, 258-263.

- Griesser, H.J., Chatelier, R.C., Gengenbach, T.R., Johnson, G., Steele, J.G.; Growth of human cells on plasma polymers - putative role of amine and amide groups. *J. Biomater. Sci.-Polym. Ed.*, 1994; 5, 6, 531-554.
- Gristina, A.G.; Biomaterial-centered infection: microbial adhesion versus tissue integration. *Science*, 1987; Sep 25, 237(4822), 1588-1595.
- Hamerli, P., Weigel, T., Groth, T., Paul, D.; Surface properties of and cell adhesion onto allylamine-plasma-coated polyethylenterephthalat membranes. *Biomaterials*, 2003; 24, 22, 3989-3999.
- Hanein, D., Geiger, B., Addadi, L.; Cell adhesion to crystal surfaces - a model for initial stages in the attachment of cells to solid substrates. *Cells Mat.*, 1995; 5, 2, 197-210.
- Harsch, A., Calderon, J., Timmons, R.B., Gross, G.W.; Pulsed plasma deposition of allylamine on polysiloxane: a stable surface for neuronal cell adhesion. *J. Neurosci. Methods*, 2000; 98, 2, 135-144.
- Hatano, K., Inoue, H., Kojo, T., Matsunaga, T., Tsujisawa, T., Uchiyama, C., Uchida, Y.; Effect of surface roughness on proliferation and alkaline phosphatase expression of rat calvarial cells cultured on polystyrene. *Bone*, 1999; 25, 4, 439-445.
- Hoene, A., Walschus, U., Patrzyk, M., Finke, B., Lucke, S., Nebe, B., Schroeder, K., Ohl, A., Schlosser, M.; In vivo investigation of the inflammatory response against allylamine plasma polymer coated titanium implants in a rat model. *Acta Biomater.*, 2010; 6, 2, 676-83.
- Hynes, R.O.; Cell adhesion: old and new questions. *Trends Biochem. Sci.*, 1999; 24, 12, M33-M37.
- Intranuovo, F., Favia, P., Sardella, E., Inghosso, C., Nardulli, M., d'Agostino, R., Gristina, R.; Osteoblast-Like Cell Behavior on Plasma Deposited Micro/Nanopatterned Coatings. *Biomacromolecules*, 2011; 12, 2, 380-387.
- Keller, J.C., Stanford, C.M., Wightman, J.P., Draughn, R.A., Zaharias, R.; Characterizations of titanium implant surfaces.3. *J. Biomed. Mater. Res.*, 1994; 28, 8, 939-946.
- Kim, J., Jung, D., Park, Y., Kim, Y., Moon, D.W., Lee, T.G.; Quantitative analysis of surface amine groups on plasma-polymerized ethylenediamine films using UV-visible spectroscopy compared to chemical derivatization with FT-IR spectroscopy XPS and TOF-SIMS. *Appl. Surf. Sci.* 2007; 253, 9, 4112-4118.
- Kokubo, T., Pattanayak, D.K., Yamaguchi, S., Takadama, H., Matsushita, T., Kawai, T., Takemoto, M., Fujibayashi, S., Nakamura, T.; Positively charged bioactive Ti metal prepared by simple chemical and heat treatments. *J. R. Soc. Interface*, 2010; 7, S503-S513.
- Kunz, F., Rebl, H., Quade, A., Matschegewski, C., Finke, B., Nebe, J. B.; Physiologically restricted osteoblasts with impaired spreading capacity benefit from positive charges of plasma polymerised allylamine. submitted to *European Cells and Materials*; minor revision.
- Lange, R., Lüthen, F., Beck, U., Rychly, J., Baumann, A., Nebe, B.; Cell-extracellular matrix interaction and physico-chemical characteristics of titanium surfaces depend on the roughness of the material. *Biomol. Eng.*, 2002; 19, 2-6, 255-261.
- Lange, R., Elter, P., Biala, K., Matschegewski, C., Stahlke, S., Löffler, R., Fleischer, M., Nebe, J.B., Kern, D., Beck, U.; Titanium surfaces structured with regular geometry - material investigations and cell morphology. *Surf. Interface Anal.*, 2010; 42, 6-7, 497-501.
- Lele, T.P., Thodeti, C.K., Pendse, J., Ingber, D.E.; Investigating complexity of protein-protein interactions in focal adhesions. *Biochem. Biophys. Res. Commun.*, 2008; 369, 3, 929-934.

- Li, B.K., Logan, B.E.; Bacterial adhesion to glass and metal-oxide surfaces. *Colloid Surf. B-Biointerfaces*, 2004; 36, 2, 81-90.
- Lim, J.Y., Liu, X., Vogler, E.A., Donahue, H.J.; Systematic variation in osteoblast adhesion and phenotype with substratum surface characteristics. *J. Biomed. Mater. Res. A*, 2004; 68A, 3, 504-512.
- Liu, X.M., Lim, J.Y., Donahue, H.J., Dhurjati, R., Mastro, A.M., Vogler, E.A.; Influence of substratum surface chemistry/energy and topography on the human fetal osteoblastic cell line hFOB 1.19: Phenotypic and genotypic responses observed in vitro. *Biomaterials*, 2007; 28, 31, 4535-4550.
- Luethen, F., Lange, R., Becker, P., Rychly, J., Beck, U., Nebe, J.G.B.; The influence of surface roughness of titanium on beta 1-and beta 3-integrin adhesion and the organization of fibronectin in human osteoblastic cells. *Biomaterials*, 2005; 26, 15, 2423-2440.
- Mannello, F.; Serum or plasma samples? The "Cinderella" role of blood collection procedures - Preanalytical methodological issues influence the release and activity of circulating matrix metalloproteinases and their tissue inhibitors, hampering diagnostic trueness and leading to misinterpretation. *Arterioscler. Thromb. Vasc. Biol.*, 2008; 28, 4, 611-614.
- Matschegewski, C., Staehlke, S., Loeffler, R., Lange, R., Chai, F., Kern, D.P., Beck, U., Nebe, B.J.; Cell architecture-cell function dependencies on titanium arrays with regular geometry. *Biomaterials*, 2010; 31, 22, 5729-5740.
- Matschegewski, C., Staehlke, S., Birkholz, H., Lange, R., Beck, U., Engel, K., Nebe, J.B.; Automatic Actin Filament Quantification of Osteoblasts and Their Morphometric Analysis on Microtextured Silicon-Titanium Arrays. 2012; 5, 1176-1195.
- Meyer-Plath, A.A., Finke, B., Schroder, K., Ohl, A.; Pulsed and cw microwave plasma excitation for surface functionalization in nitrogen-containing gases. *Surf. Coat. Technol.*, 2003; 174, 877-881.
- Mohl, C.C., Kirchgessner, N., Schafer, C., Kupper, K., Born, S., Diez, G., Goldmann, W.H., Merkel, R., Hoffmann, B.; Becoming Stable and Strong: The Interplay Between Vinculin Exchange Dynamics and Adhesion Strength During Adhesion Site Maturation. *Cell Motil. Cytoskeleton*, 2009; 66, 6, 350-364.
- Molino, P.J., Higgins, M.J., Innis, P.C., Kapsa, R.M.I., Wallace, G.G.; Fibronectin and Bovine Serum Albumin Adsorption and Conformational Dynamics on Inherently Conducting Polymers: A QCM-D Study. 2012; 28, 22, 8433-8445.
- Morra, M., Cassinelli, C., Cascardo, G., Cahalan, P., Cahalan, L., Fini, M., Giardino, R.; Surface engineering of titanium by collagen immobilization. Surface characterization and in vitro and in vivo studies. *Biomaterials*, 2003; 24, 25, 4639-4654.
- Narayanan, R., Seshadri, S.K., Kwon, T.Y., Kim, K.H.; Calcium phosphate-based coatings on titanium and its alloys. *J. Biomed. Mater. Res. Part B*, 2008; 85B, 1, 279-299.
- Navarro, M., Michiardi, A., Castano, O., Planell, J.A.; Biomaterials in orthopaedics. *J. R. Soc. Interface*, 2008; 5, 27, 1137-1158.
- Nebe, B., Finke, B., Luethen, F., Bergemann, C., Schroder, K., Rychly, J., Liefelth, K., Ohl, A.; Improved initial osteoblast functions on amino-functionalized titanium surfaces. *Biomol. Eng.*, 2007; 24, 5, 447-454.

- Nebe, J.B., Jesswein, H., Weidmann, A., Finke, B., Lange, R., Beck, U., Schroeder, K.; Osteoblast Sensitivity to Topographical and Chemical Features of Titanium; *Materials Science Forum*, 2010; 638-642, 652-657.
- Panos, M., Sen, T.Z., Ahunbay, M.G.k.; Molecular Simulation of Fibronectin Adsorption onto Polyurethane Surfaces. *Langmuir*, 2012; 28, 34, 12619-12628.
- Park, K.H., Heo, S.J., Koak, J.Y., Kim, S.K., Lee, J.B., Kim, S.H., Lim, Y.J.; Osseointegration of anodized titanium implants under different current voltages: a rabbit study. *J. Oral Rehabil.*, 2007; 34, 7, 517-527.
- Pesakova, V., Kubies, D., Hulejova, H., Himmlova, L.; The influence of implant surface properties on cell adhesion and proliferation. *J. Mater. Sci.-Mater. Med.*, 2007; 18, 3, 465-473.
- Pulliam, I.T., Trousdale, R.T.; Fracture of a ceramic femoral head after a revision operation. A case report. *J. Bone Joint Surg. Am.*, 1997; 79, 118-21.
- Ranucci, C.S., Moghe, P.V.; Substrate microtopography can enhance cell adhesive and migratory responsiveness to matrix ligand density. *J. Biomed. Mater. Res.*, 2001; 54, 2, 149-161.
- Rebl, H., Finke, B., Ihrke, R., Rothe, H., Rychly, J., Schroeder, K., Nebe, B.J.; Positively Charged Material Surfaces Generated by Plasma Polymerized Allylamine Enhance Vinculin Mobility in Vital Human Osteoblasts. *Adv. Eng. Mater.*, 2010a; 12, 8, B356-B364.
- Rebl, H., Finke, B., Schroeder, K., Nebe, J.B.; Time-dependent metabolic activity and adhesion of human osteoblast-like cells on sensor chips with a plasma polymer nanolayer. *Int. J. Artif. Organs*, 2010b; 33, 10, 738-748.
- Ren, T.B., Weigel, T., Groth, T., Lendlein, A.; Microwave plasma surface modification of silicone elastomer with Allylamine for improvement of biocompatibility. *J. Biomed. Mater. Res. Part A*, 2008; 86A, 1, 209-219.
- Schnitzer, J.; Glycocalyx Electrostatic Potential Profile Analysis: Ion, pH, Steric, and Charge Effects. *Yale J. Biol. Med.*, 1988; 61, 5, 427-446.
- Schröder, K., Finke, B., Ohl, A., Lüthen, F., Bergemann, C., Nebe, B., Rychly, J., Walschus, U., Schlosser, M., Liefeth, K., Neumann, H.G., Weltmann, K.D.; Capability of Differently Charged Plasma Polymer Coatings for Control of Tissue Interactions with Titanium Surfaces. *J. Adhes. Sci. Technol.*, 2010a; 24, 1191-1205.
- Schröder, K., Finke, B., Jesswein, H., Lüthen, F., Diener, A., Ihrke, R., Weltmann, K.D., Rychly, J., Nebe, J.B.; Similarities between Plasma Amino Functionalized PEEK and Titanium Surfaces Concerning Enhancement of Osteoblast Cell Adhesion. *J. Adhes. Sci. Technol.*, 2010b; 24, 905-923.
- Schuler, M., Owen, G.R., Hamilton, D.W., De Wilde, M., Textor, M., Brunette, D.M., Tosatti, S.G.P.; Biomimetic modification of titanium dental implant model surfaces using the RGDSP-peptide sequence: A cell morphology study. *Biomaterials*, 2006; 27, 21, 4003-4015.
- Schweikl, H., Muller, R., Englert, C., Hiller, K.A., Kujat, R., Nerlich, M., Schmalz, G.; Proliferation of osteoblasts and fibroblasts on model surfaces of varying roughness and surface chemistry. *J. Mater. Sci.-Mater. Med.*, 2007; 18, 10, 1895-1905.
- Slater, J.H., Frey, W.; Nanopatterning of fibronectin and the influence of integrin clustering on endothelial cell spreading and proliferation. *J. Biomed. Mater. Res. A*, 2008; 87A, 1, 176-195.

- Subauste, M.C., Pertz, O., Adamson, E.D., Turner, C.E., Junger, S., Hahn, K.M.; Vinculin modulation of paxillin-FAK interactions regulates ERK to control survival and motility. *J. Cell Biol.* 2004; 165, 371–381.
- Szmukler-Moncler, S., Perrin, D., Ahossi, V., Magnin, G., Bernard, J.P.; Biological properties of acid etched titanium implants: Effect of sandblasting on bone anchorage. *J. Biomed. Mater. Res. Part B*, 2004; 68B, 2, 149-159.
- Takada, Y., Ye, X., Simon, S.; The integrins. *Genome Biol.* 2007; 8, 5, 215.
- Testrich, H., Rebl, H., Finke, B., Hempel, F., Nebe, B., Meichsner, J.; Aging effects of plasma polymerized ethylenediamine (PPEDA) thin films on cell-adhesive implant coatings. *Mater. Sci. Eng.*, 2013; 33, 3875–3880.
- Thedinga, E., Kob, A., Holst, H., Keuer, A., Drechsler, S., Niendorf, R., Baumann, W., Freund, I., Lehmann, M., Ehret, R.; Online monitoring of cell metabolism for studying pharmacodynamic effects. *Toxicol. Appl. Pharmacol.*, 2007; 220, 1, 33-44.
- Thull, R., Grant, D.; Physical and Chemical Vapor Deposition and Plasma-assisted Techniques for Coating Titanium, in *Titanium in medicine*, Brunette, D.M., Tengvall, P., Textor, M., Thomsen, P., eds, Springer, Berlin, 2001, 283-341.
- Tool, B.P.; Hyaluronan in morphogenesis. *Semin. Cell Dev. Biol.*, 2001; 12, 2, 79-87.
- Toole, B.P.; Hyaluronan: From extracellular glue to pericellular cue. *Nat. Rev. Cancer*, 2004; 4, 7, 528-539.
- Walschus, U., Schröder, K., Finke, B., Nebe, B., Podbielski, A., Schlosser, M.; Application of low-temperature plasma processes for biomaterials, in *Biomaterials Applications for Nanomedicine / Book 3'*, R. e. Pignatello, Rijeka, 2011, 127-142.
- Wiest, J., Brischwein, M., Ressler, J., Otto, A.M., Grothe, H., Wolf, B.; Cellular assays with multiparametric bioelectronic sensor chips. *Chimia*, 2005; 59, 5, 243-246.
- Willumeit, R., Schuster, A., Iliev, P., Linser, S., Feyerabend, F.; Phospholipids as implant coatings. *J. Mater. Sci.-Mater. Med.*, 2007; 18, 2, 367-380.
- Wiskott, H.W.A., Belser, U.C.; Lack of integration of smooth titanium surfaces: a working hypothesis based on strains generated in the surrounding bone. *Clin. Oral Implant. Res.*, 1999; 10, 6, 429-444.
- Wojtowicz, A.M., Shekaran, A., Oest, M.E., Dupont, K.M., Templeman, K.L., Hutmacher, D.W., Guldberg, R.E., Garcia, A.J.; Coating of biomaterial scaffolds with the collagen-mimetic peptide GFOGER for bone defect repair. *Biomaterials*, 2010; 31, 9, 2574-2582.
- Yan, W.Q., Nakamura, T., Kobayashi, M., Kim, H.M., Miyaji, F., Kokubo, T.; Bonding of chemically treated titanium implants to bone. *J. Biomed. Mater. Res.*, 1997; 37, 2, 267-275.
- Zamir, E., Geiger, B.; Components of cell-matrix adhesions. *J. Cell Sci.*, 2001; 114, 20, 3577-3579.
- Zhao, G., Raines, A.L., Wieland, M., Schwartz, Z., Boyan, B.D.; Requirement for both micron- and submicron scale structure for synergistic responses of osteoblasts to substrate surface energy and topography. *Biomaterials*, 2007; 28, 18, 2821-2829.
- Zhao, J.H., Michalski, W.P., Williams, C., Li, L., Xu, H.S., Lamb, P.R., Jones, S., Zhou, Y.M., Dai, X.J.J.; Controlling cell growth on titanium by surface functionalization of heptylamine using a novel combined plasma polymerization mode. *J. Biomed. Mater. Res. Part A*, 2011; 97A, 2, 127-134.

Zhu, X., Eibl, O., Scheideler, L., Geis-Gerstorfer, J.; Characterization of nano hydroxyapatite/collagen surfaces and cellular behaviors. *J. Biomed. Mater. Res. A*, 2006; 79A, 1, 114-127.

Ziegler, W.H., Liddington, R.C., Critchley, D.R.; The structure and regulation of Vinculin. *Trends Cell. Biol.*, 2006; 16, 9, 453-460.

Zimmerman, E., Geiger, B., Addadi, L.; Initial stages of cell-matrix adhesion can be mediated and modulated by cell-surface hyaluronan. *Biophys. J.*, 2002; 82, 4, 1848-1857.

8. Appendix

List of publications

Luthen F, Bulnheim U, Mueller PD, Rychly J, Jesswein H, Nebe JGB. Influence of manganese ions on cellular behavior of human osteoblasts in vitro. *Biomol Eng* 2007 Nov;24 (5):531-536.

Nebe JB, Jesswein H, Weidmann A, Finke B, Lange R, Beck U, Schroeder K: Osteoblast sensitivity to topographical and chemical features of titanium. *Mater Sci Forum*, Vols. 638-642 (2010) 652-657.
IF 0.399

Schroder K, Finke B, Jesswein H, Luthen F, Diener A, Ihrke R, Ohl A, Weltmann KD, Rychly J, Nebe JB. Similarities between Plasma Amino Functionalized PEEK and Titanium Surfaces Concerning Enhancement of Osteoblast Cell Adhesion. *J Adhes Sci Technol* 2010;24(5):905-923. IF 1,175

Rebl H, Finke B, Rychly J, Schröder K, Nebe JB: Positively charged material surfaces generated by plasma polymerized allylamine enhance vinculin mobility in vital human osteoblasts. *Advanced Biomat.* 12 (2010) 356-364. DOI: 10.1002/adbi.200900070. IF 1,506

Rebl H, Finke B, Schroeder K, Nebe JB: Time-dependent metabolic activity and adhesion of human osteoblast-like cells on sensor chips with a plasma polymer nanolayer. *Int J Artif Organs* 2010; 33: 738 – 748
IF 1.417

Rebl A, Rebl H, Liu S, Goldammer T, Seyfert HM: Salmonid Tollip and MyD88 factors can functionally replace their mammalian orthologues in TLR-mediated trout SAA promoter activation. *Developmental and Comparative Immunology* 35 (2011) 81–87. IF 3.290

Schröder K, Finke B, Jesswein H, Lüthen F, Diener A, Ihrke R, Ohl A, Weltmann K-D, Rychly J, Nebe JB: Similarities of plasma amino functionalized PEEK and titanium surfaces concerning enhanced osteoblast cell adhesion. in “Surface and Interfacial Aspects of Cell Adhesion” (2010), 335-353. Koninklijke Brill NV, Leiden 2010.

Testrich H, Rebl H, Wienholtz F, Nebe B, Meichsner J: Biofunctional Plasma Polymerized Ethylenediamine Thin Films for Implant Coatings. Proceedings “20th European Conference on the Atomic and Molecular Physics of Ionized Gases“, 2010, 2 pages.

Meichsner J, Rebl H, Nebe B, Finke B, Testrich H: Plasma Polymerisation of Ethylenediamine (EDA) for Bioactive Implant Coating. Tagungsband „18. Neues Dresdner Vakuumtechnisches Kolloquium: Beschichtung, Modifizierung und Charakterisierung von Polymeroberflächen“, 2010, S. 42-47, ISBN: 978-3-9812550-2-7

V. Stranak, H. Wulff, H. Rebl, C. Zietz, K. Arndt, R. Bogdanowicz, B. Nebe, R. Bader, A. Podbielski, Z. Hubicka, R. Hippler, Deposition of Thin Titanium-Copper Films with Antimicrobial Effect by Advanced Magnetron Sputtering Methods, *Mat. Sci. Eng. C* 31, (2011), 1512–1519. ISSN 0928-4931
IF 2.180

Ralf Wyrwa, Birgit Finke, Henrike Rebl, Nicole Mischner, Marion Quaas, Jan Schaefer, Claudia Bergemann, J. Barbara Nebe, Karsten Schroeder, Klaus-Dieter Weltmann, and Matthias Schnabelrauch: Design of plasma surface-activated, electrospun polylactide non-wovens with improved cell acceptance. *Adv. Eng. Mater.* 13 No. 5 (2011) 165-171. IF 1,746

Finke B, Hempel F, Testrich H, Artemenko A, Rebl H, Kylian O, Meichsner J, Biederman H, Nebe B, Weltmann KD, Schroeder K. Plasma processes for cell-adhesive titanium surfaces based on nitrogen-containing coatings. *Surf Coat Technol* 2011 Jul;205: 520-524. ISSN 0257-8972 IF2.141

Finke B, Martin Polak, Frank Hempel, Henrike Rebl, Carmen Zietz, Vitezskav Stranak, Gerold Lukowski, Rainer Hippler, Rainer Bader, J. Barbara Nebe, Klaus-Dieter Weltmann, Karsten Schröder: Antimicrobial potential of copper-containing titanium surfaces generated by ion implantation and dual high power impulse magnetron sputtering. *Adv. Eng. Mater.* 2012, 14 (5), B224-B230 IF 1.185

Henrike Rebl, Birgit Finke, Regina Lange, Klaus-Dieter Weltmann, J. Barbara Nebe, Impact of plasma chemistry versus titanium surface topography on osteoblast orientation, *Acta Biomater.* 2012; 8, 10, 3840-3851; DOI: 10.1016/j.actbio.2012.06.015 online 15.6.2012 IF 4.865

H. Testrich, H. Rebl, B. Finke, F. Hempel, B. Nebe, J. Meichsner. Aging effects of plasma polymerized ethylenediamine (PPEDA) thin films on cell-adhesive implant coatings *Mater. Sci. Eng., C* 33 (2013) 3875–3880., <http://dx.doi.org/10.1016/j.msec.2013.05.024> IF 2.596

Y.J. Quan, F.M. Zhang, H. Rebl, B. Nebe, O. Kessler, E. Burkel; Ti6Al4V foams fabricated by spark plasma sintering with post-heat treatment. *Mater. Sci. Eng. A-Struct. Mater. Prop. Microstruct. Process.*, 2013; 565, 118-125. <http://dx.doi.org/10.1016/j.msea.2012.12.026> IF 2.108

A. Hoene, M. Patrzyk, U. Walschus, V. Stranak, R. Hippler, H. Testrich, J. Meichsner, B. Finke, H. Rebl, B. Nebe, C. Zietz, R. Bader, A. Podbielski, M. Schlosser; In vivo examination of the local inflammatory response after implantation of Ti6Al4V samples with a combined low-temperature plasma treatment using pulsed magnetron sputtering of copper and plasma-polymerized ethylenediamine. *J Mater Sci Mater Med.* 2013 Mar;24(3):761-71. doi: 10.1007/s10856-012-4839-4. Epub 2013 Jan 12. IF 2.141

J. Barbara Nebe, Birgit Finke, Andreas Koertge, Henrike Rebl, Susanne Staehlke; Geometrical Micropillars Combined with Chemical Surface Modifications – Independency of Actin Filament Spatial Distribution in Primary Osteoblasts. *Materials Science Forum* Vols. 783-786 (2014), 1320-1325

Matthias Schnabelrauch, Ralf Wyrwa, Henrike Rebl, Claudia Bergemann, Birgit Finke, Michael Schlosser, Uwe Walschus, Silke Lucke, Klaus-Dieter Weltmann, and J. Barbara Nebe; Surface-Coated Polylactide Fiber Meshes as Tissue Engineering Matrices with Enhanced Cell Integration Properties. *Int. J. Pol. Sci.*, Volume 2014, Article ID 439784, 12 pages, <http://dx.doi.org/10.1155/2014/439784> IF 0.765

Alexander Rebl, Henrike Rebl, Tomáš Korytář, Tom Goldammer, Hans-Martin Seyfert; The proximal promoter of a novel interleukin-8-encoding gene in rainbow trout (*Oncorhynchus mykiss*) is strongly induced by CEBPA, but not NF- κ B p65. *Developmental & Comparative Immunology*, Volume 46, Issue 2, 2014, 155–164 IF 2.238

Andreas Brietzke, Tom Goldammer, Henrike Rebl, Tomáš Korytář, Bernd Köllner, Wei Yang, Alexander Rebl, Hans-Martin Seyfert; Characterization of the interleukin 1 receptor-associated kinase 4 (IRAK4)-encoding gene in salmonid fish: The functional copy is rearranged in *Oncorhynchus mykiss* and that factor can impair TLR signaling in mammalian cells. *Fish Shellfish Immunol.* 2014 Jan;36(1):206-14 IF 2.964

Book chapters

Frank Hempel, Hartmut Steffen, Benedikt Busse, Birgit Finke, J. Barbara Nebe, Antje Quade, Henrike Rebl, Claudia Bergemann, Klaus-Dieter Weltmann and Karsten Schröder (2011). On the Application of Gas Discharge Plasmas for the Immobilization of Bioactive Molecules for Biomedical and

Bioengineering Applications, Biomedical Engineering - Frontiers and Challenges, Reza Fazel-Rezai (Ed.), ISBN: 978-953-307-309-5, InTech

Lectures

H Jesswein, B Finke, K Schröder, B Nebe: Einfluss von plasma-polymerisiertem Allylamin auf die Vinculinmobilität von humanen Osteoblasten. Thüringer Grenz- und Oberflächentage (ThGOT) und Thüringer Biomaterial-Kolloquium, 15.09. - 17.09.2009, Friedrichroda, Germany

H. Rebl: Influence of manganese ions on cell characteristics of human osteoblasts – measurements with the Bionas® 2500 analyzing system. Bionas-workshop 11.12.09, Rostock

H. Rebl: Plasmachemische Funktionalisierung von topographisch modifizierten Oberflächen: Analyse der Zellphysiologie. Statusseminar Campus PlasmaMedII, 04.04.2012, Greifswald

H. Rebl: Plasmapolymerschichten auf strukturierten Biomaterialoberflächen: Bedeutung von Topographie und Chemie auf die Zellphysiologie. Kolloquium des Forschungsverbundes „Knochenregeneration“ 2011/2012, 12.04.2012, Rostock

H. Rebl: Effects of plasma polymer layers on the cell physiology of osteoblasts. 22.06.2012, University of Cergy-Pontoise, ERRMECe (Research Team onto Relationship between Extracellular Matrix and Cells) Cergy-Pontoise, France

H. Rebl: Plasma-polymerized allylamine coatings for orthopaedic implants – cell shape analyses. 17. Workshop des ak-adp (Anwenderkreis Atmosphärendruckplasma), 3. Workshop Plasmamedizin, 02.06. - 03.06. 201,3 Berlin

Conferences/Abstracts

Lüthen F, Bulnheim U, Mueller PD, Rychly J, Jesswein H, Nebe JGB. Influence of manganese ions on cellular behavior of human osteoblasts in vitro. Symposium on Surface Functionalization Activation Biomaterials held at the 2006 E-MRS Fall Conference; 2006 Sep 04-06; Warsaw, POLAND: Elsevier Science Bv; 2006. p. 531-536.

Jesswein H, Weidmann A, Finke B, Lange R, Beck U, Stahlke S, et al. Enhanced cell-surface-contact due to positively charged, plasma polymer coated titanium. Eur J Cell Biol 2009 Mar;88:48-48.

Rebl H, Finke B, Rychly J, Schröder K, Nebe JB: Vinculin mobility in vital human osteoblasts is enhanced by positively charged material surfaces generated with plasma-polymerized allylamine. DGZ Regensburg, März 2010, EJC (European Journal of Cell Biology), Vol. 89S1, Suppl. 60, ISSN 0171-9335, p48
IF 3.314

Stranak V, Rebl H, Nebe B, Hubicka Z, Zietz C, Arndt K, Bader R, Podbielski A, Bogdanowicz R, Hippler R: Deposition of multi-structural biocompatible thin films with antimicrobial effect by pulsed magnetron sputtering. BIOMaterialien 11 (2010) 105.

Nebe JB, H. Rebl, B. Finke, C. Matschegewski, S. Stählke, U. Beck, D. Kern, K-D. Weltmann, K. Schröder: Plasmachemisch modifizierte Metalloberflächen und ihr Einfluss auf die Zellphysiologie. Workshop on Metallic Biomaterials, Geesthacht, Febr 2010.

Stranak V, Z. Hubicka, M. Cada, R. Rebl, C. Zietz, K. Arndt, B. Nebe, R. Bader, A. Podbielski, Hippler R: Deposition of Ti-Cu films with fast antimicrobial effect prepared by multicomponent High Power Impulsed Magnetron Sputtering. In: Book of abstract of 24th Symposium on Plasma Physics and Technology (SPPT 2010), Prague, June 14-17, (2010), pp.115.

Stranak V, Z. Hubicka, H. Rebl, C. Zietz, K. Arndt, B. Nebe, R. Bader, A. Podbielski, R. Hippler: DEPOSITION OF MULTI-STRUCTURAL THIN FILMS WITH ANTIMICROBIAL EFFECT BY PULSED MAGNETRON SPUTTERING. Paper # 1151, 37th International Conference on Plasma Science and 23rd Symposium on Fusion Engineering, ICOPS 2010, June 20-24, 2010, Norfolk, VA

Wyrwa R, Birgit Finke, Henrike Rebl, Nicole Mischner, J. Barbara Nebe, Karsten Schroeder, Marion Quaas, Klaus-Dieter Weltmann, Matthias Schnabelrauch: Design of plasma surface-activated, electrospun polylactide non-wovens with improved cell acceptance. JT9X6. Symp.: Functional biointerfaces. E-MRS 2010 Spring Meeting, Strasbourg, France, June 7 to 11, 2010.

Testrich H, Rebl H, Wienholtz F, Nebe B, Meichsner J: Biofunctional plasma polymerized ethylenediamine thin films for implant coatings"; ESCAMPIG-20, 13 –17 July, 2010, Novi Sad, Serbia 2010.

Rebl H, Finke B, Matschegewski C, Staehlke S, Lange R, Kern DP, Beck U, Schroeder K, Nebe J.B.: Cell architecture on plasmafunctionalized, structured metal surfaces. ESB 2010, Tampere, Finland, Sept 2010.

Finke B, Wyrwa, Rebl, Mischner, Schröder, Quaas, Weltmann, Schnabelrauch, Nebe: Plasma functionalized electrospun non-wovens with improved cell adhesion characteristics. ICPM 3, Greifswald September 23, 2010.

Stranak V., Rebl H., Nebe B., Hubicka Z., Zietz C., Arndt K., Bader R., Podbielski A., Bogdanowicz R., Hippler R.: Deposition of multi-structural biocompatible thin films with antimicrobial effect by pulsed magnetron sputtering. DGBM Heilbad Heiligenstadt, 18.11.2010.

Stranak V, Hubicka Z, Rebl H, Zietz C, Arndt K B. Nebe B, Bader R, Podbielski A, Hipper R: Multi-structural films with fast antimicrobial shock effect deposited by pulsed magnetron sputtering, In: Book of Abstracts of ICPM-3 2010 conference, Greifswald (Germany), September 19-24, 2010, (eds. K.-D. Weltmann), 75.

Meichsner J, Testrich H, Rebl H, Wienholtz F, Nebe B: Plasma Polymerized Ethylenediamine Thin Films for Biomedical Applications. Twelfth International Conference on Plasma Surface Engineering, September 13 - 17, 2010, Garmisch-Partenkirchen, Germany

Schröder K, Finke B, Testrich H, Meichsner J, Artemenko A, Kylian O, Biederman H, Rebl H, Nebe B, Weltmann K D: Plasma processes for cell-adhesive titanium surfaces based on nitrogen-containing coatings. Twelfth International Conference on Plasma Surface Engineering, September 13 - 17, 2010, Garmisch-Partenkirchen, Germany

Testrich H, Rebl H, Wienholtz F, Nebe B, Meichsner J: Cell adhesive implant coatings using plasma polymerized ethylenediamine thin films. ICPM 3, Greifswald September 23, 2010

Finke B, Rebl H, Nebe JB, Weltmann KD, Schröder K: Time dependent investigations of plasma polymerized allylamine surfaces and cell biological response. Paper 299. 20th International Symposium on Plasma Chemistry (ISPC), 24.-29. July 2011, Philadelphia, USA

Holger Testrich, Henrike Rebl, Barbara Nebe, Birgit Finke, and Jürgen Meichsner: Plasma polymerisation of ethylenediamine (EDA) for bioactive implant coatings. 20th International Symposium on Plasma Chemistry (ISPC), 24.-29. July 2011, Philadelphia, USA

Birgit Finke, Henrike Rebl, Jan Schäfer, Barbara Nebe, Klaus-Dieter Weltmann and Karsten Schröder. The Aging of Plasma Amino Functionalized Titanium Surfaces and the Response of Osteoblasts, ESB 2011 Dublin 4.-9-Sept

U. Walschus, A. Hoene, B. Finke, K. Schröder, H. Rebl, B. Nebe, C. Zietz, A. Podbielski, L. Wilhelm, M. Schlosser. An additional coating with plasma-polymerized allyl amine reduces the local tissue reactions caused in-vivo by titanium implants treated with plasma immersion ion implantation of copper for antibacterial properties, ESB 2011 Dublin 4.-9-Sept

A. Hoene, U. Walschus, V. Stranak, R. Hippler, H. Testrich, J. Meichsner, H. Rebl, B. Nebe, C. Zietz, A. Podbielski, L. Wilhelm, M. Schlosser. Time course of the local inflammatory response after implantation of low-temperature plasma modified titanium implants treated with pulsed magnetron sputtering of copper and plasma-polymerized ethylenediamine, ESB 2011 Dublin 4.-9-Sept

Vitezslav Stranak, Harm Wulff, Robert Bogdanowicz, Henrike Rebl, Carmen Zietz, Zdenek Hubicka, Kathleen Arndt, Barbara Nebe, Rainer Bader, Andreas Podbielski, and Rainer Hippler. Functional thin films prepared by high power impulse magnetron sputtering. DPG Berlin 2012

F. Hempel, B. Finke, H. Testrich, J. Meichsner, H. Rebl, B. Nebe, K.-D. Weltmann, K. Schröder. On the Aging of Nitrogen-Containing Plasma Polymer Layers on Titanium Implant Model Surfaces and Correlation with the Response of Osteoblastic Cells, 30th ICPIG, August 28th – September 2nd 2011, Belfast, Northern Ireland, UK

H. Testrich, H. Rebl, B. Nebe, J. Meichsner. Plasma polymerized ethylenediamine (PPEDA) thin films for cell-adhesive implant coatings, 30th ICPIG, August 28th – September 2nd 2011, Belfast, Northern Ireland, UK

Nebe B, Finke B, Wyrwa R, Rebl H, Bergemann C, Schröder K, Schnabelrauch M: Enhanced cell integration in electrospun polylactide fiber matrices activated by plasma-polymerized allylamine. THERMEC' 2011, August 1-5, 2011, Quebec City, Canada, Proceedings, BIOMAT-15-2, p. 89.

Nebe B, Henrike Rebl, Birgit Finke, Rainer Bader, Karsten Schröder, Klaus-Dieter Weltmann: Plasmachemisch funktionalisierte Implantate und Grenzflächeninteraktion mit Zellen. DPG Kiel, 31.03.2011.

Wyrwa R, Birgit Finke, Henrike Rebl, Nicole Mischner, Claudia Bergemann, Karsten Schroeder, Matthias Schnabelrauch and J. Barbara Nebe: Electrospun Polylactide Non-wovens with Plasma Functionalized Fibers to Improve Cell Adhesion Characteristics. ESB Dublin, Irland, 09 2011, Proceedings, no. 189.

J. B. Nebe, R. Wyrwa, B. Finke, H. Rebl, C. Bergemann, K.-D. Weltmann, M. Schnabelrauch: Plasma-deposited nanolayer on electrospun fiber mesh enhances occupancy by epithelial cells BioNanoMed, 1-2.3.2012 Krems, Austria

Vitezslav Stranak, Harm Wulff, Robert Bogdanowicz, Henrike Rebl, Carmen Zietz, Zdenek Hubicka, Kathleen Arndt, Barbara Nebe, Rainer Bader, Andreas Podbielski and Rainer Hippler: Functional thin films prepared by high power impulse magnetron sputtering, 76. Jahrestagung der DPG, 25. - 30. März 2012 Berlin

J. Barbara Nebe, Birgit Finke, Rainer Hippler, Henrike Rebl, Rainer Bader, Andreas Podbielski, Klaus-Dieter Weltmann: Plasma techniques for cell adhesive or anti-bacterial implant surfaces. 25th Symposium on Plasma Physics and Technology, Prague, June 18-21, 2012; SPPT 2012.

Henrike Rebl, Birgit Finke, Friederike Kunz, J. Barbara Nebe: Combinatory Effect of Chemical Functionalization and Surface Roughness of Titanium on Cells – Which Modification is Dominant? Materials Science Engineering (MSE) F2 Interfaces 25-27 Sept 2012, Darmstadt, Germany

B. Finke, J. Schäfer, F. Hempel, H. Rebl, K.D. Weltmann, J.B. Nebe: Analysis of the aging of cell-adhesive plasma-polymer coatings on titanium surfaces. 13th International Conference on Plasma Surface Engineering (PSE), September 10-14, 2012, Garmisch-Partenkirchen, Germany

F. Hempel, J. Schäfer, H. Rebl, J.B. Nebe, K.-D. Weltmann, B. Finke: One-year stability of a cell-adhesive plasma-polymer layer on titanium. 13th International Conference on Plasma Surface Engineering (PSE), September 10-14, 2012, Garmisch-Partenkirchen, Germany

B. Finke, F. Hempel, H. Rebl, J. Schäfer, J.B. Nebe, K.-D. Weltmann: Aging of the plasma polymer layer PPAAm and cell response. 4th International Symposium Interface Biology of Implants (IBI) 2012, from 09 - 11 May 2012, Rostock, Germany

Henrike Rebl, Birgit Finke, J. Barbara Nebe: Dominance of plasma chemistry versus the surface topography - behavior of human osteoblast-like cells, 4th International Symposium Interface Biology of Implants (IBI) 2012, from 09 - 11 May 2012, Rostock, Germany

Henrike Rebl, Birgit Finke, J. Barbara Nebe: Superiority of plasma chemistry over surface topography-characteristics of human osteoblasts. 4th International Conference on Plasma Medicine, June 17-21, 2012, Orléans, France

H. Rebl, B. Finke, J. B. Nebe: Plasma-polymerized allylamine coatings for orthopaedic implants – cell shape analyses. 1st Young Professionals Workshop in Plasma-Medicine, 17-19. September 2012 Boltenhagen, Germany

A. Rebl, H. Rebl, T. Goldammer, H.M. Seyfert. Cloning and characterization of the trout interleukin-8 promoter. *Fish & Shellfish Immunology* 34 (2013) p1732; First International Conference of Fish and Shellfish Immunology, 25 - 28,06.2013, Vigo, Spain. P-131. IF 2,96

Henrike Rebl, Holger Testrich, Jürgen Meichsner, Maryna Karmazyna, J. Barbara Nebe, Generation of fluorocarbon plasma polymers to prevent cellular adhesion on temporary implant materials in vitro, Euro BioMAT 23-24. April 2013, Weimar

Jürgen Schmidt, Christian Schrader, Birgit Finke, Henrike Rebl, J. Barbara Nebe; The combination of plasma chemical oxidized (PCO) and plasma chemical polymerized allylamine (PPAAm) coated surfaces for the improvement of cell adherent properties, Euro BioMAT 23-24. April 2013, Weimar

Jan Heeg, Andreas Podbielski, Kathleen Arndt, Henrike Rebl, Barbara Nebe, Christoph Mewes, Antje Schütz, Torsten Barfels and Marion Wienecke. Nano Composite DLC Coating for Antimicrobial Medical Applications. European Materials Research Society (E-MRS) Spring meeting 2013, 27. - 31.05.2013, Strasbourg, France

H. Rebl, B. Finke, J. B. Nebe, Plasma-polymerized allylamine coatings for orthopaedic implants – cell shape analyses, 17. Workshop des ak-adp (Anwenderkreis Atmosphärendruckplasma), 3.-4. Juni 2013, Berlin

Birgit Finke, Ralf Wyrwa, Henrike Rebl, J. Barbara Nebe, Klaus-Dieter Weltmann, Matthias Schnabelrauch. Plasma polymer-coating of electrospun fiber mesh improves cell adherent properties of osteoblasts. International symposium on plasma chemistry (ISPC), 04. – 08.08.2013, Cairns, Australia

Henrike Rebl, Holger Testrich, Jürgen Meichsner, Maryna Karmazyna, J. Barbara Nebe. Prevention of cellular adhesion on fluorocarbon plasma polymer coated metal surfaces. Jahrestagung der Deutschen Gesellschaft für Biomaterialien (DGBM), 26. – 28.09.2013, Erlangen

B. Finke, H. Rebl, B. Nebe, R. Bader, U. Walschus, M. Schlosser, K.-D. Weltmann. Anti-adhesive Finishing of temporary Implant Surfaces by a Plasma-Fluorine-Polymer. The 4th international symposium on surface and interface of biomaterials (ISSIB), 24. – 28.09.2013, Rome, Italy

B. Finke, H. Rebl, B. Nebe, R. Bader, U. Walschus, M. Schlosser, K.-D. Weltmann. ANTI-ADHESIVE FINISHING OF TEMPORARY IMPLANT SURFACES BY A PLASMA-FLUORINE-POLYMER. . International Conference on processing & manufacturing of advanced materials THERMEC '2013, 02. – 06.12.2013, Las Vegas, USA

J. B. Nebe, C. Matschegewski, B. Finke, H. Rebl, R. Lange, S. Stählke. Geometrical micropillars combined with chemical surface modifications – independency of actin filament spatial distribution in primary osteoblasts. International Conference on processing & manufacturing of advanced materials THERMEC '2013, 02. – 06.12.2013, Las Vegas, USA

Matthias Schnabelrauch, Ralf Wyrwa, Birgit Finke, Henrike Rebl, Claudia Bergemann, Michael Schlosser, Uwe Walschus, Silke Lucke, Klaus-Dieter Weltmann, J. Barbara Nebe. Plasma-activated electrospun polylactide fiber meshes as matrices for tissue engineering. . International Conference on processing & manufacturing of advanced materials THERMEC '2013, 02. – 06.12.2013, Las Vegas, USA

J. Meichsner, H. Testrich, H. Rebl, B. Nebe; Fluorocarbon plasma polymer coating for temporary implants, XXII Europhysics Conference on Atomic and Molecular Physics of Ionized Gases (ESCAMPIG) 15.-19.07.2014 Greifswald, Germany

Appendix II

Method Bionas Analyzer 2500

For the continuous measurement of adhesion and metabolism (respiration and acidification) the cells were seeded onto microchips. The Bionas® 2500 analyzing system with the metabolic chips SC 1000 (Bionas GmbH, Rostock, Germany) was used. This chip type is equipped with three sensor types: IDES (interdigitated electrode structure) sensors for cell adhesion, Clark type sensors for respiration and ISFET (ion-sensitive field effect transistor) sensors for acidification measurements. Prior to the experiments, the metabolic chips SC 1000 used as controls were decontaminated with 70% ethanol and washed with phosphate buffer solution (PBS; PAA Laboratories GmbH, Pasching, Austria). Additionally, the chip surface was functionalized with plasma polymerized allylamine (PPAAm). The Bionas® 2500 analyzing system technology is based on a flow system, where fresh medium (in our experiments Dulbecco's modified Eagle medium + 0.1% fetal calf serum) is steadily supplied to the cells. During the entire course of the experiment a pump phase of 4 minutes was followed by a steady phase (no flow) of 4 minutes. The flow rate in the system was adjusted to the lowest value of 56 µl/min to avoid shear stress. The temperature in the operating chamber was 37°C. In the Bionas® 2500 analyzing system, six measurement places work in parallel; therefore different surface treatments can directly be compared in the same experiment.

For cell adhesion measurements, the metabolic chips SC 1000 (total area of the cell culture surface=70.88 mm²) were equipped with IDES sensors (cell culture surface of the IDES-sensor: 29 mm², with a finger width and interfinger space of 50 µm each). Impedance measurements were used to detect insulating cell membranes near the measuring electrodes. Sinusoidally oscillating fields with a frequency of 10 kHz were used [Ehret et al. 1997]. The insulating cell membrane of intact cells on the electrodes and their distance to the electrodes determine the current flow and thus the sensor signal. When the membranes are destroyed or cell-cell contacts are opened, there are fewer obstacles for an oscillating electrical field compared to the situation with intact cells. Thus higher capacitance values indicate the presence of damaged or opened cell membranes on the IDES. The cell adhesion is then calculated from the inverted raw values of capacitance (nF). The empty, cell-free chip (ca. 47 nF) was referred to as 0% adhesion; 0 nF corresponds to 100% adhesion. The metabolic activity was assessed by respiration (Clark type sensor) and acidification (ISFET) measurements. The accumulation of metabolic products, e.g., lactate leads to a decrease in the pH-value of the medium. When fresh medium is supplied, the pH- value rises again. This creates characteristic peaks and the slope of the curve represents the acidification rate. The respiration rate was calculated analogously. For further processing of the values, Microsoft Excel software (Microsoft Office 2007) was used.

R. Ehret, W. Baumann, M. Brischwein, A. Schwinde, K. Stegbauer & B. Wolf; Monitoring of cellular behavior impedance measurements on interdigitated electrode structures; *Biosensors & Bioelectronics* Vol. 12, No. 1, pp. 29-41, 1997

Supplementary data

A

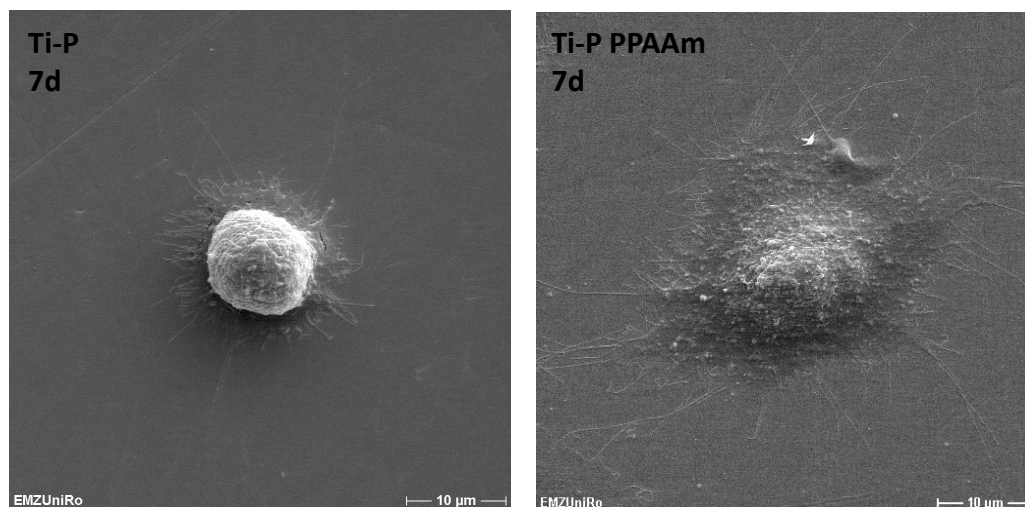


Figure 5: Scanning electron images of MG-63 cells grown on polished titanium +/- coating with PPAAm for 30 min. The cells on PPAAm spread much faster and express a lot more filopodia than cells grown on pure titanium. (bar=10 µm, scanning electron microscope DMS 960A)

B

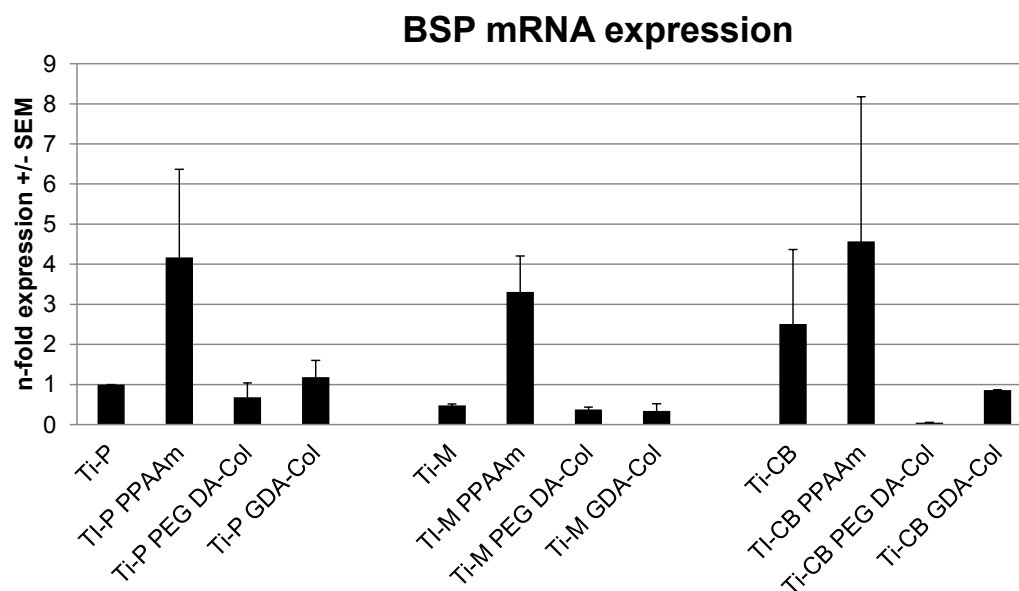


Figure 6: mRNA expression of the late osteogenic marker bone sialoprotein (BSP) on topographically and chemically modified titanium surfaces after 24h. None of the samples is significantly different from Ti-P although a trend to higher values on PPAAm can be observed. (n=3, Student's t-test)

Danksagung

Mein außerordentlicher Dank gebührt Frau Professor Barbara Nebe für die hervorragende Betreuung und intensive Unterstützung während der Durchführung der Promotion. Durch viele motivierende Diskussionen und konstruktive Anregungen hat sie entscheidend zum Entstehen dieser Arbeit beigetragen.

Ich danke allen Kollegen im Projekt „Campus PlamaMed“ für die gute und zielstrebige Zusammenarbeit und die interdisziplinären Diskussionen, aus denen ich viel lernen konnte.

Ein besonders herzlicher Dank gilt den Kollegen des AB Zellbiologie. Dr. Claudia Bergemann danke ich für die Hilfe bei der Durchführung der PCR und für die vielen erfreuenden Gespräche zwischendurch. Dr. Frank Lüthen danke ich für die Unterstützung, besonders bei der konfokalen Mikroskopie. Außerdem möchte ich mich bei Frau A. Peters, Frau Dr. Müller, Janine Wetzel und Frau Seidel bedanken, die mich tatkräftig unterstützt haben und mir stets hilfreich zur Seite standen.

Ganz besonders möchte ich mich bei meinem Mann Alexander bedanken - für seine Ausdauer und Ermutigung diese Arbeit fertigzustellen. Meinen Kindern Kira und Jan danke ich für die Kraft die sie mir gegeben haben. Meinen Eltern möchte ich dafür danken, dass sie mir Zeit zum Erholen und Kräftesammeln geschenkt haben.

Erklärung

Hiermit versichere ich, dass ich die vorliegende Arbeit selbstständig angefertigt und ohne fremde Hilfe verfasst habe, keine außer den von mir angegebenen Hilfsmitteln und Quellen dazu verwendet habe und die den benutzten Werken inhaltlich und wörtlich entnommenen Stellen als solche kenntlich gemacht habe.

 Ort, Datum

 Unterschrift
Erklärung zum eigenen Anteil an der Veröffentlichung:

Hiermit erkläre ich, dass drei der Veröffentlichungen, die in der vorliegenden Arbeit zusammengefasst sind, von mir selbstständig verfasst wurden. Dabei erhielt ich Supervision von Frau Professor Barbara Nebe.

Mein eigener Anteil an den Veröffentlichungen beschreibt sich wie folgt:

- 1) Durchführung der Datenerhebung im Labor
- 2) Statistische Auswertung der Daten
- 3) Diskussion und Interpretation der Daten
- 4) Entwurf und Verfassen der Manuskripte inkl. Literaturrecherche und Erstellung von Tabellen und Abbildungen

Mein Anteil an der als Studie IV benannten Veröffentlichung beläuft sich auf

- 1) Durchführung der zellbiologischen Untersuchungen
- 2) Statistische Auswertung der Daten
- 3) Diskussion und Verfassen des zellbiologischen Teils des Manuskriptes inklusive Erstellung der Abbildungen

Die vorliegende Arbeit wurde im Rahmen des Projektes “Campus PlasmaMed” im Teilprojekt “PlasmaImp” (www.campus-plasmamed.de, 10/2012, grant No. 13N9775, 13N11183) angefertigt, welches von Frau Professor Barbara Nebe koordiniert wurde.

Alle Co-Autoren haben die Manuskripte der Veröffentlichungen redigiert.

 Ort, Datum

 Unterschrift